4-9247

DIRECT PRODUCTION OF GASOLINE RANGE HYDROCARBONS FROM SYNGAS IN A DUAL BED REACTOR SYSTEM

DSS CONTRACT #OST84-00321

Report Submitted by:

N.N. Bakhshi
Catalysis & Chemical Reaction Engineering Laboratory
Department of Chemical Engineering
University of Saskatchewan
Saskatoon, Saskatchewan, Canada
S7N 0W0

May 5, 1986

AUG 15 1986
MICROMEDIA

161 pp

LIST OF CONTENTS

	PAGE
ABSTRACT	(ii)
INTRODUCTION	2
EXPERIMENTAL	4
(i) Preparation of Fischer-Tropsch Catalysts	4
Preparation of 5% Ni/Zirconia Catalyst (The base catalyst)	4
Preparation of 10% Co/base and 2% Ni-5% Co/base Catalysts	5
(ii) Characterization of Fischer-Tropsch Catalysts	5
(iii) Preparation of Zeolite Catalyst HZSM-5	6
(iv) Characterization of the HZSM-5 Catalyst	6
Determination of the Constraint Index (C.I.)	7
(v) Apparatus and Procedure for Syngas Conversion	7
(vi) General Comments on Product Distribution Versus Time-On-Stream Behavior	9
RESULTS AND DISCUSSION	10
(i) Testing of FT/HZSM-5 Catalysts in the Dual-Packed Bed Reactor System	10
I. Catalyst Combination 10% Co/base and HZSM-5	10
Material Balance	13
II. Catalyst Combination 2% Ni-5% Co/base and HZSM-5	15
Material Balance	17
(ii) Regeneration Characteristics of the FT Catalyst	20
SUMMARY AND CONCLUSIONS	21
REFERENCES	24
APPENDIX A	26
APPENDIX B	28
APPENDIX C	38
TABLES	62
FIGURES	102

ABSTRACT

Conversion of synthesis gas (CO/H_2=1) to hydrocarbons was studied at atmospheric and elevated pressures using a 1/2 inch i.d. dual reactor system containing a Fischer-Tropsch (FT) catalyst followed by zeolite HZSM-5. Two FT catalysts, viz. 10% Co/base and 2% Ni-5% Co/base were used. The base catalyst was 5% Ni/ZrO_2 and was prepared by the coprecipitation method. The FT catalysts were prepared in the laboratory and characterized by temperature programmed reduction (TPR), BET surface area and atomic absorption. The ZSM-5 catalyst was also prepared in the laboratory and characterized by BET surface area, atomic absorption, x-ray diffraction and constraint index determination techniques.

The conversion reactions were carried out at various HZSM-5/FT ratios (1-4 by wt.) and operating pressures (0.101-2 MPa). The temperature of the FT reactor was fixed at 250°C, while the HZSM-5 reactor temperature was varied in the range 350-400°C.

The product distributions obtained using the two different FT catalysts combined with HZSM-5 were found to be different only slightly. However, the effects of the operating conditions on product distribution for the two FT catalysts were almost similar.

At atmospheric pressure conditions (0.101 MPa), the catalysts showed high activity and selectivity to liquid hydrocarbons and produced high octane gasoline even after long periods of operation. Thus, under favorable conditions of operation, the C_5^+ fraction produced was about 52% containing about 22% aromatic hydrocarbons. Almost all the C_5^+ hydrocarbons produced were in the gasoline range terminating at about C_{11}. The regeneration characteristics of the FT catalyst (10% Co/base used for CO conversion at 250°C and 0.101 MPa) showed that the catalyst could be regenerated fully to its initial activity by passing hydrogen over the catalyst at 425°C for 16 h.

In general, at atmospheric pressure the effect of the increase in the HZSM-5 reactor temperature was to decrease the C_5^+ hydrocarbons, while total aromatics remained almost constant or decreased only slightly. The isobutane selectivity also decreased with increase in the HZSM-5 reactor temperature.

The effect of increasing the pressure in the reactor (from 0.101 MPa to 2 MPa) was to shift the whole product distribution toward the lower molecular weight hydrocarbons with methane as the major product. At high pressure operation, the aromatic hydrocarbon-make was reduced to almost zero and the product contained small amounts of olefins. This intriguing behavior cannot be explained at the present. Further work needs to be done to understand this behavior.

This report covers the work done under the following Tasks:

Task 1: Preparation and Characterization of Catalysts

Task 2: Design and Construction of a 13 mm (1/2 in.) Diameter Dual Packed Bed Reactor System

Task 3: Testing of FT-HZSM-5 in the Dual Packed Bed Reactor System

INTRODUCTION

The world energy problem and particularly the threat of the rapid exhaustion of the world petroleum reserves in the last decade suggested a search for new energy sources, especially those from more abundant resources such as coal. The Fischer-Tropsch (FT) process is well known for hyrocarbon production from syngas. Recent catalytic work has combined a Fischer-Tropsch synthesis function with a shape-selective acid function to convert synthesis gas directly to liquid fuels (1-6). Most conventional Fischer-Tropsch catalysts produce a wide spectrum of hydrocarbon products (7). However, if combined with a shape-selective catalyst, a more selective hydrocarbon product can be produced in one step. In a single stage process, the shape-selective acid function such as HZSM-5 is physically admixed with a CO reduction catalyst such as FT catalyst or methanol synthesis catalyst (1,2). Although this single stage process is indeed effective in producing products having a substantial quantity of aromatics, there are some disadvantages associated in the single stage process. The FT catalyst usually deactivates faster than the HZSM-5 catalyst. Therefore, the FT catalyst may require regeneration or replacement while the HZSM-5 is still active. Furthermore, the regeneration procedures for the FT catalyst are different from those for the HZSM-5 catalyst. Also, this single stage process does not permit the operation of each component at its optimum reaction conditions. Therefore, it is highly desirable to separate the two catalysts so that each catalyst bed can be operated at its optimum condition.

In a sequentially arranged two-stage process, the product obtained from the FT reactor is passed through a second reactor containing zeolite HZSM-5 (8). The main advantages of the two-step process are: (i) the dual-bed reactor system allows for considerable flexibility with respect to both reaction conditions and products and (ii) the dual-bed reactor system allows the operation of each component at its own optimum reaction conditions. In general, the operating temperature of the FT catalyst is lower than that of HZSM-5 by about 100 - 200°C. High temperatures over the FT catalyst will cause increased formation of methane and fast deterioration of the catalyst. Furthermore, the dual-bed system permits easier rengeration and replacement of the spent catalyst.

In the present investigation, the conversion of synthesis gas to gasoline-range hydrocarbons was investigated with cobalt-nickel-zirconia and HZSM-5 catalysts combination, using 13 mm (1/2-inch) dual-bed reactor system.

EXPERIMENTAL

(i) Preparation of Fischer-Tropsch Catalysts

Preparation of 5% Ni/Zirconia Catalyst (The base catalyst)

One of the problems associated with preparing the base catalyst is the time required to wash the catalyst. The Ni/Zirconia catalyst is gelatinous in nature, thus making filtration extremely difficult. In order to speed up the process, we designed a filtration/washing unit which allows a large volume of water to be used per wash.

Basically, the apparatus is similar to a Büchner funnel. As can be seen in Figure 1, the cylindrical vessel is split roughly in half by an acrylic filter paper support (thickness = 5/16 inch). This support has holes drilled through it (drill size = 1/16 inch); number of holes $\simeq$ 400) in the same manner as in a Büchner funnel. Vacuum is applied at the lower section. The catalyst is kept in suspension by an impeller and baffles arrangement in the upper portion to enhance the mixing of the catalyst and water. Also, this arrangement prevents the settling of the gelatinous suspension, thus avoiding plugging of the pores of the filter paper.

Previously, using a Büchner funnel, it took approximately four days to complete the washing of the catalyst in order to produce $\simeq$ 40 g of the base catalyst. With this system, washing was completed within four hours to produce the same amount of the base catalyst.

The base catalyst (5% Ni/ZrO_2) was prepared by the co-precipitation of zirconyl nitrate and nickel nitrate solutions by excess alkali solution. Thus, 100 g zirconium dinitrate oxide [$Zr(NO_3)_2 \cdot H_2O$ containing 40.2% ZrO_2 from Alfa products] was dissolved in 200 mL water. Also, another solution was made with 10 g nickel nitrate salt [$Ni(NO_3)_2 \cdot 6\ H_2O$] in 200 mL water. The two solutions were mixed and added, drop by drop, with continuous mechanical stirring to 400 mL of 10% NaOH solution under a nitrogen atmosphere. The resulting cake was washed with distilled water and filtered under nitrogen atmosphere

until the pH of the filtrate was neutral using the above-mentioned filtration/washing unit. This was followed by two washings with acetone and drying in a vacuum oven at 60°C for 24 h.

Preparation of 10% Co/base and 2% Ni-5% Co/base Catalysts

The base catalyst (5% Ni/ZrO_2) thus prepared was used as support for the preparation of the two zirconia-based Fischer-Tropsch catalysts (10% Co/base and 2% Ni-5% Co/base) of varying Ni and Co contents. The impregnation of this support with aqueous solutions of nickel and cobalt salts [$Ni(NO_3)_2 \cdot 6\ H_2O$ and $Co(NO_3)_2 \cdot 6\ H_2O$] was carried out using the incipient wetness technique. The impregnated FT catalysts were dried in an oven at 100°C followed by calcination in a muffle furnace at 500°C for 24 h. About 50 g of each catalyst thus prepared was stored in a dessicator.

(ii) Characterization of Fischer-Tropsch Catalysts

The Fischer-Tropsch catalysts were characterized by BET surface area and atomic absorption. The results of atomic absorption analyses and surface area measurements are given in Table 1.

The 10% Co/base catalyst was characterized by temperature-programmed reduction (TPR). The details and procedure used for temperature-programmed reduction are described elsewhere (9). A mixture of 3% H_2 in nitrogen (Matheson, high purity) was used as the carrier gas. It was further purified by passing through a hydrogen deoxo purifier (Engelhard) followed by indicating drierite and molecular sieve 5X, used as a moisture trap. The carrier gas was split into two streams of equal flow rates of 30 mL/min. One stream passed through a quartz U-tube reactor containing 0.0536 g of the FT catalyst, a 5X molecular sieve-trap (to remove water formed during reduction) and then through one arm of the thermal conductivity cell. The other stream passed directly through the reference arm of the cell. The catalyst sample contained in the U-tube reactor was heated at a linearly programmed rate of 6 K/min. The hydrogen uptake due to the

reduction of the catalyst was monitored by the detector and displayed along with the corresponding reduction temperature on a two-pen recorder. The temperature was raised from 293 K to 900 K at the above rate, followed by isothermal reduction for 1 h. The TPR profile obtained is shown in Figure 2 and shows two stages of reduction, an initial one at 600 K and a major one at 683-693 K. As seen from the shape of the curve, maximum reduction seems to take place in the range 683-693 K.

(iii) Preparation of Zeolite Catalyst HZSM-5

ZSM-5 catalyst was prepared according to the method reported in the patent literature (U.S. Patent, 4,112,056 (1973)). The details of the procedure are given in Appendix A. The H^+ form was made by acid leaching using HCl. Finally, the catalyst was dried in air at 110°C and calcined in a muffle furnace at 400°C for 4 h.

(iv) Characterization of the HZSM-5 Catalyst

The zeolite was characterized by x-ray diffraction for crystal structure, by atomic absorption for SiO_2/Al_2O_3 weight ratio and by Constraint Index (C.I.) determinations for information on the necessary constrained accessibility in the zeolite to the desirable molecules.

As shown in Table 2, the x-ray diffraction pattern for HZSM-5 is identical to that reported in U.S. Patent 3,702,886.

The atomic absorption analysis of the sample showed that SiO_2/Al_2O_3 weight ratio was 56. The minimum required SiO_2/Al_2O_3 ratio of HZSM-5 type zeolite is around 30. The ratio of the prepared HZSM-5 is well above the minimum specified. The BET surface area of this zeolite was 341 m^2/g.

Determination of the Constraint Index (C.I.)

The experiments for the determination of the C.I. were carried out in the newly constructed microreactor apparatus as shown in Figure 3. The apparatus consisted of 1/4 inch OD reactor-preheater assembly. The C.I. was determined at atmospheric pressure using the following procedure as reported in the U.S. Patent 4,279,830. Zeolite in the powder form was first pelletized and then crushed to a particle size of -12 +24 mesh. A weighed amount of zeolite (0.2 g) was loaded in the microreactor. Prior to testing, the zeolite was treated with a stream of air (flow rate of air = 20 mL/min) at 375°C for 1 h. The zeolite was then flushed with helium at that temperature for 1/2 h. Then a mixture of equal weights of n-hexane and 3-methylpentane was passed continuously over the zeolite sample with helium dilution to give a helium to total hydrocarbon mole ratio of 4:1. The hydrocarbon mixture with helium dilution was made by continuously passing helium through a bubbler containing the mixture of liquid hydrocarbons at room temperature. After 20 min. on stream, a sample of the effluent gas was analyzed by GC using 10% OV-101 column to determine the fraction remaining unchanged for each of the two hydrocarbons.

The Constraint Index was calculated as follows:

$$\text{Constraint Index} = \frac{\log_{10}(\text{fraction of n-hexane remaining})}{\log_{10}(\text{fraction of 3-methylpentane remaining})}$$

The operating conditions and results for C.I. determination are given in Table 3. The C.I. value for our zeolite sample was determined as 1.25. This value is within the range (C.I. = 1-12) as reported in the U.S. Patent 4,279,830.

(v) Apparatus and Procedure for Syngas Conversion

Fixed-bed continous flow reactors were used and were made from stainless steel tube (i.d. 13 mm). The schematic diagram of the apparatus is shown in Figure 4. The apparatus consisted of sequen-

tially arranged dual reactor system of which the first reactor contained the FT catalyst and the second reactor contained the HZSM-5 catalyst. In the first reactor, the syngas mixture reacts over the FT catayst resulting in the formation of C_1 to C_{30} hydrocarbons and oxygenates. The product obtained from this FT reactor was fed to the second reactor containing the HZSM-5 zeolite. The effluent from the HZSM-5 reactor was passed directly through the GC System for product analysis via heated tubes. The reactor and preheater sections of both the reactors were surrounded by metal block heaters and were equipped with independent temperature control. The FT reactor was surrounded by a metal block heater whose temperature was controlled to $\pm 2°C$. The HZSM-5 reactor furnace was split in two halves to give independent control of the upper and lower sections thereby reducing the temperature gradient across the reactor. The temperature drop across the reactor was $\pm 3°C$, and the temperatures of the HZSM-5 reactor was controlled to $\pm 2°C$. The feed gas was a premixed mixture of CO and H_2 (ratio 1:1) containing 5% Ar which served as an internal standard for product analysis.

The FT catalyst was pretreated in-situ under flowing hydrogen at 450°C for 16 h, while the HZSM-5 was pretreated with air at 450°C for 16 h. The catalyst temperature was lowered to the reaction temperature before introducing the feed gas.

The reaction products were analyzed by on-line gas chromatography. The GC operating conditions are given in Table 4. The following columns are used for product analysis.

1. 10% TCEP on Chromosorb P AW - for C_1 - C_{15} hydrocarbons and aromatics distribution.
2. Chromosorb 102 - for C_1 - C_4 hydrocarbons.
3. Carbopack C/0.19% Picric acid - C_4 components.
4. Carbosieve S column - for CO, CO_2, Ar and CH_4.

All the peak areas were measured by Hewlett-Packard electronic integrators. The calibration was carried out using various calibration mixtures and pure compounds.

Experiments were performed under the following operating conditions:

Particle size of the FT catalysts	: -10 +20 mesh
Particle size of the HZSM-5 catalyst	: -12 +24 mesh
H_2/CO ratio	: 1:1
WHSV	: 1.0 h^{-1}
FT reactor temperature	: 250°C
HZSM-5 reactor temperature	: 350°C, 375°C and 400°C
Pressure	: 0.101 MPa, 1 MPa and 2 MPa (1 atm. = 0.101 MPa)
FT/HZSM-5 ratio	: 1:1, 1:2.5 and 1:4

(vi) General Comments on Product Distribution Versus Time-On-Stream Behavior

The variation of the product distribution was studied under various operating conditions with time on stream. These results are reported later in this report. In general, it was observed that in order to obtain a true steady state, often long periods (about 10 - 30 hours) were required, particularly for atmospheric pressure operation. However, the induction periods were found to be much shorter (about 5 - 6 hours) under the conditions of higher pressures and higher ZSM-5 reactor temperatures. In order to compare the product distribution, a time-on-stream period of 5 - 8 hours was used. This was found to be adequate for all practical purposes. Any small drift in the product distribution at longer periods can be reasonably ignored keeping in view the accuracy of our GC analytical system which is known to be about $\pm$10%. In fact, several previous investigators (23,24) have allowed similar or even shorter periods of time-on-stream for the comparison of product distribution (in some studies time required to achieve the steady state has not even been reported).

RESULTS AND DISCUSSION

The FT catalysts were found to have insufficient mechanical strength for high pressure operation. This was a completely unexpected behavior and required an intensive effort to overcome this problem. It almost took 5 - 6 weeks to find a solution to this problem. In order to facilitate operation at high pressures, the mechanical strength of the FT catalyst had to be increased. Methods used to increase the mechanical strength of the FT catalyst are given in Appendix B.

Preliminary high pressure studies in the dual-bed 13 mm (1/2 in.) reactor showed that the hydrocarbon product contained mainly methane with small amounts of C_5^+ hydrocarbons and no aromatics. A detailed study had to be carried out with FT catalyst alone as well as with FT + HZSM-5 combination in order to clarify why mainly methane was produced at high pressure operation. These results are discussed in Appendix C.

(i) Testing of FT-HZSM-5 Catalyst in the Dual-Packed Bed Reactor System

I. Catalyst Combination: 10% Co/base (first reactor)
and HZSM-5 (second reactor)

Experiments were carried out for CO hydrogenation in the 1/2 inch dual-bed reactor arrangement for various HZSM-5/FT ratios and pressures. The HZSM-5 reactor temperature was varied from 350-400°C. Table 5 gives the operating conditions for the experiments using HZSM-5/FT=1. The results are reported in Tables 6 - 8 and are plotted in Figures 5 - 10.

Figure 5 shows that the selectivities of C_1-C_4 fractions increase with increase in the temperature of the HZSM-5 reactor at 0.101 MPa. However, the C_1-C_4 selectivities remain constant with temperature at 1 and 2 MPa. Figure 5 also shows that C_1-C_4 selectivities increase with increase in pressure. The total C_5^+ hydrocarbons (including aromatics) (Figure 6) decrease with increase in the temperature of the HZSM-5 reactor at 0.101 MPa. However, at 1 and 2 MPa, these selectivities

remained almost constant with temperature. Also, the C_5^+ hydrocarbon selectivity decreased with increase in pressure. At 0.101 MPa, as the temperature increases from 350 to 400°C, the C_1-C_4 hydrocarbons increase (see Figure 5) as a result of secondary cracking reactions. Thus, increasing the temperature in the range 350 - 400°C decreases the C_5^+ fraction (see Fig. 6). Derouane et al. (14) and Chang et al. (15) also reported that increasing the temperature from 300 - 400°C leads to a decrease in the C_5^+ hydrocarbons for methanol conversion reaction over HZSM-5.

Figure 7 shows that at 0.101 MPa, total aromatic hydrocarbon make slightly decreases with increase in the temperature of the HZSM-5 reactor and remains almost constant at zero at 1 and 2 MPa. Figure 7 also shows that aromatic hydrocarbon production decreases as the pressure increases. Figures 8 and 9 show that with increase in the temperature of the HZSM-5 reactor, the $C_2^=/C_2$ and $C_3^=/C_3$ fractions increase at 0.101 MPa, but remain constant at 1 and 2 MPa. As the pressure increases, the $C_2^=/C_2$ and $C_3^=/C_3$ fractions decrease (see Figures 8 and 9). By comparing Figures 8 and 9 at 0.101 MPa, it is seen that the decrease in the olefinicity of the C_3 fraction is much higher compared to that of the C_2 fraction. A large decrease in the olefinicity of C_3 fraction compared to the C_2 fraction suggests that propylene is more reactive compared to ethylene in the formation of aromatics. This conclusion is in agreement with the recent studies dealing with the conversion of the olefins over HZSM-5 (10, 11) indicating that, among the olefins, ethylene is the least reactive over HZSM-5. The isobutane selectivity decreases with increase in the temperature of the HZSM-5 reactor at 0.101 MPa and exhibits a slight maximum at 375°C at 1 and 2 MPa (see Figure 10). Figure 10 also shows that i-C_4 fraction increases with increase in pressure. The operating conditions and results for HZSM-5/FT ratio of 2.5 and 4 are reported in Tables 9 - 16 and are plotted in Figures 11 - 22. As seen, the trends observed are similar to those discussed above for HZSM-5/FT ratio of 1, although the magnitude of various fractions differs due to the increased amount of HZSM-5.

As discussed in Appendix C, Ni/ZrO_2 (the base catalyst) catalyst shows unusual activity and selectivity in the Fischer-Tropsch reaction at atmospheric pressure (6, 12). Whereas nickel on most common supports is a methanation catalyst (13), with zirconia (at atmospheric pressure) the selectivity shifts to higher hydrocarbons with a high proportion of olefins in the product (6, 12). As reported in Appendix C, at high pressure operation, the FT catalyst (10% Co/base) produces mainly lower hydrocarbons in the Fischer-Tropsch Synthesis. Bruce et al. (12) also reported that for the Ni/ZrO_2 (the base catalyst) the effect of increasing the pressure in the reactor (to 0.503 MPa) was to shift the whole product distribution toward the lower molecular weight hydrocarbons. Thus, at 1 and 2 MPa, mainly lower molecular weight hydrocarbons are produced over the FT catalyst with very little amounts of olefins. This may be the reason why little or no aromatic hydrocarbons were produced in the dual-bed reactor system at 1 and 2 MPa.

The effects of HZSM-5 reactor temperature on product distribution at 0.101 MPa are summarized as follows:

(i) The selctivity of C_1-C_4 fractions increases with increase in temperature in the range 350 - 400°C.

(ii) The total C_5^+ hydrocarbons decrease with increase in temperature.

(iii) Total aromatic hydrocarbon-make slightly decreases with increase in temperature.

(iv) $C_2^=/C_2$ and $C_3^=/C_3$ fractions increase while the isobutane selectivity decreases with increase in temperature of the HZSM-5 reactor.

The effects of HZSM-5 reactor temperature on product distribution at 1 and 2 MPa are summarized as follows:

(i) The whole product distribution is shifted to the lower molecular weight hydrocarbons at high pressures. The selectivity of C_1-C_4 fractions remains constant with increase in temperature.

(ii) The total C_5^+ hydrocarbon remains almost constant with increase in temperature of the HZSM-5 bed.

(iii) The aromatic hydrocarbon make is found to be almost zero.

(iv) The $C_2^=/C_2$ and $C_3^=/C_3$ fractions remain constant with temperature at 1 and 2 MPa while the isobutane selectivity exhibits a slight maximum at 375°C at 1 and 2 MPa.

Material Balance

Material balance runs were carried out over the 10% Co/base + HZSM-5 catalyst combination using the 1/2 inch dual-bed reactor system. These tests were carried out to fulfill the following objectives:

(i) To study the catalyst performance at higher conversion levels.

(ii) To make the overall material balance for the system operated for a long period of time.

(iii) To study the deactivation characteristics of the catalysts under the given operating conditions.

The experiments were run continuously for a period of 100 h at atmospheric pressure. The operating conditions are shown in Table 17. The products were condensed using two traps in series: (i) cooled with water and (ii) cooled with liquid N_2 + hexane mixture. The condensate collected from the cold water condenser was found to be mainly water, therefore, it was rejected. The condensate sample collected from liquid N_2 + hexane condenser was weighed and analyzed by GC/MS for product identification. The results are given in Table 17a. It shows that the condensate is a mixture of aliphatics and aromatics terminating at C_{14}. The aromatics are mainly methyl and ethyl substituted benzenes (see Table 17a).

The fresh and used catalyst samples were analyzed using a Leco Induction Furnace for the deposited carbon. The analyses are reported in Table 18. It is seen that fresh FT catalyst contains some carbon, which is mainly due to graphite (graphite is added as a binder to the FT catalyst in order to avoid the crumbling effect). The fresh HZSM-5 catalyst also contains a very small amount of carbon which is probably due the organic templates used in its manufacture.

Since the conversion and product distribution varied during the test run (time on stream = 100 h), the average values of the runs were calculated in order to make an overall material balance. The material balance is summarized in Figure 23.

The variations of CO conversion and hydrocarbon distribution with time on stream for the above set of experiments are given in Table 19 and are plotted in Figure 24 - 27. As shown in Figure 24, the CO conversion declines with time on stream and the major decline takes place during the initial stages of the operation. This decline in CO conversion is essentially due to the slow deactivation of the FT catalyst caused by the carbonaceous deposit formed as a result of dissociation of CO on the FT catalyst surface and grows with time on stream. This inactive overlayer reduces the sites available for CO dissociation and, therefore, the conversion declines. Figure 25 shows the variations of hydrocarbon selectivity with time on stream. As seen from Figure 25, the methane selectivity slightly decreases during the initial stages. However, there is a slight increase in the methane selectivity after about 60 h with time on stream. These results indicate that the deactivation of the FT catalyst not only causes a decline in CO conversion, but also promotes the formation of methane. Higher methane selectivity for the deactivated catalyst has also been reported in the literature. Figure 25 also shows that a sharp increase in the selectivity of C_5^+ fraction with a simultaneous drop in the selectivity of C_2-C_4 fraction is observed during the first 6 h of time on stream. This is attributed to various cracking and aromatization reactions taking place over HZSM-5. After 6 h, there is little variation in the C_2-C_4 and C_5^+ selectivities.

As seen from Figure 26, the C_5^+ (aliphatics) fraction varies very little with time on stream while the total aromatics fraction shows a dramatic increase during the initial periods of operation and then remains constant with time on stream. The amount of aromatics formation was low initially, but increased rapidly with time on stream. This is analogous to that reported for conversion of methanol to hydrocarbons. Ono (16) reported time-on-stream behaviour of methanol conversion in a close-circulation system at 239°C over HZSM-5. The reaction was very slow for the first 3 h, and then the hydrocarbon yield increased sharply 4 - 5 h after starting the reaction, giving an induction period of about 10 h at 219°C. The duration of the induction periods can be greatly shortened by the addition of olefins or olefins precursors, such as alcohols. This is attributed to the autocatalytic character of the reaction (17). Since there is no significant decline in the aromatic selectivity (see Figure 26) with increased aging of the catalyst over the total 100 h test period, it indicates that the rate of coke deposition over the zeolite component is low. This is in accordance with the deactivation characteristics of the intermediate pore zeolites such as HZSM-5. The carbon formation in HZSM-5 zeolites has been shown to be a shape-selective reaction (18).

Figure 27 gives the fractions of ethylene in $C_2(C_2^=/C_2)$ and propylene in $C_3(C_3^=/C_3)$ and isobutane in $C_4(i\text{-}C_4/C_4)$ as a function of time on stream. The C_2 and C_3 fractions initially increase up to about 50 h and then remain constant with time-on-stream. The $i\text{-}C_4/C_4$ ratio remains almost constant with time-on-stream.

II. Catalyst Combination: 2% Ni-5% Co/base (first reactor)
and HZSM-5 (second reactor)

Further experiments were carried out with 2% Ni-5% Co/base + HZSM-5 catalyst combination for various HZSM-5/FT ratios and pressures, and the HZSM-5 reactor temperature was varied from 350 - 400°C. Table 20 gives the operating conditions for HZSM-5/FT=1, and the results are reported in Tables 21 - 23 and are plotted in Figures 28 - 33.

Figure 28 shows that the selectivities of C_1-C_4 fractions increase, with increase in temperature of the HZSM-5 reactor at 0.101 and 2 MPa. However, there is a slight drop in C_1-C_4 selectivity with temperature at 1 MPa. Figure 28 also shows that C_1-C_4 selectivity increases with increase in pressure. The total C_5^+ hydrocarbons (Figure 29) decrease with increase in the temperature of the HZSM-5 bed at 0.101 and 2 MPa. The C_5^+ hydrocarbon selectivity also decreases with increase in pressure. As mentioned earlier, as the temperature increases from 350 - 400°C, C_1-C_4 hydrocarbons begin to rise (see Figure 28) as a result of the secondary cracking reactions. These results indicate that increasing the temperature of the HZSM-5 bed (in the range 350 - 400°C) decreases the C_5^+ fraction.

Figure 30 shows that at 0.101 MPa, total aromatic hydrocarbon make remains almost constant with increase in temperature of the HZSM-5 reactor and is almost zero at 1 and 2 MPa. At higher pressures, the aromatic hydrocarbon production was found to be zero. Figures 31 and 32 show that with increase in the temperature of the HZSM-5 reactor, the $C_2^=/C_2$ and $C_3^=/C_3$ fractions increase at 0.101 MPa and remain constant with temperature at 1 and 2 MPa. As the pressure increases, the $C_2^=/C_2$ and $C_3^=/C_3$ fractions decrease (see Figures 31 and 32). The isobutane selectivity decreases with increase in temperature of the HZSM-5 reactor for 0.101 MPa and remains almost constant at 1 and 2 MPa (see Figure 33). Figure 33 also shows that the i-C_4 fraction increases with the increase in pressure. Approximately similar trends were observed for similar experiments with HZSM-5/FT ratio of 2.5 and 4, although the magnitude of various fractions differs due to the increased amount of HZSM-5. The operating conditions and results for HZSM-5/FT ratio of 2.5 and 4 are reported in Tables 24 - 31 and are plotted in Figures 34 - 45.

As mentioned earlier, for FT catalyst alone, the effect of increasing the pressure in the reactor was to shift the whole product distribution toward the lower molecular weight hydrocarbons. Thus, at 1 and 2 MPa, mainly low molecular weight hydrocarbons with small amounts of olefins were obtained. It may be the reason why little or no aromatic hydrocarbons are formed in the dual-bed reactor system at 1 and 2 MPa.

The effects of HZSM-5 reactor temperature on product distribution at 0.101 MPa are summarized as follows:

(i) The selectivity of C_1-C_4 fractions increases with increase in temperature of the HZSM-5 reactor in the range 350 - 400°C.

(ii) The total C_5^+ hydrocarbons decrease with increase in temperature of the HZSM-5 bed.

(iii) Total aromatic hydrocarbons remain almost constant with increase in temperature.

(iv) $C_2^=/C_2$ and $C_3^=/C_3$ fractions increase while the isobutane selectivity decreases with increase in temperature of the HZSM-5 reactor.

The effects of HZSM-5 reactor temperature on product distribution at 1 and 2 MPa are summarized as follows:

(i) The whole product distribution is shifted to the lower molecular weight hydrocarbons. The selectivity of C_1-C_4 fractions remains almost constant with increase in temperature.

(ii) The total C_5^+ hydrocarbons decrease with increase in temperature of the HZSM-5 bed.

(iii) The aromatic hydrocarbon make is found to be almost zero.

(iv) The $C_2^=/C_2$ and $C_3^=/C_3$ fractions remain almost constant with temperature at 1 and 2 MPa while the isobutane selectivity slightly decreases with increase in temperature of HZSM-5 reactor.

Material Balance

Material balance runs were carried out over the 2% Ni-5% Co/base + HZSM-5 catalyst combination using the 1/2 inch dual-bed reactor system. The experiments were run continuously for a period of 100 h at atmos-

pheric pressure. The operating conditions are shown in Table 32. The products were condensed using LN_2 + Hexane trap. The condensate sample collected from the condenser was weighed and analyzed. The condensate was analysed using GC/MS. It shows that the condensate is aromatic-containing mainly methyl and ethyl substituted benzene, terminating at about A_{11} (see Table 32a). At the end of the experiment, fresh and used catalysts were analyzed for carbon content using Leco Induction Furnace. The analyses are given in Table 33. As seen in Table 33, fresh FT catalyst contains some carbon, which is mainly due to graphite (graphite is added as a binder to the FT catalyst in order to avoid the crumbling effect). The fresh HZSM-5 catalyst also contains some carbon which is due to its preparation with organic solutions. Since the conversion and product distribution varied during the test run (time-on-stream = 100 h), the average values of the runs were calculated in order to make an overall material balance. The material balance is summarized in Figure 46.

The variations of CO conversion and hydrocarbons distribution with time-on-stream for the above set of experiments are given in Table 34 and are plotted in Figure 47 - 50. As shown in Figure 47, the CO conversion declines with time-on-stream, and the major decline takes place during the initial stages of operation. This decline in CO is essentially due to the slow deactivation of the FT catalyst caused by the carbonaceous deposit formed as a result of the dissociation of CO on the FT catalyst surface which grows with time-on-stream. Figure 48 shows the variations of hydrocarbon selectivity with time-on-stream. As seen from Figure 48, during the initial stages, methane selectivity decreases. However, there is a slight increase in methane selectivity after about 30 h with time-on-stream. These results indicate that the deactivation of the FT catalyst not only causes a decline in CO conversion, but also promotes the formation of methane. Figure 48 also shows that a drop in the selectivity of the C_2-C_4 fraction with a simultaneous increase in the selectivity of the C_5^+ fraction is observed during the first 10 h of operation. This is attributed to various cracking and aromatization reactions taking place over HZSM-5 catalyst. After about 30 h, there is almost no variation in the C_2-C_4 and C_5^+ selectivi-

ties. Due to the presence of HZSM-5, the C_5^+ fraction contains both aliphatics and aromatics. The product analysis indicated the complete absence of hydrocarbons with carbon number > 11. This limited distribution results from the unique molecular shape selectivity of the zeolite HZSM-5 (18, 19).

As seen from Figure 49, the C_5^+ (aliphatics) fraction remains almost constant with time-on-stream while the total aromatics fraction shows a dramatic increase during the initial periods of operation and then remains constant with time-on-stream. The induction period for aromatic formation is about 6 - 8 h. This is analogous to that reported for conversion of methanol to hydrocarbons. Ono (16) found an induction period of about 10 h for the formation of hydrocarbons from methanol at 219°C over HZSM-5 zeolite in a recycle reactor. Langner (20) also found induction periods of more than 2 h for the reaction of methanol on the NaH-Y at 250°C. Varma et al. (21) also found that an induction period of 15 - 20 h exists for the formation of aromatics from syngas over the admixed cobalt-nickel-zirconia and HZSM-5 catalyst at 250°C. The duration of the induction period can be influenced by the addition of olefins like ethylene or cis-2-butene (16). This is attributed to the autocatalytic character of the reaction. The autocatalytic step is believed to involve mainly alkylation by reactive C_1 intermediate generated from oxygenates (17-19). Several reactions take place over HZSM-5 catalyst in sequence, which apparently cause the induction periods observed; these have already been discussed elsewhere (3, 18, 21). Since there is no significant decline in the aromatic selectivity with increased aging of the catalyst up to the total test period of 100 h, it indicates that the rate of coke deposition over the zeolite component is low. This is in accordance with the deactivation characteristics of intermediate pore zeolites such as HZSM-5. Coke formation and deactivation of the catalyst has been reported to be much faster in small pore and large pore zeolites. On the other hand, HZSM-5 has shown low tendency for coke formation (20). The carbon formation in zeolites has been shown to be a shape-selective reaction (18).

Figure 50 gives the fractions of ethylene in $C_2(C_2^=/C_2)$ and propylene in $C_3(C_3^=/C_3)$ and isobutane in $C_4(i\text{-}C_4/C_4)$ as a function of time-on-stream. The C_2 and C_3 fractions initially increase up to about 20 h and then remain constant with time-on-stream. The $i\text{-}C_4/C_4$ ratio remains constant with time-on-stream. Figure 50 also shows that the reduction in the olefinicity of the C_3 fraction is much higher compared to that in the C_2 fraction. This substantiates the conclusions by earlier workers that propylene is more reactive over HZSM-5 compared to ethylene (11).

On the basis of the above presented results, a comparison can be made between the performances of the two FT catalysts (viz. 10% Co/base and 2% Ni-5% Co/base catalysts) when combined with HZSM-5 in a dual-bed reactor. These results indicate that although there are minor differences in the product distributions obtained; however, in general, the trends and conclusions drawn from the results for these two catalysts are almost similar.

(ii) Regeneration Characteristics of the FT Catalyst

It is important to know whether the FT catalyst can be regenerated after use. Measurements of CO/H_2 conversion activity and product selectivity were performed at atmospheric pressure in a newly constructed high pressure microreactor in order to study the regeneration characteristics of the FT catalyst (10% Co/base). The schematic diagram of the microreactor system is shown in Figure 51.

Fresh FT catalyst was reduced under flowing hydrogen (flow rate = 15 mL/min) at 450°C for 16 h before the activity measurements. The catalyst bed temperature was lowered to the reaction temperature under flowing hydrogen before introducing the pre-mixed feed gas. The product distributions were recorded with time-on-stream under the fixed operating conditions. The operating conditins are given in Table 35. The reaction products were analyzed by on-line gas chromatography.

At the end of the fresh catalyst cycle (after about 30 h time-on-stream), the catalyst was regenerated for 16 h in flowing H_2 (flow rate of H_2 = 15 mL/min) at 425°C, a method originally suggested by Sinfelt (1968). After regeneration, the hydrogen flow was stopped and the reaction was carried out (1st cycle). Similarly, 2nd and 3rd cycle experiments were performed. The results are reported in Table 36 and are plotted in Figures 52 - 55. As shown in Figure 52, CO conversion declines with time-on-stream and the major decline takes place during the initial stages of operation. This decline in CO conversion is essentially due to the slow deactivaion of the FT catalyst caused by the carbonaceous deposit formed as a result of dissociation of CO on the FT catalyst surface which grows with time-on-stream. This inactive overlayer reduces the sites available for CO dissociation and therefore the conversion declines. Figure 53 shows the C_5^+ hydrocarbons remain constant with time-on-stream for all the cycles. Figures 54 and 55 show that the olefin selectivity increases with time-on-stream. As seen from figures 54 and 55, the olefinicity of the C_2 fraction is much lower than the C_3 fraction. This is in good agreement with the CO hydrogenation reaction over FT catalyst where ethylene is known to be more reactive compared to propylene (22). As seen from Figures 52 - 55, the catalyst could be regenerated fully; i.e., the activity of the catalyst approaches its initial activity even after three regenerations.

SUMMARY AND CONCLUSIONS

Synthesis gas conversion reaction was carried out at atmospheric and high pressure using 1/2 inch i.d. dual-bed reactor system. Two Fischer-Tropsch (FT) catalysts (10% Co/base and 2% Ni-5% Co/base) were prepared and characterized by TPR, BET surface area, atomic absorption, etc. ZSM-5 zeolite catalyst was prepared and characterized by BET surface area, atomic absorption, x-ray diffraction and constraint index determination.

Both the FT catalysts were tested for activity and product selectivity for CO hydrogenation combined with HZSM-5 catalyst in the dual-bed reactor for various HZSM-5/FT ratios and pressures. The temperature of the FT

catalyst was fixed at 250°C while the HZSM-5 reactor temperature was varied from 350 - 400°C. A summary of experimental runs including the ranges of operating conditions and analyses of typical runs is presented in Table 37.

I. Catalyst Combination: 10% Co/base and HZSM-5

The effect of increasing the pressure in the reactor (0.101 MPa to 2 MPa) was to shift the whole product distribution toward the lower molecular weight hydrocarbons with very small proportion of olefins in the product. Also at high pressure operation, the aromatic hydrocarbon make was found to be zero.

The major conclusions of the effect of HZSM-5 reactor temperature on product distribution at 0.101 MPa are as follows:

1. The total C_5^+ hydrocarbons decrease with increase in temperature.

2. Total aromatic hydrocarbon make slightly decreases with increase in temperature.

3. $C_2^=/C_2$ and $C_3^=/C_3$ fractions increase while the isobutane selectivity decreases with increase in temperature of the HZSM-5 reactor.

4. The selectivity of C_1-C_4 fractions increases with increase in temperature in the range 350 - 400°C.

II. Catalyst Combination: 2% Ni-5% Co/base and HZSM-5

Similar to 10% Co/base and HZSM-5 catalyst combination, the effect of increasing the pressure in the reactor was to shift the whole product distribution toward the lower molecular weight hydrocarbons. At high pressure, the aromatic hydrocarbon make was found to be almost zero.

The major conclusions of the effect of HZSM-5 reactor temperature on product distributions at 0.101 MPa are as follows:

1. The total C_5^+ hydrocarbons decrease with increase in temperature of the HZSM-5 bed.

2. Total aromatic hydrocarbons remain almost constant with increase in temperature.

3. In general, the $C_2^=/C_2$ and $C_3^=/C_3$ fractions increase while the isobutane selectivity decreases with increase in temperature of the HZSM-5 reactor. However, at HZSM-5/FT=4, the $C_2^=/C_2$ and $C_3^=/C_3$ fractions were found to decrease with increase in temperature of HZSM-5 reactor.

4. The selectivity of C_1-C_4 fractions increases with increase in temperature of the HZSM-5 reactor in the range 350 - 400°C.

At this point, we do not understand the behavior of the product distributions at high pressure operation. Bruce et al. (12) have also reported that for the Ni/ZrO_2 catalyst (the base catalyst), the effect of increasing the pressure to 0.503 MPa was to shift the product distribution toward the lower molecular weight hydrocarbons. It may be possible that this behavior is observed due to the increased temperature within the catalyst pores caused by the increased reaction rates at high pressures. However, more work needs to be done to clarify this situation.

REFERENCES

1. Chang, C.D., W.H. Lang and A.J. Silvestri, "Synthesis Gas Conversion to Aromatic Hydrocarbons", J. Catal. 56, 268-273 (1979).

2. Caesar, P.D., J.A. Brennan, W.E. Garwood and J. Ciric, "Advances in Fischer-Tropsch Chemistry", J. Catal. 56, 274-278 (1979).

3. Bruce, L.A., G.J. Hope and J.F. Mathews, "Conversion of Synthesis Gas to Aromatic-Containing Hydrocarbons under Mild Conditions", Appl. Catal. 9, 351-359 (1984).

4. Pennline, H.W., R.J. Gormley and R.R. Schehl, "Process Studies with a Promoted Transition Metal-Zeolite Catalyst", Ind. Eng. Chem. Prod. Res. Dev. 23, 388-393 (1984).

5. Shamsi, A., U.S. Rao, R.J. Gormley, R.T. Obermyer, R.R. Schehl and J.M. Stencel, "Zeolite-Supported Cobalt Catalysts for the Conversion of Synthesis Gas to Hydrocarbon Products", Ind. Eng. Chem. Prod. Res. Dev. 23, 513-519 (1984).

6. Varma, R.L., N.N. Bakhshi, J.F. Mathews and S.H. Ng, "Performance of Combined Cobalt-Nickel-Zirconia and HZSM-5 Catalyst Systems for Carbon Monoxide Hydrogenation", Can. J. Chem. Eng. 63, 612-617 (1985).

7. Henrici-Olive, G. and S. Olive, "The Fischer-Tropsch Synthesis: Molecular Weight Distribution of Primary Products and Reaction Mechanism", Angew. Chem. Int. Ed. Engl. 15, 136-141 (1976).

8. Haag, W.O. and T.J. Huang, "Conversion of Synthesis Gas to Hydrocarbon Mixtures Utilizing Dual Reactors", U.S. Patent 4,279, 830 (1981).

9. Varma, R.L., J.F. Mathews and N.N. Bakhshi, "Characterization of Manganese Oxide-Supported Metal Catalysts by Temperature-Programmed Reduction" in "Frontiers in Chemical Reaction Engineering", L.K. Doraiswamy and R.A. Mashelkar-Editors, Vol. II, pp. 118-128, Wiley Eastern Limited, New Delhi, (1984).

10. Anderson, J.R., K. Foger, F.A. Rajadhyaksha and J.V. Sanders, "Reactions on ZSM-5 Type Zeolite Catalysts", J. Catal. 58, 114-130 (1979).

11. Garwood, W.E., "Conversion of C_2-C_{10} to Higher Olefins over Synthetic Zeolite ZSM-5", ACS Symp. Series 218, 383-396 (1983).

12. Bruce, L. and J.F. Mathews, "The Fischer-Tropsch Activity of Nickel-Zirconia", Appl. Catal. 4, 353-370 (1982).

13. Vannice, M.A., "The Catalytic Synthesis of Hydrocarbons from Carbon Monoxide and Hydrogen", Catal. Rev.-Sci. Eng. 14,(2), 153-191 (1976).

14. Derouane, E.G., J.B. Nagy, P. Dejaifve, J.H.C. Van Hoof, B.P. Spekman, J.C. Vedrine and C. Naccache, "Elucidation of the Mechanism of Conversion of Methanol and Ethanol to Hydrocarbons on a New Type of Synthetic Zeolites", J. Catal. 53, 40-55 (1978).

15. Chang, C.D., J.C.W. Kuo, W.H. Lang, S.M. Jacob, J.J. Wise and A.J. Silvestri, "Process Studies on the Conversion of Methanol to Gasoline", Ind. Eng. Chem. Process Des. Dev. 17, 255-260 (1978).

16. Ono, Y., "Role of Basic Sites in Catalysis by Zeolites" in "Catalysis by Zeolites", (Eds. B. Imelik et al.), Elsevier, Vol. 5, p. 19-27, Amsterdam, 1980.

17. Chen, N.Y. and W.J. Reagan, "Evidence of Autocatalysis in Methanol to Hydrocarbon Reactions over Zeolite Catalysts", J. Catal. 59, 123-129 (1979).

18. Chang, C.D., "Hydrocarbons from Methanol", Catal. Rev.-Sci. Eng. 25, 1-118 (1983).

19. Chang, C.D., "Methanol Conversion to Light Olefins", Catal. Rev.-Sci. Eng. 6, 323-345 (1984).

20. Langner, B.E., "Reactions of Methanol on Zeolites with Different Pore Structures", Appl. Catal. 2, 289-302 (1982).

21. Varma, R.L., K. Jothimurugesan, N.N. Bakhshi, J.F. Mathews and S.H. Ng, "Direct Conversion of Synthesis Gas to Aromatic Hydrocarbons: Variation of Product Distribution with Time-On-Stream", Can. J. Chem. Eng. 64, 141-148 (1986).

22. Rautavouma, A.O.I. and H.S. Van Der Baan, "Kinetics and Mechanism of the Fischer-Tropsch Hydrocarbon Synthesis on a Cobalt on Alumina Catalyst", Appl. Catal. 1, 247-272 (1981).

23. Yashima, T., A. Yoshimura, Y. Wakushima and S. Namba, "Hydrocarbon Synthesis from Syngas on Zn-Cr/HZSM-5 Catalyst", Pan-Pacific Synfuels Conference, Nov. 17-19, 1982, Tokyo, pp. 130-136.

24. Chen. Y.W., H.T. Wang and J.G. Goodwin, Jr., J. Catal. 83, 415 (1983).

APPENDIX A

Reference: Preparation of Zeolites by Chen et al., U.S. Pat. 4,112,056 (1973)

Preparation of HZSM-5

A. Materials required:

(i) Sodium Aluminate
(ii) Sodium Hydroxide Pellets
(iii) Sodium Silicate Solution, Tech. (Fischer Scientific)
(iv) Tetrapropylammonium Bromide (Aldrich)
(v) Sulfuric Acid (98%)
(vi) Sodium Chloride
(vii) Hydrochloric Acid

B. Equipment required:

(i) 3-L Round Bottom Flask
(ii) Condenser
(iii) Magnetic Stirrer
(iv) Electric Heater
(v) Waring Blender
(vi) 4-L Beaker
(vii) 18 cm dia. Buckner Funnel
(viii) 2-L Filtering Flask
(ix) Waterman Filtering Paper
(x) Variac

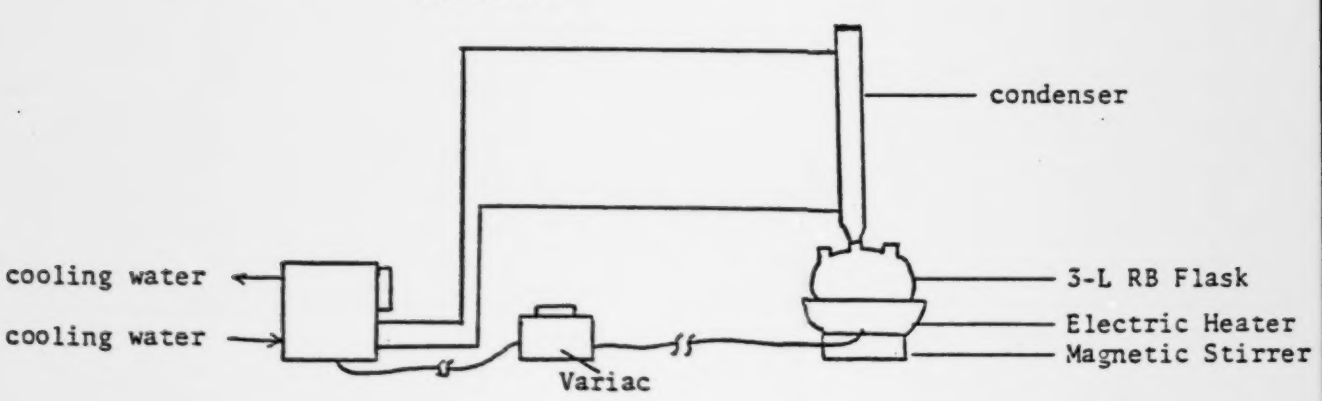

C. Experimental Procedure:

1. The initial step in producing HZSM-5 is the preparation of the following solutions:

Solution A:
- 2.5 gm Sodium Aluminate
- 0.17 gm Sodiam Hydroxide
- 66.0 gm Distilled water

Solution B:
- 211.2 gms Sodium Silicate
- 2.64 gms Distilled water

Solution C: - 26.4 gms Tetrapropylammonium Bromide
- 132.0 gms Distilled water

Solution D: - 21.0 gms Sulfuric Acid
- 66.0 gms Distilled water

Solution E: - 79.2 gms Sodium Chloride
- 95.0 gms Distilled water

2. Solutions B, C, D and E are combined and mixed in a waring blender for approximately 10 minutes.

3. The mixture is then placed in a 3-L round bottom flask and was heated to 100°C with a magnetic stirring providing agitation.

4. 10% of solution A is added initially.

5. The resulting mixture is maintained at a temperature of 100°C and refluxed for a 240 h period.

6. Solution A is added to the heated mixture in the following sequence:

   - 10% of solutions A for the first three days
   - 57% of remaining solution A is added for each succeeding day after three days.

7. After refluxing for 10 days, the mixture is cooled to room temperature and then filtered through fast qualitative filter paper under vacuum.

8. The crystals are then washed three times with hot distilled water and then dried at 110°C.

9. The crystals are then put in a muffle furnace at 550°C for 16 h to remove organic molecules.

10. The crystals are then reflexed for 24 h in 2.0 L of 0.5 M HCl to ion exchange impurities in the crystal and to set sodium in crystal.

11. The crystals are then filtered and washed as before (steps 7 - 8).

12. The crystals are then dried in air at 110°C and finally in a muffle furnace at 400°C for 4 h.

APPENDIX B

A problem was encountered when operating the dual-bed reactor system at high pressures. A few experiments were conducted at high pressures. The synthesis gas was passed through the first reactor containing the FT catalyst, and the resulting product mixture was fed to the second reactor containing HZSM-5 catalyst. The effluent from the HZSM-5 reactor was directly passed through the GC System for product analysis. The first sample for product analysis was taken after about 1 h of operation. The product analysis showed that the hydrocarbon product contains mainly methane. After about 3 h of operation, it was found that there was no flow through the system. The reactors were then opened and it was found that the FT catalyst was reduced to powder. The initial catalyst particle size was -12 +24 mesh. Further, this powder was found to be compressed into a plug, thus resulting in the plugging of the FT reactor. Thus, the 10% Co/base (FT) catalyst was found to have insufficient mechanical strength for high pressure operation.

In order to facilitate operation at high pressuers, the mechanical strength of the FT catalyst had to be increased. Two methods of increasing the mechanical strength were examined:

(i) Higher calcination temperature (800°C)
(ii) Binders (i.e., Magnesium stearate, stearic acid, graphite, etc.)

We first examined the effect of the calcination temperature on the mechanical strength of the FT catalyst. A 5 g sample of 10% Co/base was prepared and then calcined for 16 h at 800°C in a muffle furnace. The catalyst strength was found to be greatly improved. The activity of the catalyst was tested in the 1/2 inch dual-bed reactor system. The operating conditions are shown in Table B1. Table B2 shows the product distribution as a function of time-on-stream for 0.101 MPa and 2 MPa pressures (0 and 280 psig). As seen in Table B2, the C_5^+ fraction and total aromatics increase up to 6 h of operation and then decrease with time-on-stream at 0.101 MPa (0 psig). The $C_2^=/C_2$, $C_3^=/C_3$ and $i\text{-}C_4/C_4$ fractions increases while the CO conversion decreases with time-on-stream at 0.101 MPa (0 psig). Runs 55 and 56 (Table B2) show the product distribution at 2 MPa (280 psig). As seen in

Table B2, no aromatics were produced at 2 MPa (280 psig). After about 2.5 h of operation, the FT reactor was found to be plugged for the same reason as mentioned earlier.

Since the higher calcination temperature did not improve the mechanical strength of the FT catalyst, the effect of binders on the mechanical strength of the FT catalyst was examined next.

To increase the mechanical strength of the FT catalyst, various binders were physically mixed with the powdered 10% Co/base catalyst (calcined at 500°C) and then pelletized in a tableting machine at 5,000 psig. The pellets were then crushed to a particle size of -12 +24 mesh. The binders were examined and their effect on the catalyst strength is given qualitatively in Table B3.

Then, a 5 g batch of 10% Co/base (FT catalyst calcined at 500°C) was physically mixed with 1% magnesium stearate, pelletized at 5,000 psig and finally crushed to a particle size of -10 +24 mesh. The activity of this FT catalyst was then checked in the 1/2 inch dual-bed reactor for CO hydrogenation at 2.1 MPa (290 psig). During the time-on-stream runs, the flow rate of syngas was not steady (i.e., the flow rate of syngas slowly decreased with time) and after about 3.5 h of operation, it was found that there was no flow through the system. We then opened the FT reactor and found that almost 60% of the FT catalyst was reduced to powder form.

Next, a 5 g batch of 10% Co/base (FT catalyst calcined at 500°C) was mixed with 2% stearic acid, pelletized at 5,000 psig and finally crushed to a particle size of -10 +20 mesh. The activity of this catalyst was checked for CO hydrogenation in the 1/2 inch dual-bed reactor system. The operating conditions are shown in Table B4. Table B5 shows the product distribution as a function of time-on-stream at 0.101 and 2.1 MPa (0 and 290 psig). CO conversion decreases, while the C_5^+ fraction, total aromatics, $C_2^=/C_2$, $C_3^=/C_3$ and $i\text{-}C_4/C_4$ fractions increases with time-on-stream at 0.101 MPa (0 psig). The trend is exactly the same as found in previous studies. Run 70 - 73 (Table B5) shows the product distribution at 2.1 MPa (290 psig). During these runs, the flow rate of syngas was not steady. The product analysis

showed that (see Table B5) the hydrocarbon product contains mainly methane and small amounts of C_5^+ hydrocarbons and aromatics. We then opened the reactor and found that almost 40% of the FT catalyst had been reduced to powder.

Further work was carried out by adding graphite powder to the FT catalyst. A.B. Stiles (Catalyst Manufacture, Marcl Dekker, Inc., New York, 1983) has reported that graphite is one of the most effective binders in producing the hard pellets.

To increase the mechanical strength of the FT catalyst, a 5 g sample of 10% Co/base was mixed with 1.5% graphite, pelletized at 2,000 psig and finally crushed to a particle size of -10 +20 mesh. The activity of the catalyst was checked in the 1/2 inch dual-bed reactor system. The operating conditions are shown in Table B6. Table B7 shows the product distribution as a function of time-on-stream at 0 and 290 psig. As seen in Table B7 at 0.101 MPa (0 psig) (runs 80 - 83), C_5^+ fraction, total aromatics, $C_2^=/C_2$, $C_3^=/C_3$ and $i\text{-}C_4/C_4$ fractions increase while the CO conversion decreases with time-on-stream. This trend is similar to what was observed previously. Runs 84 - 86 (Table B7) show the product distribution at 2.1 MPa (290 psig). The product analysis showed that the hydrocarbon product contained mainly methane (73-80%), small amounts of C_5^+ hydrocarbons and no aromatics. During these runs, the flow rate of syngas was steady. At the end of the run, we opened the FT reactor and found that the FT catalyst had not been crushed at all.

Since large concentration of graphite binder in the catalyst may be detrimental to the catalyst activity, we decided to reduce the graphite content. A 5 g sample of 10% Co/base was then mixed with 1% graphite + 1% stearic acid and tested in the reactor. The FT catalyst had not been crushed at all.

All the runs in Task 3 were carried out by mixing the FT catalyst (calcined at 500°C) with 1% graphite + 1% stearic acid, pelletized at 2,000 psig and finally crushed to a particle size of -10 +20 mesh size.

Table B1. Operating Conditions (Runs 51-56)

HZSM-5/FT	:	4
FT Catalyst	:	10% Co/base (Calcined at 800°C for 16 h)
Wt of FT Catalyst	:	3.0030 g
Particle size of FT catalyst	:	-12+24 mesh
Wt. of HZSM-5	:	11.9990 g
Particle size of HZSM-5	:	-12+24 mesh
Feed Composition	:	47.5% CO, 47.5% H_2, 5% Ar
Temp. of FT Reactor	:	250°C
Temp. of HZSM-5 reactor	:	310°C
Pressure	:	0.101 MPa, 2 MPa (0, 280 psig)

Table B2. **Product Distribution as a Function of Time-on-Stream**

Run No.	51	52	53	54	55	56
WHSV, h^{-1}	0.18	0.18	0.18	0.18	1.3	0.62
Temp. of FT reactor, °C	250	250	250	250	250	250
Temp. of HZSM-5 reactor, °C	310	310	310	310	310	310
Time-on-stream, h	1	3	6	22	1	2
Pressure, MPa	0.101	0.101	0.101	0.101	2	2
CO conversion, %	17.1	15.5	14.2	13.1	10.0	10.1
Hydrocarbon Distribution, Wt %						
C_1	25.6	12.8	9.2	21.6	38.0	38.1
C_2	18.8	8.3	3.3	7.3	5.3	4.5
C_3	23.6	12.2	9.1	16.3	21.4	20.0
C_4	15.8	11.0	16.0	27.7	16.9	21.1
C_5^+ (incl. arom.)	16.2	55.7	62.4	27.1	18.4	16.3
A_6	0.0	5.8	5.3	0.0	0.0	0.0
A_7	0.0	19.2	19.3	8.0	0.0	0.0
A_8	0.0	0.0	12.6	6.2	0.0	0.0
A_9	0.0	0.0	0.0	0.6	0.0	0.0
Total Arom., wt%	0.0	25.0	37.2	14.8	0.0	0.0
$C_2^=$/Total C_2, wt%	13.6	16.5	15.3	20.2	0.0	0.0
$C_3^=$/Total C_3, wt%	5.1	5.5	6.0	12.6	0.0	0.0
iC_4/Total C_4, wt%	40.4	58.2	79.2	78.3	77.0	72.4

Table B3. 10% Co/base catalyst prepared with various binders

S. No.	FT Catalyst	Binders	Condition of catalyst
1	10% Co/base	1.5% Sodium aluminate	Soft
2	10% Co/base	1.5% Sodium silicate	Soft
3	10% Co/base	3% Aluminium nitrate	Soft
4	10% Co/base	4.5% Aluminum nitrate + 0.5% K_2CO_3	Soft

Table B4. Operating Conditions (Runs 66-73)

HZSM-5/FT	:	4
FT Catalyst	:	10% Co/base (Mixed with 2% stearic acid)
Wt of FT Catalyst	:	3.0019 g
Particle size of FT catalyst	:	-10+20 mesh
Wt. of HZSM-5	:	11.9990 g
Particle size of HZSM-5	:	-12+24 mesh
Feed Composition	:	47.5% CO, 47.5% H_2, 5% Ar
Temp. of FT Reactor	:	250°C
Temp. of HZSM-5 reactor	:	300°C
Pressure	:	0.101, 2.1 MPa (0, 290 psig)

Table B5. Product Distribution as a Function of Time-on-Stream

Run No.	66	67	68	69	70	71	72	73
WHSV, h^{-1}	0.16	0.16	0.16	0.16	0.63	0.70	1.7	0.5
Temp. of FT reactor, ^{o}C	250	250	250	250	250	250	250	250
Temp. of HZSM-5 reactor, ^{o}C	300	300	300	300	300	300	300	300
Time-on-stream, h	1	3	6	21	1	2	4.5	7.25
Pressure, MPa	0.101	0.101	0.101	2.1	2.1	2.1	2.1	2.1
CO conversion, %	44.2	35.9	35.6	30.1	76.2	77.2	68.8	55.7
Hydrocarbon Distribution, wt%								
C_1	29.3	20.0	22.5	14.0	90.9	90.1	77.1	67.7
C_2	6.4	4.3	4.3	2.7	2.4	2.4	5.4	8.0
C_3	24.3	20.8	18.7	18.9	2.9	4.1	9.2	15.9
C_4	31.0	28.1	25.2	31.7	2.5	2.3	4.6	5.2
C_5^+ (incl. arom.)	9.0	26.8	29.3	32.7	1.3	1.1	3.7	3.2
A_6	0.2	2.6	2.6	3.1	0.1	0.1	0.1	0.2
A_7	0.0	9.4	10.0	10.8	0.1	0.1	0.3	0.3
A_8	0.0	4.7	5.5	5.9	0.0	0.0	0.0	0.0
A_9	0.2	1.5	2.9	3.3	0.0	0.0	0.0	0.0
Total aromatics, wt%	0.4	18.2	21.0	23.1	0.2	0.2	0.4	0.5
$C_2^=$/Total C_2, wt%	3.4	6.6	7.0	11.0	0.0	0.0	1.8	0.4
$C_3^=$/Total C_3, wt%	1.0	1.1	1.6	1.4	0.0	0.0	18.0	2.8
i-C_4/Total C_4, wt%	69.9	71.3	72.9	76.4	60.1	62.8	20.1	48.0

Table B6. Operating Conditions (Runs 80-86)

HZSM-5/FT	:	4
FT Catalyst	:	10% Co/base (Mixed with 1.5% graphite)
Wt of FT Catalyst	:	3.0215 g
Particle size of FT catalyst	:	-10+20 mesh
Wt. of HZSM-5	:	11.9990 g
Particle size of HZSM-5	:	-12+24 mesh
Feed Composition	:	47.5% CO, 47.5% H_2, 5% Ar
Temp. of FT Reactor	:	250°C
Temp. of HZSM-5 reactor	:	300°C
Pressure	:	0.101, 2.1 MPa (0, 290 psig)

Table B7. Product Distribution as a Function of Time-on-Stream

Run No.	80	81	82	83	84	85	86
WHSV, h^{-1}	0.16	0.16	0.16	0.16	1.5	1.5	1.5
Temp. of FT reactor, °C	250	250	250	250	250	250	250
Temp. of HZSM-5 reactor, °C	300	300	300	300	300	300	300
Time-on-stream, h	1	3	5	8	2	4	6
Pressure, psig	0.101	0.101	0.101	0.101	2.1	2.1	2.1
CO conversion, %	39.6	36.5	35.9	34.3	67.9	76.3	62.3
Hydrocarbon Distribution, wt%							
C_1	24.4	22.1	22.2	22.1	75.1	80.1	73.0
C_2	6.0	5.2	4.9	4.6	6.5	4.6	6.7
C_3	25.5	21.7	20.5	18.3	8.8	9.2	14.0
C_4	30.9	27.6	26.2	25.3	7.3	4.4	4.8
C_5^+ (incl. Arom.)	13.2	23.4	26.2	29.7	2.3	1.7	1.5
A_6	0.3	2.3	2.1	2.2	0.0	0.0	0.0
A_7	0.0	9.1	8.9	9.5	0.0	0.0	0.0
A_8	0.2	0.4	3.8	5.9	0.0	0.0	0.0
A_9	1.2	0.8	1.0	2.0	0.0	0.0	0.0
Total Aromatics, wt%	1.7	12.6	15.8	19.6	0.0	0.0	0.0
$C_2^=$/Total C_2, wt%	4.4	5.7	6.5	7.3	0.0	0.0	0.0
$C_3^=$/Total C_3, wt%	1.2	1.4	1.6	2.0	0.0	0.0	0.0
iC_4/Total C_4, wt%	66.6	68.5	69.8	70.5	55.8	59.3	61.7

APPENDIX C

Preliminary studies of the dual-bed 1/2 inch reactor at high pressure showed that the hydrocarbon product contained mainly methane (70-80%), small amounts of C_5^+ hydrocarbons and no aromatics. A detailed study was carried out in order to clarify why mainly methane was produced at high pressure operation. In the first stage of this study, the activity of the FT catalyst only (10% Co/base) was checked three times for reproducibility in the 1/2 inch dual-bed reactor system at 0.101, 0.446, 0.788 and 2.1 MPa (0, 50, 100 and 290 psig). The operating conditions are shown in Table C1. The results of the product analysis for FT catalyst only are shown in Tables C2-C5 and plotted in Figures C1-C5.

As shown in Figure C1, the CO conversion slightly declines with time-on-stream for 0.101, 0.446 and 2.1 MPa (0, 50 and 290 psig). This decline in conversion is essentially due to the slow deactivation of the FT catalyst caused by the carbonaceous surface layer that forms from the dissociation of CO on the FT catalyst surface and grows with time-on-stream (5). This inactive overlayer reduces the sites available for CO dissociation and, therefore, the conversion declines. However, there is a sharp increase in CO conversion during initial hours of start-up at 0.788 MPa (100 psig) and which becomes constant with further time-on-stream. As the pressure increases from 0.101 to 0.788 MPa (0 to 100 psig), conversion increases. Further increase in pressure to 2.1 MPa (290 psig) resulted in a decrease in CO conversion. The C_5^+ hydrocarbons slightly increase with time-on-stream for all the pressures as seen from Figure C2. However, the C_5^+ hydrocarbons decrease with increase in pressure (see Figure C2). The $C_2^=/C_2$ and $C_3^=/C_3$ fractions increase with time-on-stream for 0.101, 0.446 and 0.788 MPa (0, 50 and 100 psig) and are almost zero at 2.1 MPa (290 psig) as seen from Figures C3 and C4. The $C_2^=/C_2$ and $C_3^=/C_3$ fractions decrease with increase in pressure (see Figures C3 and C4). As seen from Figures C3 and C4, the olefinicity of the C_2 fraction is much lower than that of the C_3 fraction over the FT catalyst. This is in good agreement with CO hydrogenation reaction over FT catalyst where ethylene is known to be more reactive compared to propylene (22). Figure C5 shows that isobutane fraction was zero for all the pressures.

Ni/ZrO_2 (the base catalyst) catalysts show unusual activity and selectivity in the Fischer-Tropsch reaction at atmospheric pressure, especially when prepared by co-precipitation method (6, 12). Whereas, nickel on most common supports is a methanation catalyst (13), with zirconia at atmospheric pressure the selectivity is moved to higher hydrocarbons, with a high proportion of olefins in the product (6, 12). From the above results, it appears that, at high pressure operation, cobalt-nickel-zirconia catalyst increases the hydrogenation activity and thus produces lower hydrocarbon in the Fischer-Tropsch synthesis. Bruce et al. (12) also reported that for the Ni/ZrO_2 (the base catalyst) catalysts, the effect of increasing the pressure in the reactor (to 0.503 MPa) was to shift the whole product distribution toward the lower molecular weight hydrocarbons.

The effects of pressure on the performance of FT catalyst only (10% Co/base) are summarized as follows:

1. As the pressure increases from 0.101 to 0.788 MPa (0 to 100 psig), the CO conversion increases. However, further increase in pressure results in a decrease in CO conversion.

2. C_5^+ hydrocarbons, $C_2^=/C_2$ and $C_3^=/C_3$ fractions decrease with increase in pressure.

3. The effect of increasing the pressure in the reactor from 0.101 MPa to 2.1 MPa (0 - 290 psig) was to shift the whole product distribution toward the lower molecular weight hydrocarbons as seen from Tables C2 - C5.

Next, experiments were carried out for FT + HZSM-5 catalysts in the 1/2 inch dual-bed reactor. The activity of the catalysts was checked three times for reproducibility. The operating conditions are shown in Table C6. The results of the FT + HZSM-5 experiments are shown in Tables C7 - C10 and plotted in Figures C6 - C11. As seen from Figure C6, as observed with FT catalyst alone, the CO conversion slightly decreases with time-on-stream for 0.101, 0.446 and 2.1 MPa (0, 50 and 290 psig). As has been mentioned earlier, this decline in CO conversion is essentially due to the slow deactivation of the FT component. Figure C6 also shows that, as the pressure

increases from 0.101 MPa to 0.446 MPa (0 - 50 psig), conversion increases. Further increase in pressure from 0.788 MPa to 2.1 MPa (from 100 - 290 psig) results in a decrease in conversion. As shown in Figure C7, the total C_5^+ hydrocarbons decreases with increase in pressure. Due to the presence of HZSM-5, the C_5^+ fraction contains both aliphatics and aromatics. Figure C8 shows that as the pressure increases from 0.446 - 2.1 MPa (50 - 290 psig), the production of the aromatic hydrocarbons becomes negligible. Figure C9 and C10 show that as the pressure increases from 0.446 - 2.1 MPa (50 - 290 psig), the $C_2^=/C_2$ and $C_3^=/C_3$ fractions also become negligible. Figure C11 shows that the isobutane fraction decreases with increase in pressure.

As has been mentioned earlier, the effect of increasing the pressure on the FT catalyst alone was to shift the whole product distribution toward the lower molecular weight hydrocarbons. Therefore, the HZSM-5 catalyst was not able to modify the product distribution at high pressure operation.

The effects of pressure on the performance of FT + HZSM-5 catalysts are summarized as follows:

1. As the pressure increases from 0 to 50 psig, the CO conversion increases. However, further increase in pressure results in a decrease in CO conversion.

2. C_5^+ hydrocarbons and aromatics hydrocarbons decrease with increase in pressure. Beyond 0.446 MPa (50 psig), the production of aromatic hydrocarbons was found to be negligible.

3. $C_2^=/C_2$, $C_3^=/C_3$ and $i\text{-}C_4/C_4$ fractions decrease with increase in pressure.

4. The effect of increasing the pressure in the reactor from 0.101 - 2.1 MPa (0 - 290 psig) was to shift the whole product distribution toward the lower molecular weight hydrocarbons as seen from Tables C7 - C10.

Table C1. Operating Conditions

FT Catalyst	:	10% Co/base (Mixed with 1% graphite & 1% stearic acdi)
Wt of FT Catalyst	:	3.0002 g
Particle size of FT catalyst	:	-10+20 mesh
Feed Composition	:	47.5% CO, 47.5% H_2, 5% Ar
Temp. of FT Reactor	:	250°C
WHSV	:	1.0 h^{-1}
Pressure	:	0, 50, 100, 290 psig (0.101, 0.446, 0.788, 2.1 MPa)

Table C2. Product Distribution as a Function of Time-on-Stream for FT Catalyst only at 0 psig (0.101 MPa)

Run No.	94	95	96	97	106	107	108	109	114	115	116	117
WHSV, h^{-1}	1.0	1.0	1.0	1.0	1.0	1.0	1.0	1.0	1.0	1.0	1.0	1.0
Temp. of FT Reactor, °C	250	250	250	250	250	250	250	250	250	250	250	250
Time-on-Stream, h	1	3	5	7	1	3	5	7	1	3	5	7
Pressure, psig	0	0	0	0	0	0	0	0	0	0	0	0
CO Conversion, %	15.4	14.9	14.8	14.0	14.4	14.1	13.0	12.8	13.9	12.9	13.1	12.6
Hydrocarbon Distribution, Wt. %												
C_1	17.1	17.7	17.9	18.4	19.7	18.1	17.8	18.9	18.7	19.3	19.5	19.3
C_2	4.2	4.1	4.0	4.0	4.4	3.8	3.7	3.9	4.1	3.9	4.1	3.9
C_3	9.5	8.9	8.7	8.7	10.0	8.5	8.9	8.5	9.6	8.3	8.1	8.5
C_4	9.0	8.1	6.5	6.6	8.8	7.6	5.5	5.2	8.7	7.8	6.7	6.1
C_5^+	60.2	61.2	62.9	62.3	57.1	62.0	64.1	63.5	58.9	60.7	61.6	62.2
$C_2^=$/Total C_2, wt%	65.3	67.3	67.4	69.8	62.5	71.1	71.6	71.0	64.3	70.8	71.5	69.6
$C_3^=$/Total C_3, wt%	89.9	91.6	95.0	100.0	95.0	91.8	89.6	100.0	88.4	100.0	100.0	92.1
i-C_4/Total C_4, wt%	0.0	0.0	0.0	0.0	0.0	0.0	0.0	0.0	0.0	0.0	0.0	0.0

Table C3. Product Distribution as a Function of Time-on-Stream for FT Catalyst Only at 50 Psig (0.446 MPa)

Run No.	118	119	120	121	122	123	124	125	126	127	128	129
WHSV, h^{-1}	1.1	1.0	1.0	0.9	1.1	1.0	1.0	0.9	1.0	0.9	1.0	1.0
Temp. of FT reactor, °C	250	250	250	250	250	250	250	250	250	250	250	250
Time-on-Stream, h	1	3	5	7	1	3	5	7	1	3	5	7
Pressure, Psig	50	50	50	50	50	50	50	50	50	50	50	50
CO Conversion, %	25.2	27.7	24.9	24.2	16.2	16.5	16.8	17.8	19.6	20.0	18.0	18.1
Hydrocarbon Distribution, Wt%												
C_1	26.4	21.3	18.9	15.8	26.6	20.0	17.8	17.8	26.1	19.2	17.7	17.3
C_2	8.4	6.7	5.8	4.8	9.6	7.2	6.4	6.4	9.1	6.6	5.8	5.9
C_3	20.0	16.6	14.3	12.7	21.1	16.2	15.0	15.1	21.9	16.1	14.1	14.0
C_4	15.5	14.4	11.5	13.1	13.8	12.7	12.8	12.9	18.3	13.8	12.4	12.4
C_5^+	29.7	41.0	49.5	53.6	28.9	43.9	48.0	47.8	24.6	44.3	50.0	50.4
$C_2^=$/Total C_2, Wt%	19.4	19.7	21.2	22.6	33.2	35.0	34.5	31.9	30.5	29.3	33.9	33.5
$C_3^=$/Total C_3, Wt%	69.2	68.5	72.7	73.2	83.3	81.4	81.7	81.7	76.9	78.9	80.8	81.3
i-C_4/Total C_4, Wt%	0.0	0.0	0.0	0.0	0.0	0.0	0.0	0.0	0.0	0.0	0.0	0.0

Table C4. Product Distribution as a Function of Time-on-Stream for FT Catalyst only at 100 Psig (0.788 MPa)

Run No.	142	143	144	145	146	147	148	149	151	152	153
WHSV, h^{-1}	1.0	0.9	0.9	1.0	1.0	1.0	0.9	1.0	1.1	1.1	1.1
Temp. of FT reactor, °C	250	250	250	250	250	250	250	250	250	250	250
Time-on-Stream, h	1	3	5	7	1	3	5	7	3	5	7
Pressure, Psig	100	100	100	100	100	100	100	100	100	100	100
CO Conversion, %	13.7	22.5	23.3	22.6	11.1	20.7	20.0	20.2	15.5	15.4	15.4
Hydrocarbon Distribution, Wt%											
C_1	34.7	27.5	24.3	22.0	43.0	30.4	25.6	23.3	32.5	27.4	25.7
C_2	10.9	10.1	9.0	8.0	8.7	11.4	9.5	8.3	12.7	10.5	9.5
C_3	24.2	22.5	21.2	18.7	14.2	24.0	21.0	18.0	22.9	19.7	17.8
C_4	6.1	14.3	15.9	15.8	9.2	15.6	16.2	14.9	14.9	15.1	13.6
C_5^+	24.1	25.6	29.6	35.5	24.9	18.6	27.7	35.5	17.0	27.3	33.4
$C_2^=$/Total C_2, Wt%	41.5	18.7	19.2	20.5	68.7	23.2	22.4	23.2	27.9	26.2	24.1
$C_3^=$/Total C_3, Wt%	77.0	70.1	70.3	70.9	70.0	70.1	70.8	71.8	73.0	73.0	73.1
i-C_4/Total C_4, Wt%	0.0	0.0	0.0	0.0	0.0	0.0	0.0	0.0	0.0	0.0	0.0

Table C5. Product Distribution as a Function of Time-on-Stream for FT catalyst only at 290 Psig (2.1 MPa)

Run No.	182	183	184	185	186	187	188	189	190	191	192	193
WHSV, h^{-1}	1.0	1.2	1.2	1.2	1.0	1.0	0.9	0.9	1.0	1.0	1.0	1.0
Temp. of FT reactor, °C	250	250	250	250	250	250	250	250	250	250	250	250
Time-on-Stream, h	1	3	5	7	1	3	5	7	1	3	5	7
Pressure, Psig	290	290	290	290	290	290	290	290	290	290	290	290
CO Conversion, %	10.2	10.1	9.5	10.7	9.7	10.3	10.9	10.1	9.7	9.7	9.9	11.0
Hydrocarbon Distribution, Wt%												
C_1	64.3	89.4	87.8	76.5	80.4	80.1	72.9	70.4	72.4	71.7	71.2	73.0
C_2	11.4	0.0	0.0	2.3	2.0	1.8	3.4	5.4	4.3	0.0	0.0	1.8
C_3	9.3	0.0	0.0	2.6	5.8	5.0	8.6	12.2	9.2	0.0	0.0	0.0
C_4	8.3	0.0	0.0	0.0	0.0	0.0	4.8	0.0	0.0	0.0	0.0	0.0
C_5^+	6.7	10.6	12.2	18.6	11.8	13.1	10.3	12.0	14.1	28.3	28.8	25.2
$C_2^=$/Total C_2, Wt%	0.0	0.0	0.0	0.0	0.0	0.0	0.0	0.0	0.0	0.0	0.0	0.0
$C_3^=$/Total C_3, Wt%	0.0	0.0	0.0	0.0	0.0	0.0	0.0	0.0	0.0	0.0	0.0	0.0
i-C_4/Total C_4, Wt%	0.0	0.0	0.0	0.0	0.0	0.0	0.0	0.0	0.0	0.0	0.0	0.0

Table C6. Operating Conditions

HZSM-5/FT	:	4
FT Catalyst	:	10% Co/base (Mixed with 1% graphite & 1% stearic acid)
Wt of FT Catalyst	:	3.0002 g
Particle size of FT catalyst	:	-10+20 mesh
Wt. of HZSM-5	:	11.9990 g
Particle size of HZSM-5	:	-12+24 mesh
Feed Composition	:	47.5% CO, 47.5% H_2, 5% Ar
Temp. of FT Reactor	:	250°C
Temp. of HZSM-5 reactor	:	300°C
WHSV	:	1.0 h^{-1}
Pressure	:	0, 50, 100, 290 psig (0.101, 0.446, 0.788, 2.1 MPa)

Table C7. Product Distribution as a Function of Time-on-Stream for FT + HZSM-5 Catalysts at 0 psig (0.101 MPa)

Run No.	98	99	100	101	102	103	104	105	110	111	112	113
WHSV, h^{-1}	1.0	1.0	1.0	1.0	1.0	1.0	1.0	1.0	1.0	1.0	1.0	1.0
Temp. of FT reactor, °C	250	250	250	250	250	250	250	250	250	250	250	250
Temp. of HZSM-5 reactor, °C	300	300	300	300	300	300	300	300	300	300	300	300
Time-on-stream, h	1	3	5	7	1	3	5	7	1	3	5	7
Pressure, psig	0	0	0	0	0	0	0	0	0	0	0	0
CO Conversion, %	16.6	15.5	14.7	15.2	15.3	14.6	14.4	14.2	14.5	13.3	13.4	13.4
Hydrocarbon Distribution, Wt%												
C_1	19.3	17.2	16.8	15.4	19.9	18.2	17.2	16.9	20.4	17.1	17.2	18.0
C_2	8.3	6.2	5.9	5.9	6.5	5.8	5.4	5.8	7.3	6.6	5.8	5.9
C_3	15.6	13.7	13.4	13.7	14.7	13.5	13.6	14.0	14.2	14.5	13.4	13.7
C_4	25.5	25.7	24.2	24.5	25.7	24.0	24.3	24.4	24.1	24.2	24.7	23.6
C_{5+} (incl. Arom.)	31.3	37.2	39.7	40.5	33.2	38.5	39.5	38.9	34.0	37.6	38.9	38.8
A_6	1.0	1.1	1.2	1.3	0.9	1.1	1.1	1.2	0.7	1.0	1.0	1.0
A_7	5.0	6.0	6.6	6.6	4.7	6.5	6.1	5.6	6.3	6.6	6.2	6.1
A_8	2.7	5.8	6.0	6.4	3.5	5.5	6.0	5.5	5.1	5.7	5.8	5.8
A_9	0.7	2.5	4.2	4.2	1.2	3.0	4.2	4.1	1.5	2.0	3.6	4.1
Total Aromatics, wt%	9.4	15.4	18.0	18.5	10.3	16.1	17.4	16.4	13.6	15.3	16.6	17.0
$C_2^=$/Total C_2, wt%	11.5	18.8	27.3	32.4	28.3	34.0	37.8	40.2	28.6	34.0	40.0	40.8
$C_3^=$/Total C_3, wt%	13.8	17.2	17.9	21.3	19.3	21.5	23.3	23.4	19.3	24.3	23.0	25.2
i-C_4 Total C_4, wt%	70.0	67.5	70.7	67.9	73.0	70.6	71.2	74.7	68.1	66.6	69.3	74.6

Table C8. Product Distribution as a Function of Time-on-Stream for FT+HZSM-5 Catalysts at 50 Psig (0.446 MPa)

Run No.	130	131	132	133	134	135	136	137	138	139	140	141
WHSV, h^{-1}	1.1	1.0	0.9	0.9	1.0	1.0	1.1	1.1	1.1	1.1	1.1	1.1
Temp. of FT reactor, °C	250	250	250	250	250	250	250	250	250	250	250	250
Temp. of HZSM-5 reactor, °C	300	300	300	300	300	300	300	300	300	300	300	300
Time-on-Stream, h	1	3	5	7	1	3	5	7	1	3	5	7
Pressure, Psig	50	50	50	50	50	50	50	50	50	50	50	50
CO Conversion, %	17.4	16.4	17.3	17.9	16.5	15.9	15.2	15.3	16.0	14.8	14.5	14.4
Hydrocarbon Distribution, Wt%												
C_1	29.5	21.6	21.8	21.3	26.4	22.6	22.2	21.4	28.6	23.0	20.9	20.4
C_2	10.5	8.2	7.9	7.9	9.0	8.1	7.4	7.2	9.0	7.6	7.0	6.7
C_3	21.9	21.5	21.5	21.7	20.5	21.4	19.1	19.3	19.2	19.7	19.5	19.0
C_4	27.0	30.1	30.2	29.6	29.3	31.4	29.2	29.1	29.3	29.9	31.0	29.7
C_5^+ (Incl. Arom)	11.1	18.6	18.6	19.5	14.8	16.5	22.1	23.0	13.9	19.8	21.6	24.2
A_6	0.0	0.0	1.0	1.3	0.0	0.0	1.3	1.3	0.0	0.0	1.1	1.3
A_7	0.0	0.0	0.3	1.7	0.0	0.0	1.4	3.4	0.0	0.0	1.5	3.4
A_8	0.0	0.0	0.0	0.0	0.0	0.0	0.0	0.0	0.0	0.0	0.0	0.0
A_9	0.0	0.0	0.0	0.0	0.0	0.0	0.0	0.0	0.0	0.0	0.0	0.0
Total Aromatics	0.0	0.0	1.3	3.0	0.0	0.0	2.7	4.7	0.0	0.0	2.6	4.7
$C_2^=$/Total C_2, Wt%	0.0	0.0	0.0	0.0	0.0	0.0	0.0	0.0	0.0	0.0	0.0	0.0
$C_3^=$/Total C_3, Wt%	0.0	0.0	0.0	0.0	0.0	0.0	0.0	0.0	0.0	0.0	0.0	0.0
i-C_4/Total C_4, Wt%	70.7	67.9	68.1	68.2	68.5	68.2	68.9	69.2	69.8	69.9	70.0	70.3

Table C9. Product Distribution as a Function of Time-on-Stream for FT+HZSM-5 Catalysts at 100 Psig (0.788 MPa)

Run No.	154	155	156	157	158	159	160	161	163	164	165
WHSV, h^{-1}	1.4	1.1	1.1	1.1	0.9	0.9	0.9	0.9	1.0	1.1	1.0
Temp. of FT reactor, °C	250	250	250	250	250	250	250	250	250	250	250
Temp. of HZSM-5 reactor, °C	300	300	300	300	300	300	300	300	300	300	300
Time-on-Stream, h	1	3	5	7	1	3	5	7	3	5	7
Pressure, Psig	100	100	100	100	100	100	100	100	100	100	100
CO Conversion, %	9.6	13.2	13.6	14.6	9.6	13.6	15.1	16.0	13.4	12.2	12.1
Hydrocarbon Distribution, Wt%											
C_1	51.0	30.2	28.6	29.1	17.8	25.1	25.2	25.1	37.5	33.0	31.8
C_2	3.8	11.9	10.9	11.8	10.5	9.5	10.4	10.4	12.7	12.1	11.6
C_3	7.1	20.6	20.8	21.8	31.2	22.0	24.7	24.0	19.3	19.1	19.6
C_4	22.4	25.5	26.9	26.1	22.8	29.0	28.9	28.5	24.0	25.3	25.1
C_5^+ (Incl. Arom)	15.7	11.8	12.8	11.2	17.7	14.4	10.8	12.0	6.5	10.5	11.9
A_6	0.0	0.0	0.0	0.0	0.0	0.0	0.0	0.0	0.0	0.0	0.0
A_7	0.0	0.0	0.0	0.0	0.0	0.0	0.0	0.0	0.0	0.0	0.0
A_8	0.0	0.0	0.0	0.0	0.0	0.0	0.0	0.0	0.0	0.0	0.0
A_9	0.0	0.0	0.0	0.0	0.0	0.0	0.0	0.0	0.0	0.0	0.0
Total Aromatics	0.0	0.0	0.0	0.0	0.0	0.0	0.0	0.0	0.0	0.0	0.0
$C_2^=$/Total C_2, Wt%	0.0	0.0	0.0	0.0	0.0	0.0	0.0	0.0	0.0	0.0	0.0
$C_3^=$/Total C_3, Wt%	0.0	0.0	0.0	0.0	0.0	0.0	0.0	0.0	0.0	0.0	0.0
i-C_4/Total C_4, Wt%	70.0	69.7	68.7	69.7	82.1	71.2	69.7	69.4	73.6	71.5	70.8

Table C10. Product Distribution as a Function of Time-on-Stream for FT+HZSM-5 Catalysts at 290 Psig (2.1 MPa)

Run No.	166	167	168	169	170	171	172	173	174	175	176	177
WHSV, h^{-1}	0.9	1.1	0.9	1.0	1.1	1.1	1.0	1.0	0.9	0.9	1.0	1.0
Temp. of FT reactor, °C	250	250	250	250	250	250	250	250	250	250	250	250
Temp. of HZSM-5 reactor, °C	300	300	300	300	300	300	300	300	300	300	300	300
Time-on-Stream, h	1	3	5	7	1	3	5	7	1	3	5	7
Pressure, Psig	290	290	290	290	290	290	290	290	290	290	290	290
CO Conversion, %	10.3	10.4	10.4	10.2	10.4	10.3	10.5	10.8	9.7	10.0	10.0	10.3
Hydrocarbon Distribution, %												
C_1	76.4	80.9	81.3	79.7	77.6	76.5	78.2	77.3	87.7	87.0	82.6	86.3
C_2	4.3	6.5	5.3	6.3	3.8	3.5	4.1	4.7	1.6	1.6	3.7	2.3
C_3	10.3	7.6	6.3	8.5	5.0	3.9	4.1	5.1	1.7	1.6	4.9	2.2
C_4	0.0	0.0	0.0	0.0	0.0	0.0	0.0	0.0	0.0	0.0	0.0	0.0
C_5^+	9.0	5.0	7.1	5.5	13.6	16.1	13.6	12.9	9.0	9.8	8.8	9.2
(Incl. Arom)												
A_6	0.0	0.0	0.0	0.0	0.0	0.0	0.0	0.0	0.0	0.0	0.0	0.0
A_7	0.0	0.0	0.0	0.0	0.0	0.0	0.0	0.0	0.0	0.0	0.0	0.0
A_8	0.0	0.0	0.0	0.0	0.0	0.0	0.0	0.0	0.0	0.0	0.0	0.0
A_9	0.0	0.0	0.0	0.0	0.0	0.0	0.0	0.0	0.0	0.0	0.0	0.0
Total Aromatics	0.0	0.0	0.0	0.0	0.0	0.0	0.0	0.0	0.0	0.0	0.0	0.0
$C_2^=$/Total C_2, Wt%	0.0	0.0	0.0	0.0	0.0	0.0	0.0	0.0	0.0	0.0	0.0	0.0
$C_3^=$/Total C_3, Wt%	0.0	0.0	0.0	0.0	0.0	0.0	0.0	0.0	0.0	0.0	0.0	0.0

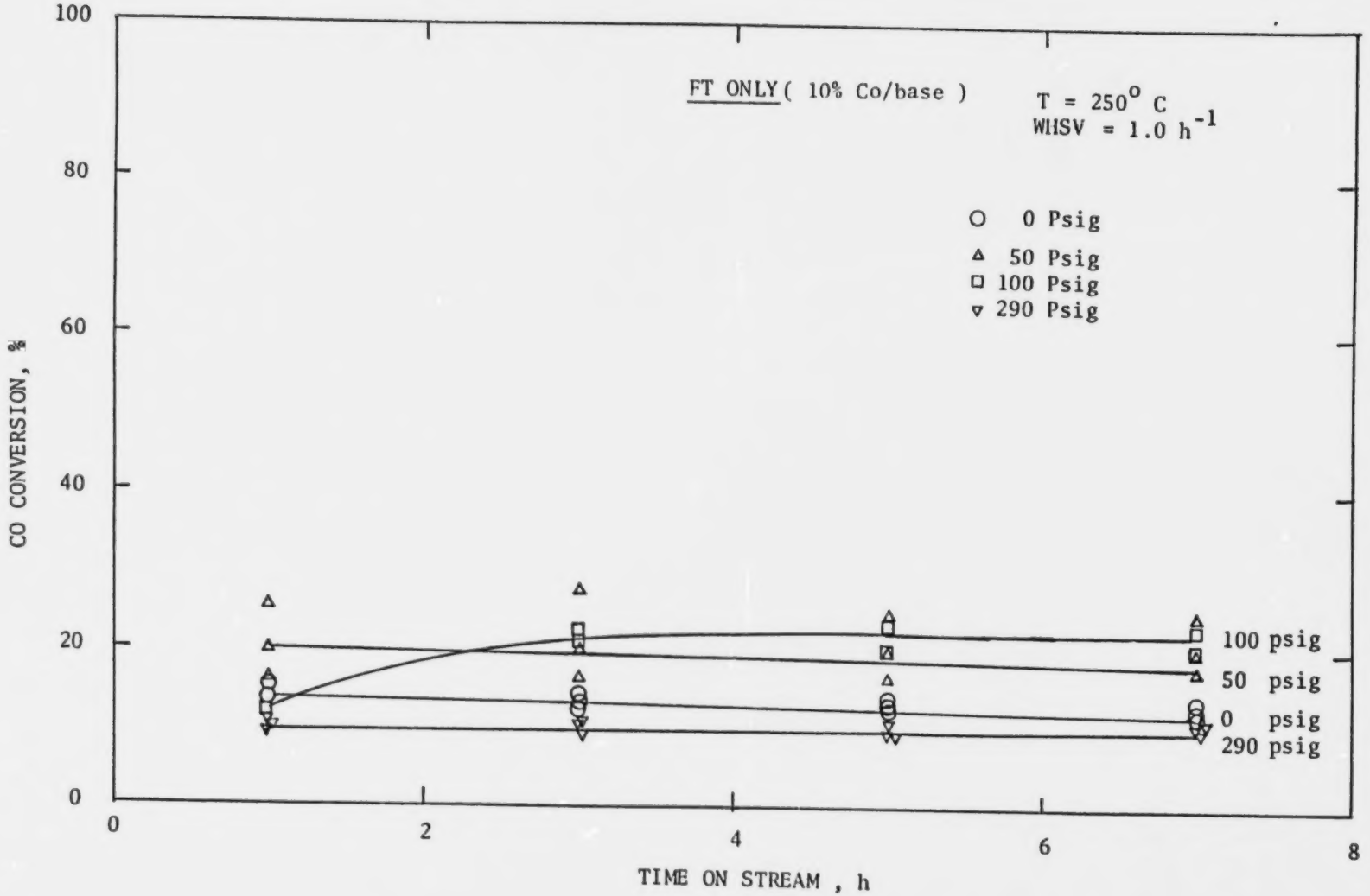

Figure C1. Variation of Carbon Monoxide Conversion with Time-on-Stream for FT Catalyst

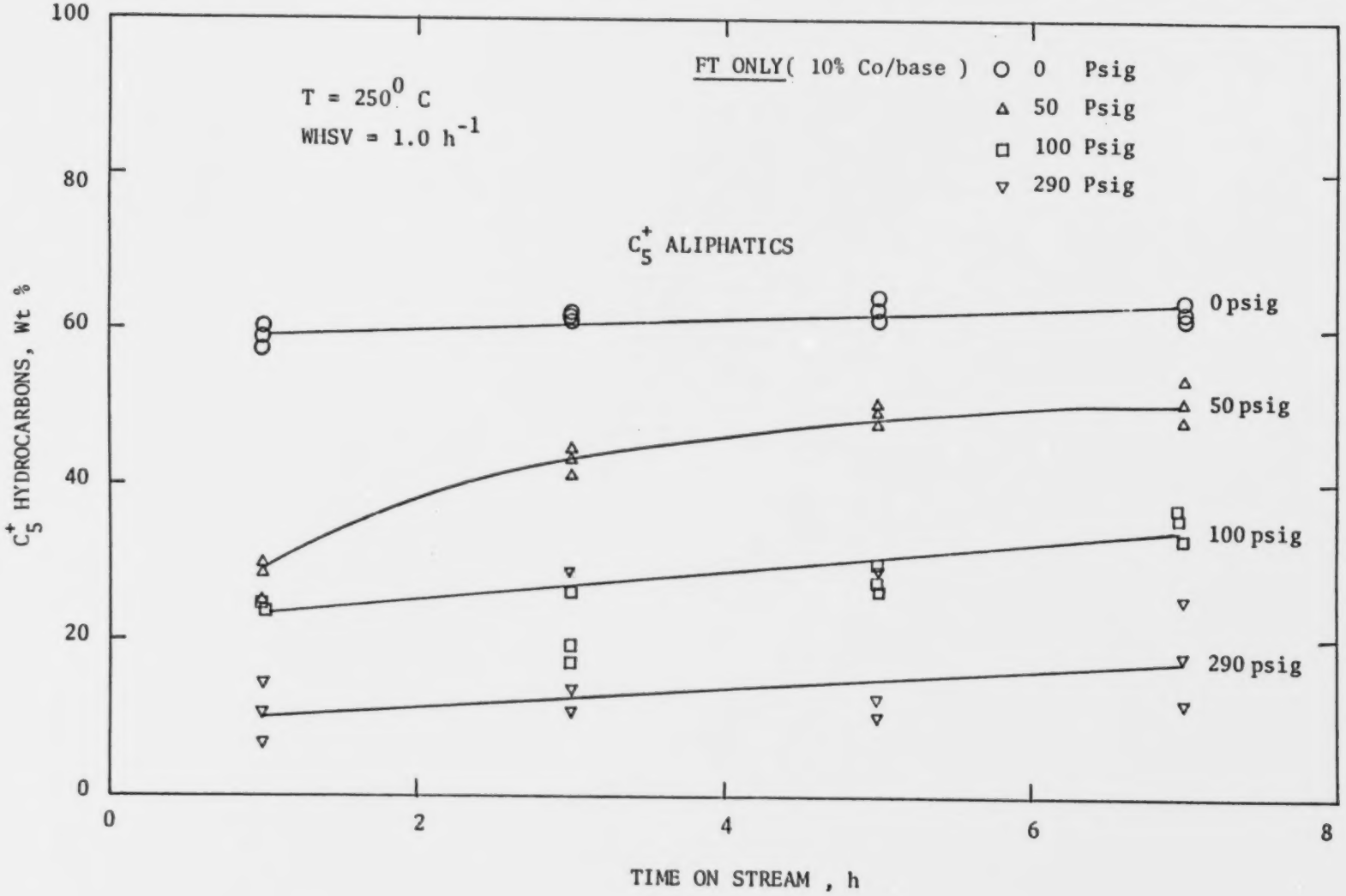

Figure C2 . C_5^+ Aliphatics Hydrocarbons in the Hydrocarbon Product with Time-on-Stream for FT Catalyst

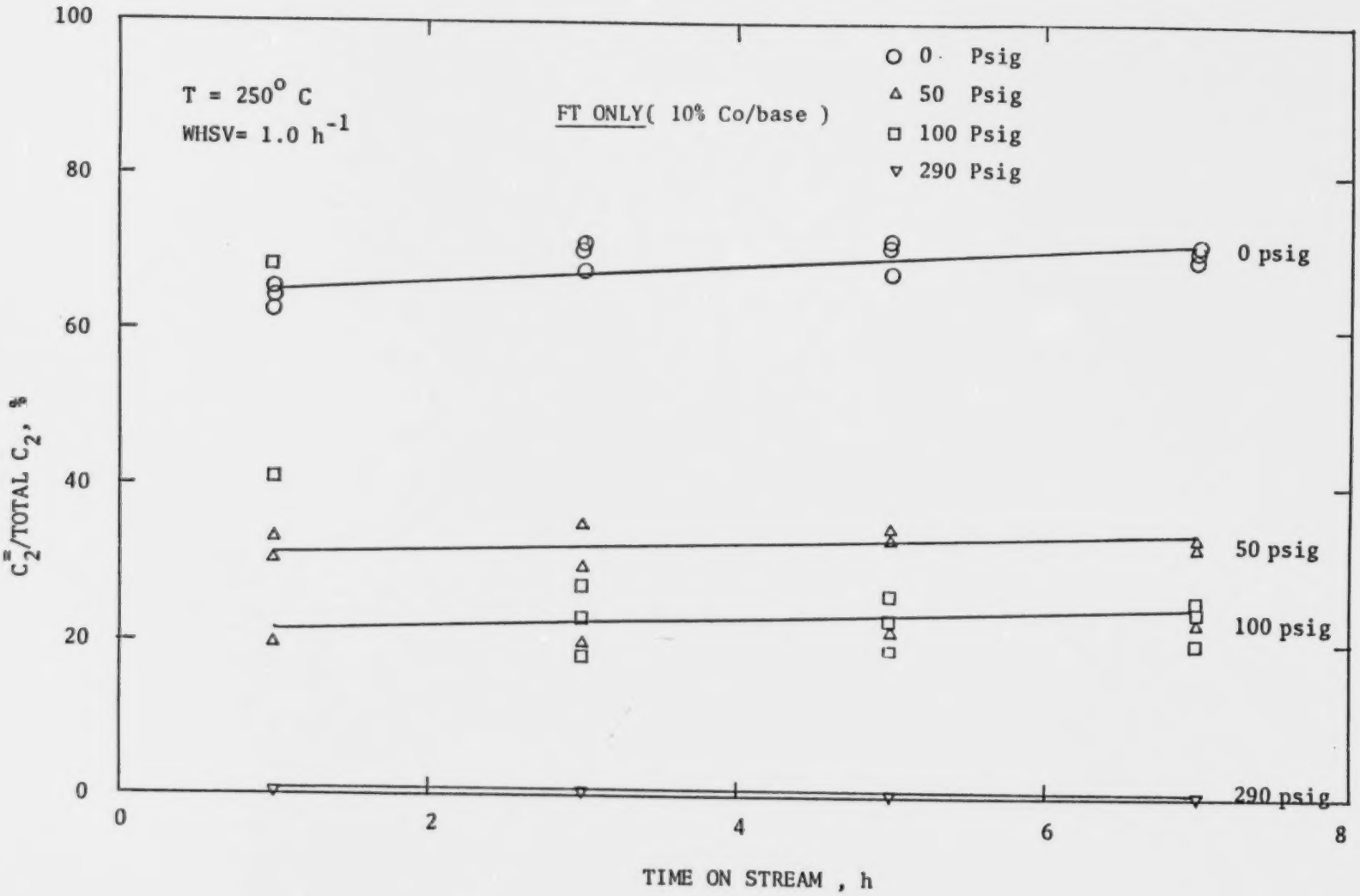

Figure C3. $C_2^=/C_2$ Fraction in the Hydrocarbon Product with Time-on-Stream for FT Catalyst

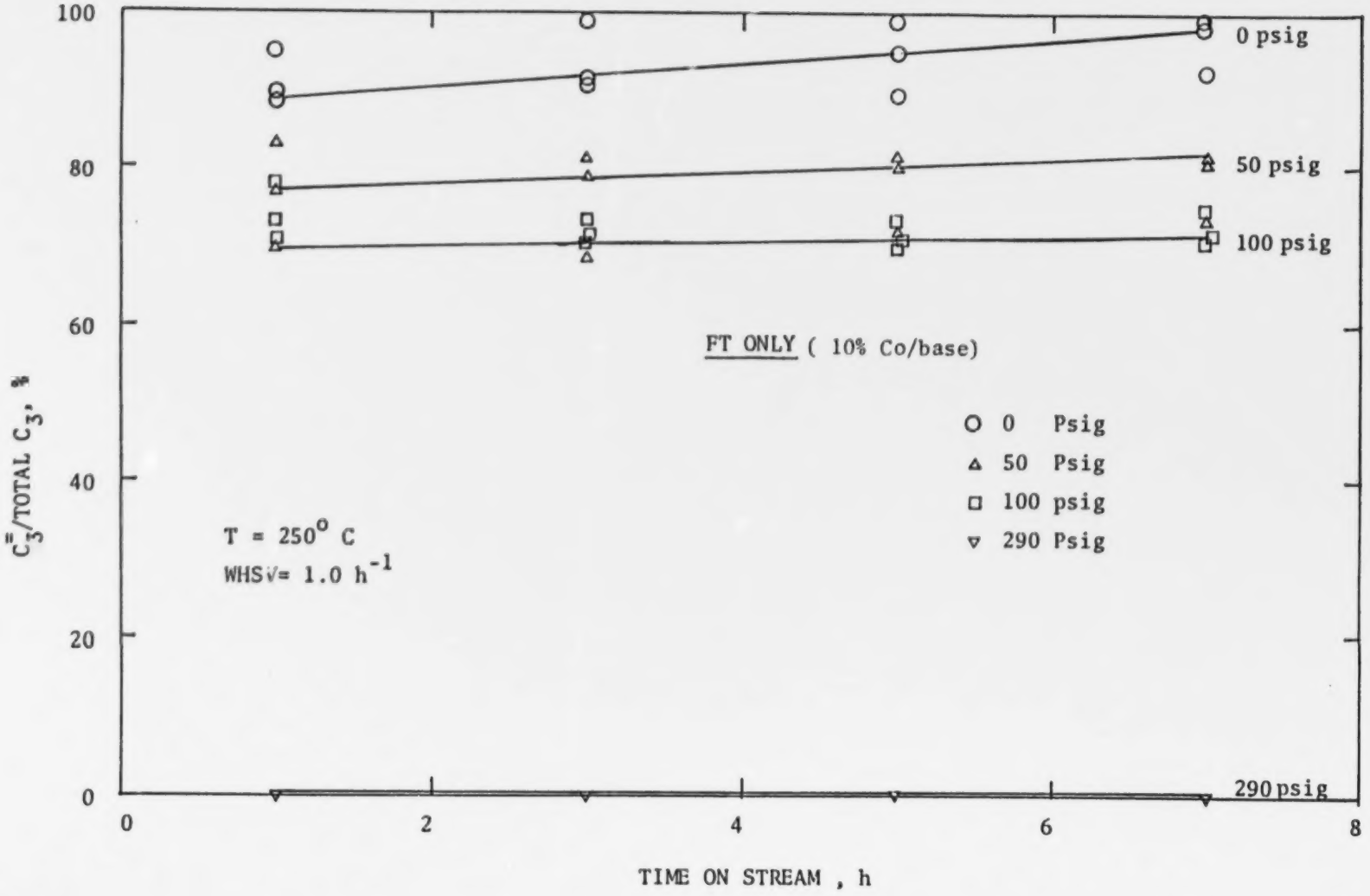

Figure C4. $C_3^=/C_3$ Fraction in the Hydrocarbon Product with Time-on-Stream for FT Catalyst

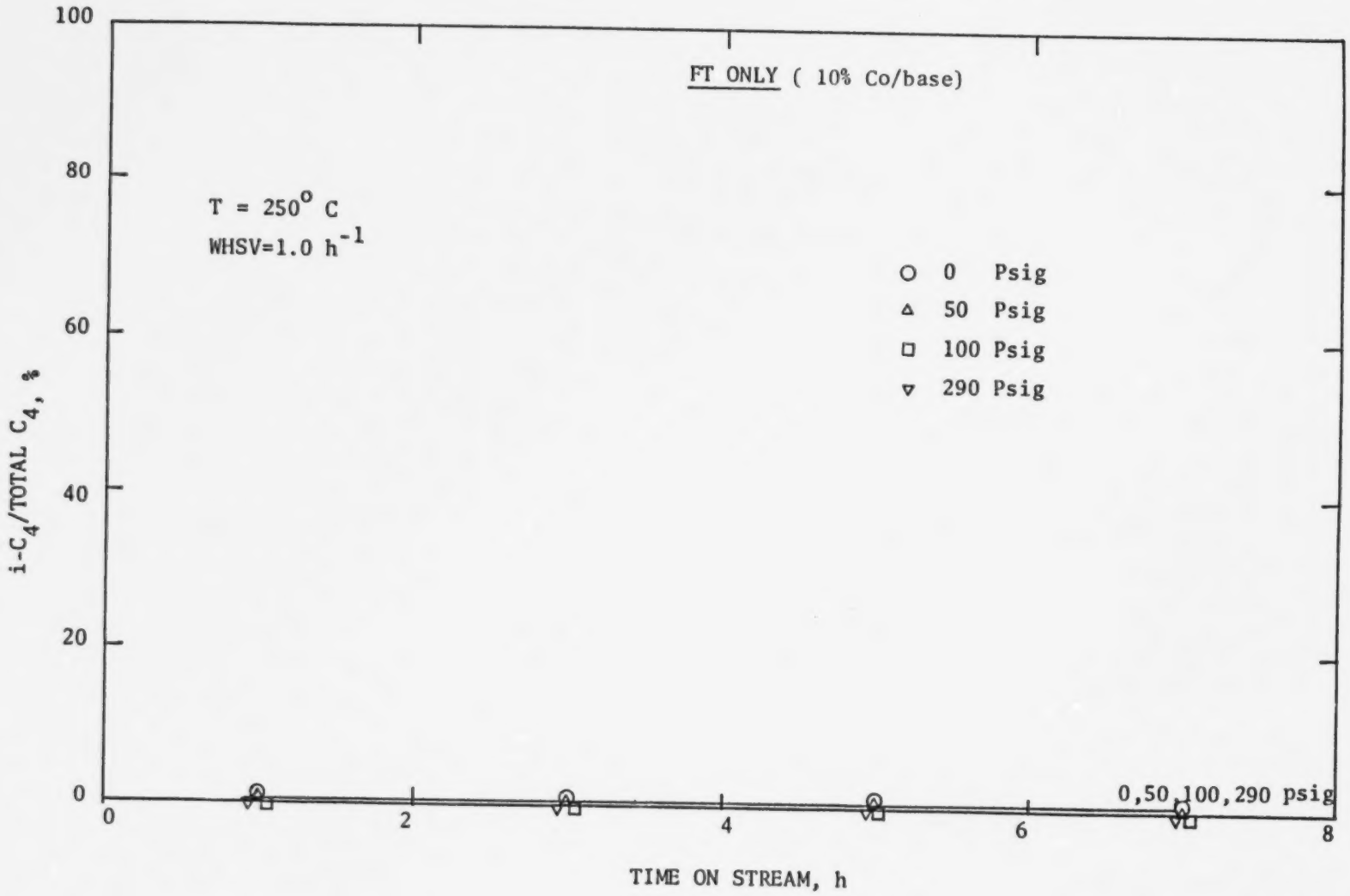

Figure C5. i-C_4/C_4 Fraction in the Hydrocarbon Product with Time-on-Stream for FT Catalyst

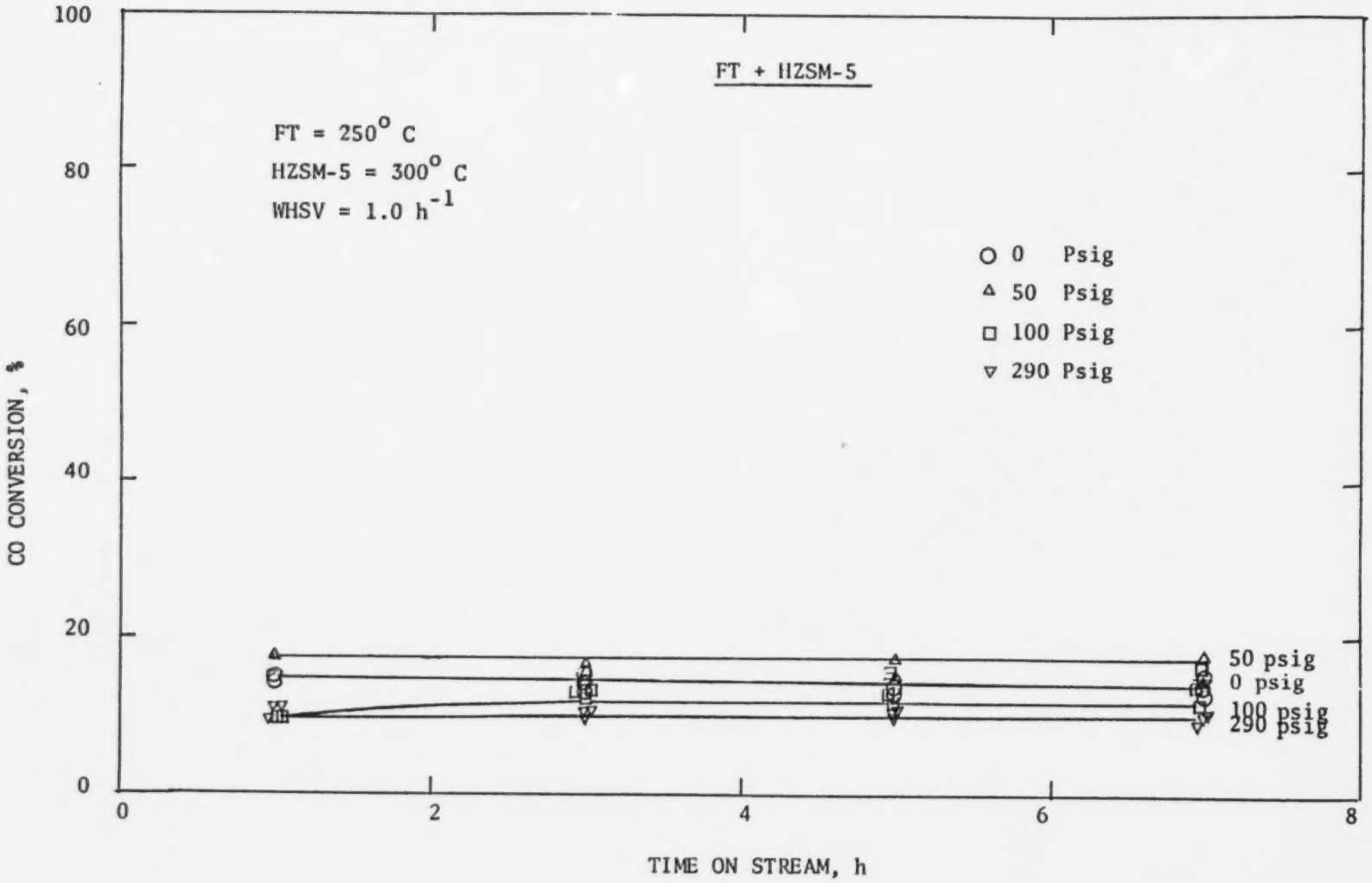

Figure C6. Variation of Carbon Monoxide Conversion with Time-on-Stream for FT + HZSM-5 Catalysts

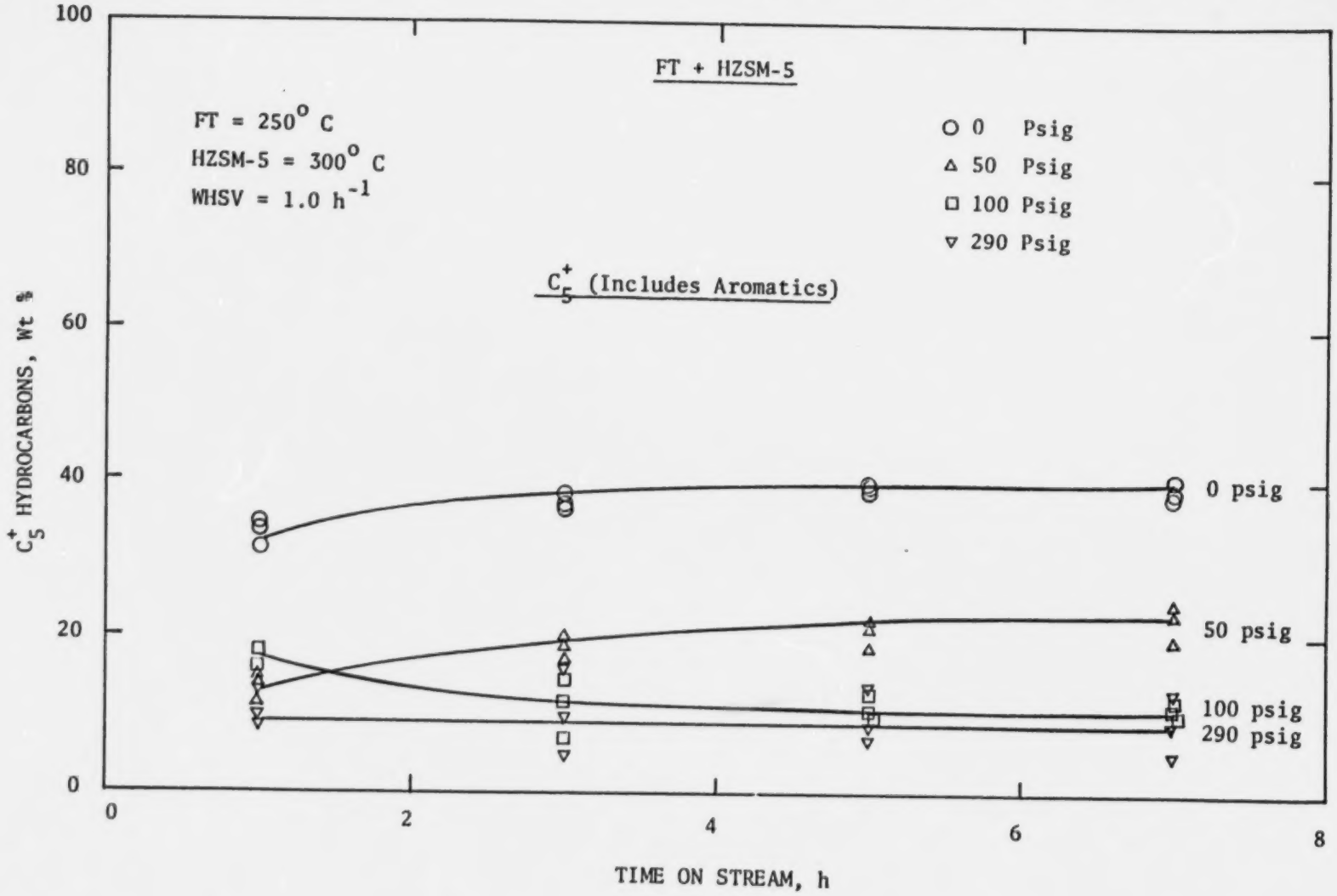

Figure C7. C_5^+ Hydrocarbons in the Hydrocarbon Product with Time-on-Stream for FT+HZSM-5 Catalysts

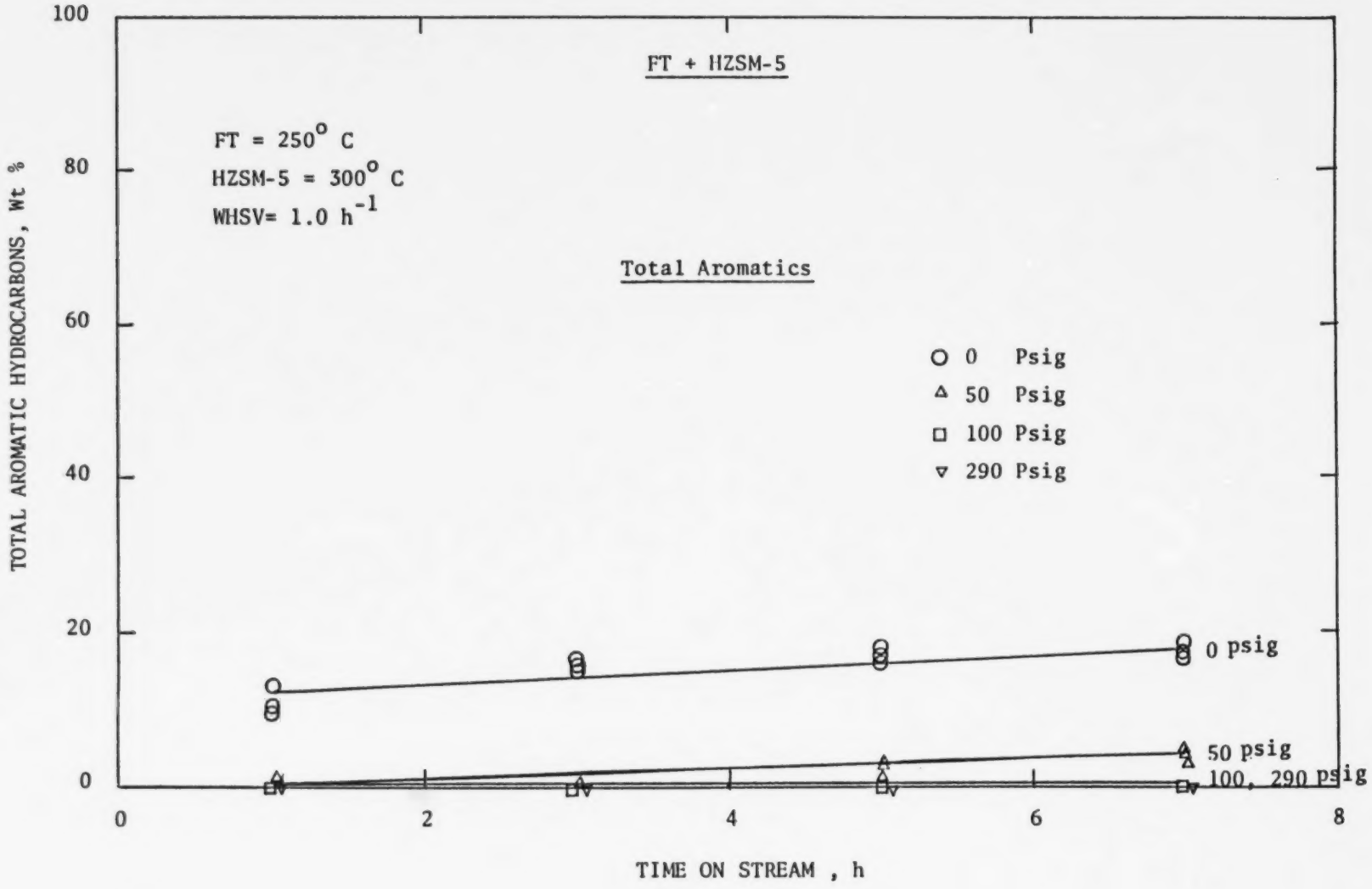

Figure C8. Total Aromatic Hydrocarbons in the Hydrocarbon Product with Time-on-Stream for FT+HZSM-5 Catalysts

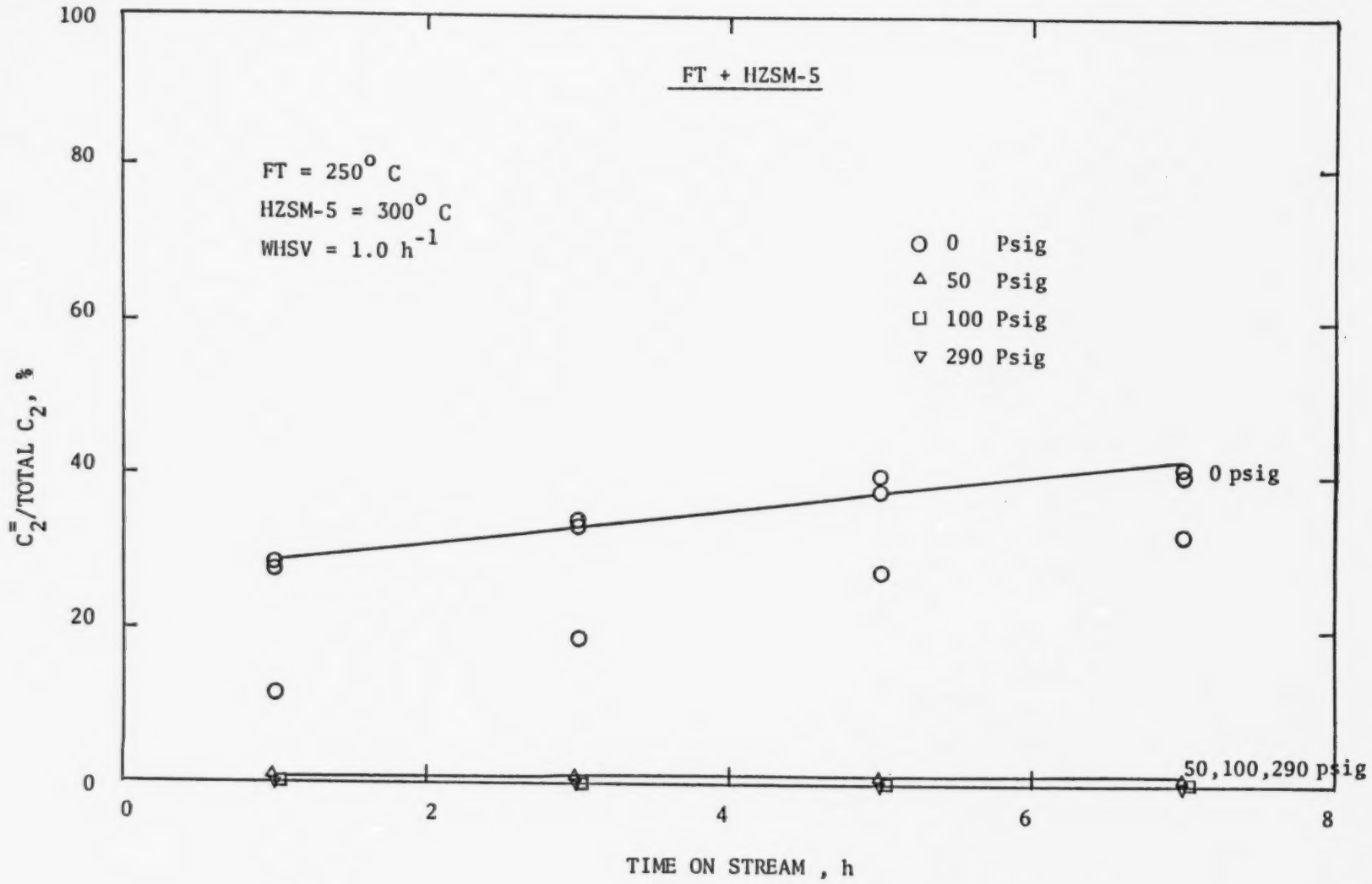

Figure C9. $C_2^=/C_2$ Fraction in the Hydrocarbon Product with Time-on-Stream for FT + HZSM-5 Catalysts

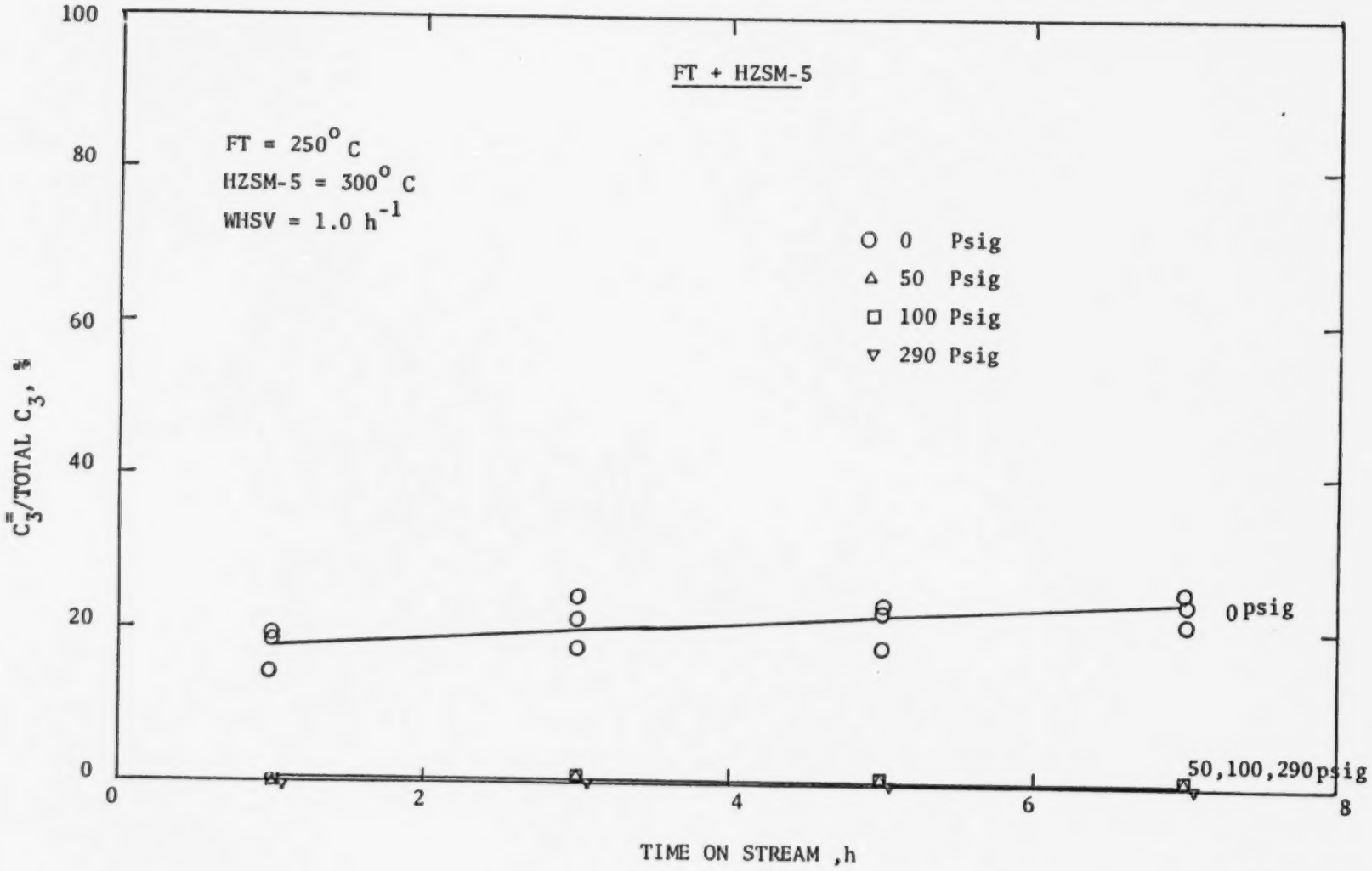

Figure C10. $C_3^=/C_3$ Fraction in the Hydrocarbon Product with Time-on-Stream for FT + HZSM-5 Catalysts

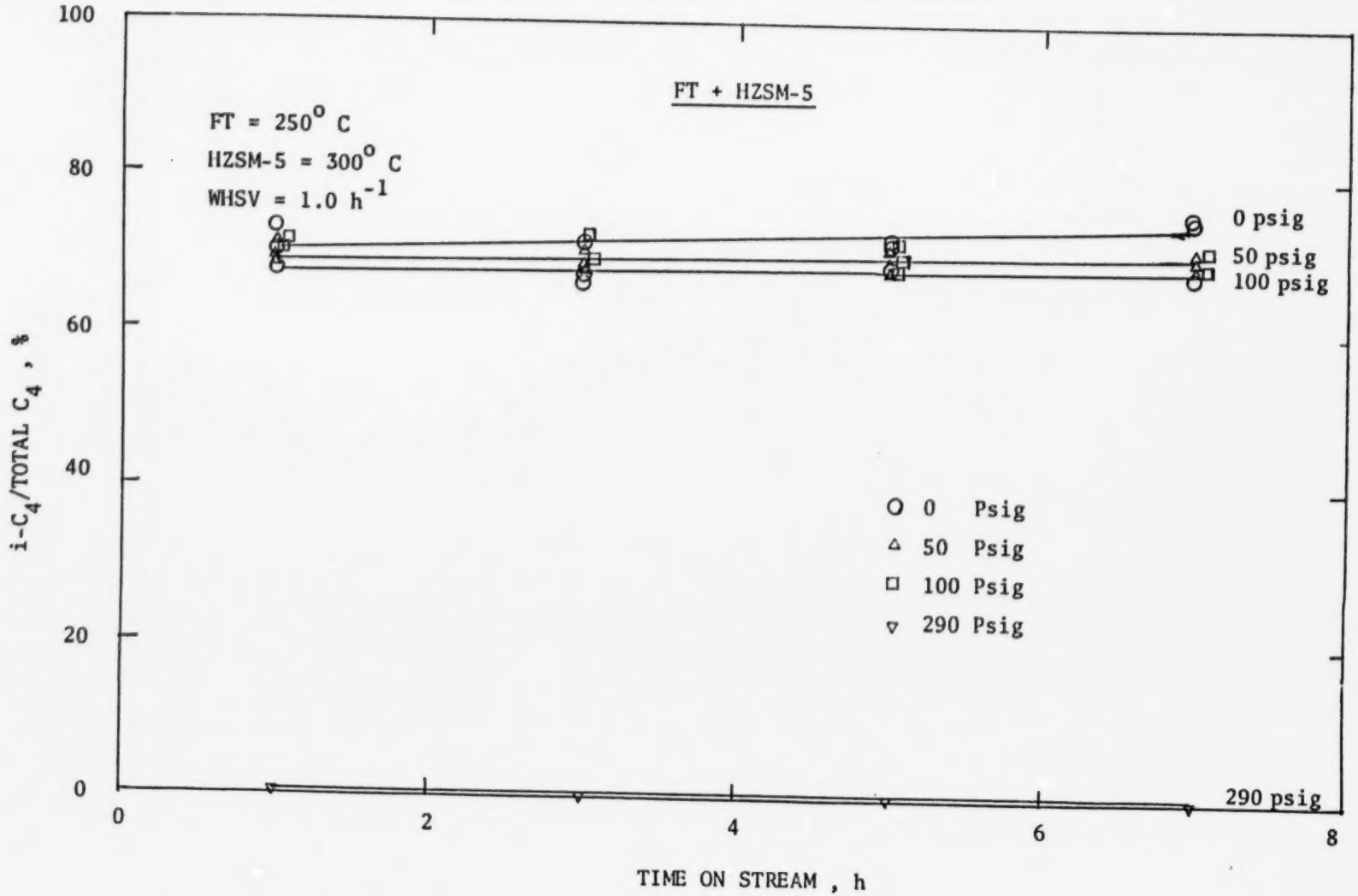

Figure C11. $i\text{-}C_4/C_4$ Fraction in the Hydrocarbon Product with Time-on-Stream for FT + HZSM-5 Catalysts

Table 1. Physico-Chemical Characteristics of FT Catalysts

No.	Catalyst	BET Surface Area, m^2/g	Metal analysis, wt% Ni	Co
1	10% Co/base	90	3.0	10.0
2	2%Ni-5% Co/base	70	6.9	5.6

TABLE 2. X-ray diffraction data for HZSM-5

HZSM-5		From Patent literature U.S. Patent: 3,702,886	
Interplanar spacing d(Å)	Relative Intensity	Interplanar spacing d (Å)	Relative Intensity
1.8697	W		
1.9141	W		
1.9509	W		
1.9935	W		
2.0102	W		
2.4013	W		
2.4846	W		
2.5996	W		
2.7263	W		
2.8621	W	2.94 ± 0.02	W
2.9785	W	2.99 ± 0.02	W
3.0480	W	3.04 ± 0.03	W
3.2433	W		
3.3143	W		
3.4399	W		
3.6405	W		
3.7154	S	3.71 ± 0.05	S
3.8420	V.S.	3.85 ± 0.07	V.S
4.0042	W		
4.2603	W	4.25 ± 0.08	W
4.3638	W		
4.5988	W	4.60 ± 0.08	W
4.9967	W	5.01 ± 0.1	W
5.3402	W		
5.5737	W	5.56 ± 0.1	W
5.7166	W		
5.9854	W	5.97 ± 0.1	W
6.3708	W	6.3 ± 0.1	W
6.7071	W		
7.4367	W	7.4 ± 0.15	W
9.9355	S	10.0 ± 0.2	S
11.0510	S	11.0 ± 0.2	S

W = weak
S = strong
V.S.= very strong

Table 3. Operating Conditions and Results for C.I. Determination

Weight of the HZSM-5	=	0.1998 g
Bulk volume of the catalyst	=	0.46 mL
Flow rate of helium	=	17.0 mL/min
Volumetric flow rate of liquid hydrocarbon	=	1.37 mL/h
Liquid hourly space velocity	=	3.0 h^{-1}
Mole ratio of helium/total hydrocarbon	=	4.0
Fraction of n-hexane unconverted	=	0.7884
Fraction of 3-methylpentane unconverted	=	0.8234

$$\text{Constraint Index} = \frac{\log_{10}(0.7884)}{\log_{10}(0.8234)} = 1.25$$

Table 4. GC Operating Conditions

Column	Analysis	Detector	GC	Column Conditions
10% TCEP on Chromosorb P AW	Hydrocarbon C_1 - C_{15}	FID	HP 5880	Dimension 8ft x 1/8" Carrier gas He, 30 mL/min. Detector temp. 250°C Inj. port temp. 200°C Ramp 5°C/min.
80/100 Carbosieve -S	Ar, CO, CO_2, CH_4	TCD	Erograph Model A-90P	Dimension 1.5m x 3mm Carrier gas He, 30 mL/min. Detector temp. 230°C Inj. port temp. 135°C Ramp 5°C/min.
60/80 Chromosorb 102	Hydrocarbon C_1 to C_4	FID	F&M Model700A-99E	Dimension 1.8 x 3 mm Carrier gas He, 30 mL/min. Detector temp. 180°C Inj. port temp. 135°C Ramp 5°C/min.
80/100 Carbopack C/0.19% picric acid	C_4 components	FID	HP 5880	Dimension 2 m x 3 mm Carrier gas He, 30 mL/min. Detector temp. 250°C Inj. port temp. 200°C Ramp 5°C/min.
Activated Charcoal	H_2	TCD	F&M 720	Dimension 8ft x 1/4"

Table 5. Operating Conditions (Runs 209-232)

HZSM-5/FT	:	1
FT Catalyst	:	10% Co/base (Mixed with 1% graphite + 1% Stearic acid)
Wt of FT Catalyst	:	3.0000 g
Particle size of FT catalyst	:	-10 + 20 mesh
Wt. of HZSM-5	:	3.0007 g
Particle size of HZSM-5	:	-12 + 24 mesh
Feed Composition	:	47.5% CO. 47.5% H_2, 5% Ar
Temp. of FT Reactor	:	250^{o}C
Temp. of HZSM-5 reactor	:	350, 375, 400^{o}C
WHSV	:	1.0 h^{-1}
Pressure	:	0.101, 1.0, 2.0 MPa

Table 6.

Effect of the HZSM-5 Reactor Temperature on the Product Distribution at 0.101 MPa (HZSM-5/FT Ratio = 1)

Run No.	209	210	211	212	214	215	216	217	218	220	221	222	223	224	226
WHSV, h^{-1}	1.0	1.0	1.0	1.0	1.0	1.0	1.0	1.0	1.0	1.0	1.0	1.0	1.0	1.0	1.0
Temp. of FT reactor, ^{o}C	250	250	250	250	250	250	250	250	250	250	250	250	250	250	250
Temp. of HZSM-5 reactor, ^{o}C	350	350	350	350	350	375	375	375	375	375	400	400	400	400	400
Time-on-stream, h	1	3	5	7	24	25	27	29	31	48	49	51	53	55	72
Pressure, MPa	.101	.101	.101	.101	.101	.101	.101	.101	.101	.101	.101	.101	.101	.101	.101
CO Conversion,%	18.7	18.2	17.4	17.8	15.3	15.4	14.4	16.7	15.1	14.9	14.2	13.8	14.6	14.1	13.4
Hydrocarbon Distribution, wt%															
C_1	19.2	19.2	19.7	21.0	21.3	19.9	20.3	23.8	22.0	24.0	21.8	21.5	23.5	22.2	23.2
C_2	7.7	7.2	9.3	8.9	7.7	10.7	10.6	10.8	10.2	11.0	14.8	15.4	16.1	14.8	15.4
C_3	17.7	16.8	15.4	15.5	16.6	19.8	19.6	19.3	18.6	19.4	22.0	22.1	21.8	22.4	22.0
C_4	21.9	21.0	18.9	19.5	19.0	17.7	17.7	17.4	17.8	17.0	15.7	14.7	14.1	15.2	14.3
C_5+ (Includes Aromatics)	33.5	35.8	36.7	35.1	35.4	31.9	31.8	28.7	31.4	28.6	25.7	26.3	24.5	25.4	25.1
A_6	1.4	1.3	1.4	1.2	1.1	1.2	1.2	1.0	1.1	1.0	0.9	0.9	0.9	1.0	0.9
A_7	6.4	6.6	6.9	5.6	5.3	4.8	4.9	4.1	4.6	3.9	3.2	3.5	3.2	3.3	3.1
A_8	2.2	5.1	6.8	6.1	6.0	5.7	5.0	4.5	4.9	4.3	4.2	3.9	3.2	3.5	3.4
A_9	0.0	0.0	0.0	0.0	0.0	0.0	0.0	0.0	0.0	0.0	0.0	0.0	0.0	0.0	0.0
Total Aromatics, wt%	10.0	13.0	15.1	12.9	12.4	11.7	11.1	9.6	10.6	9.2	8.3	8.3	7.3	7.8	7.4
$C_2^{=}$ /total C_2, wt%	68.9	72.5	66.7	76.1	77.0	83.4	83.0	79.7	82.1	82.4	87.1	88.0	85.4	86.3	87.5
$C_3^{=}$ /total C_3, wt%	39.4	39.0	40.2	41.0	49.1	53.6	53.7	52.3	55.4	58.3	62.1	63.5	61.8	62.3	64.1
iC_4/total C_4, wt%	52.9	54.4	52.7	53.6	56.6	45.6	45.9	46.5	44.7	44.5	37.8	37.8	32.3	38.7	37.6

Table 7. Effect of the HZSM-5 Reactor Temperature on the Product Distribution at 1 MPa (HZSM-5/FT Ratio = 1)

Run No.	227	228	229
WHSV, h^{-1}	1.0	1.0	1.0
Temp. of FT reactor, ^{o}C	250	250	250
Temp. of HZSM-5 reactor, ^{o}C	350	375	400
Time-on-stream, h	5.0	6.5	8.0
Pressure, MPa	1.0	1.0	1.0
CO Conversion, %	43.2	43.0	43.5
Hydrocarbon Distribution, wt%			
C_1	52.4	48.8	46.1
C_2	11.0	10.1	11.5
C_3	25.0	27.7	29.4
C_4	9.4	10.7	10.1
C_5+ (Includes Aromatics)	2.2	2.7	2.9
A_6	0.0	0.0	0.0
A_7	0.1	0.1	0.1
A_8	0.1	0.1	0.1
A_9	0.0	0.0	0.0
Total Aromatics, wt%	0.2	0.2	0.2
$C_2^{=}$ /total C_2, wt%	1.0	1.1	1.8
$C_3^{=}$ /total C_3, wt%	0.0	0.0	0.0
iC_4/total C_4, wt%	56.4	60.4	57.1

Table 8. Effect of the HZSM-5 Reactor Temperature on the Product Distribution at 2 MPa (HZSM-5/FT Ratio = 1)

Run No.	230	231	232
WHSV, h^{-1}	1.0	1.0	1.0
Temp. of FT reactor, ^{o}C	250	250	250
Temp. of HZSM-5 reactor, ^{o}C	350	375	400
Time-on-stream, h	5.0	6.5	8.0
Pressure, MPa	2.0	2.0	2.0
CO Conversion, %	66.7	40.6	46.5
Hydrocarbon Distribution, wt%			
C_1	74.2	85.9	79.7
C_2	6.3	4.8	6.1
C_3	14.1	6.4	8.4
C_4	4.9	2.4	5.1
C_5+ (Includes Aromatics)	0.5	0.5	0.7
A_6	0.0	0.0	0.0
A_7	0.0	0.0	0.0
A_8	0.0	0.0	0.0
A_9	0.0	0.0	0.0
Total Aromatics, wt%	0.0	0.0	0.0
$C_2^=$ /total C_2, wt%	0.9	1.3	1.4
$C_3^=$ /total C_3, wt%	0.0	0.0	0.0
iC_4/total C_4, wt%	61.4	70.8	59.7

Table 9. Operating Conditions (Runs 233-241)

HZSM-5/FT	:	2.5
FT Catalyst	:	10% Co/base (Mixed with 1% graphite & 1% stearic acid)
Wt of FT Catalyst	:	3.0060 g
Particle size of FT catalyst	:	-10+20 mesh
Wt. of HZSM-5	:	7.5040 g
Particle size of HZSM-5	:	-12+24 mesh
Feed Composition	:	47.5% CO, 47.5% H_2, 5% Ar
Temp. of FT Reactor	:	250°C
Temp. of HZSM-5 reactor	:	350, 375, 400°C
WHSV	:	1.0 h^{-1}
Pressure	:	0.101, 1.0, 2.0 MPa

Table 10. Effect of the HZSM-5 Reactor Temperature on the Product Distribution at 0.101 MPa (HZSM-5/FT Ratio = 2.5)

Run No.	233	234	235
WHSV, h^{-1}	1.0	1.0	1.0
Temp. of FT reactor, ^{o}C	250	250	250
Temp. of HZSM-5 reactor, ^{o}C	350	375	400
Time-on-stream, h	5.0	6.5	8.0
Pressure, MPa	0.101	0.101	0.101
CO Conversion, %	22.3	22.2	21.1
Hydrocarbon Distribution, wt%			
C_1	21.4	21.1	20.7
C_2	5.6	7.5	10.2
C_3	16.9	19.5	21.8
C_4	22.2	20.0	17.5
C_5+ (Includes Aromatics)	33.9	31.9	29.8
A_6	2.3	2.3	2.3
A_7	9.4	8.8	8.3
A_8	6.8	8.1	8.5
A_9	0.0	0.0	0.0
Total Aromatics, wt%	18.5	19.2	19.1
$C_2^=$ /total C_2, wt%	56.2	68.8	69.5
$C_3^=$ /total C_3, wt%	20.0	25.8	31.0
iC_4/total C_4, wt%	62.3	58.8	54.2

Table 11. Effect of the HZSM-5 Temperature on the Product Distribution at 1 MPa (HZSM-5/FT Ratio = 2.5)

Run No.	236	237	238
WHSV, h^{-1}	1.0	1.0	1.0
Temp. of FT reactor, ^{o}C	250	250	250
Temp. of HZSM-5 reactor, ^{o}C	350	375	400
Time-on-stream, h	5.0	6.5	8.0
Pressure, MPa	1.0	1.0	1.0
CO Conversion, %	54.9	52.2	51.5
Hydrocarbon Distribution, wt%			
C_1	63.9	30.3	32.8
C_2	8.6	6.0	7.8
C_3	22.6	50.6	38.8
C_4	4.4	12.5	19.0
C_5+ (Includes Aromatics)	0.5	0.6	1.6
A_6	0.0	0.0	0.0
A_7	0.0	0.0	0.0
A_8	0.0	0.0	0.0
A_9	0.0	0.0	0.0
Total Aromatics, wt%	0.0	0.0	0.0
$C_2^=$ /total C_2, wt%	1.0	1.5	2.4
$C_3^=$ /total C_3, wt%	0.0	0.0	0.0
iC_4/total C_4, wt%	74.8	76.2	65.2

Table 12. Effect of the HZSM-5 Reactor Temperature on the Product Distribution at 2 MPa (HZSM-5/FT Ratio = 2.5)

Run No.	239	240	241
WHSV, h^{-1}	1.0	1.0	1.0
Temp. of FT reactor, ^{o}C	250	250	250
Temp. of HZSM-5 reactor, ^{o}C	350	375	400
Time-on-stream, h	5.0	6.5	8.0
Pressure, MPa	2.0	2.0	2.0
CO Conversion, %	96.7	88.4	69.3
Hydrocarbon Distribution, wt%			
C_1	98.1	95.8	89.5
C_2	1.1	2.6	5.0
C_3	0.3	0.9	4.4
C_4	0.2	0.3	0.7
C_5+ (Includes Aromatics)	0.3	0.4	0.4
A_6	0.0	0.0	0.0
A_7	0.0	0.0	0.0
A_8	0.0	0.0	0.0
A_9	0.0	0.0	0.0
Total Aromatics, wt%	0.0	0.0	0.0
$C_2^=$ /total C_2, wt%	2.4	0.9	0.8
$C_3^=$ /total C_3, wt%	0.0	0.0	0.0
iC_4/total C_4, wt%	66.3	70.9	72.7

Table 13. Operating Conditions (Runs 242-250

HZSM-5/FT	:	4
FT Catalyst	:	10% Co/base (Mixed with 1% graphite & 1% stearic acid)
Wt of FT Catalyst	:	2.9992 g
Particle size of FT catalyst	:	-10+20 mesh
Wt. of HZSM-5	:	12.0020 g
Particle size of HZSM-5	:	-12+24 mesh
Feed Composition	:	47.5% CO, 47.5% H_2, 5% Ar
Temp. of FT Reactor	:	250°C
Temp. of HZSM-5 reactor	:	350, 375, 400°C
WHSV	:	1.0 h^{-1}
Pressure	:	0.101, 1.0, 2.0 MPa

Table 14. Effect of the HZSM-5 Reactor Temperature on the Product Distribution at 0.101 MPa (HZSM-5/FT Ratio = 4)

Run No.	242	243	244
WHSV, h^{-1}	1.0	1.0	1.0
Temp. of FT reactor, ^{o}C	250	250	250
Temp. of HZSM-5 reactor, ^{o}C	350	375	400
Time-on-stream, h	5.0	6.5	8.0
Pressure, MPa	0.101	0.101	0.101
CO Conversion, %	21.2	21.4	19.9
Hydrocarbon Distribution, wt%			
C_1	20.3	18.4	20.3
C_2	5.0	8.2	9.0
C_3	16.5	18.9	19.6
C_4	20.3	18.9	14.8
C_5+ (Includes Aromatics)	37.9	35.6	36.3
A_6	2.0	2.0	2.1
A_7	8.7	7.7	6.6
A_8	11.3	10.2	9.6
A_9	0.0	0.0	0.0
Total Aromatics, wt%	22.0	19.9	18.3
$C_2^=$ /total C_2, wt%	59.8	77.6	72.3
$C_3^=$ /total C_3, wt%	18.4	32.0	26.9
iC_4/total C_4, wt%	62.2	54.9	56.1

Table 15. Effect of the HZSM-5 Reactor Temperature on the Product Distribution at 1 MPa (HZSM-5/FT Ratio = 4)

Run No.	245	246	247
WHSV, h^{-1}	1.0	1.0	1.0
Temp. of FT reactor, ^{o}C	250	250	250
Temp. of HZSM-5 reactor, ^{o}C	350	375	400
Time-on-stream, h	5.0	6.5	8.0
Pressure, MPa	1.0	1.0	1.0
CO Conversion, %	49.8	50.8	48.9
Hydrocarbon Distribution, wt%			
C_1	65.1	50.0	44.1
C_2	8.2	7.8	9.3
C_3	21.8	32.9	36.7
C_4	3.7	8.1	8.2
C_5+ (Includes Aromatics)	1.2	1.2	1.7
A_6	0.0	0.0	0.0
A_7	0.1	0.1	0.1
A_8	0.0	0.0	0.0
A_9	0.0	0.0	0.0
Total Aromatics, wt%	0.1	0.1	0.1
$C_2^=$ /total C_2, wt%	0.8	0.9	1.9
$C_3^=$ /total C_3, wt%	0.0	0.0	0.0
iC_4/total C_4, wt%	68.5	67.3	61.6

Table 16. Effect of the HZSM-5 Reactor Temperature on the Product Distribution at 2 MPa (HZSM-5/FT Ratio = 4)

Run No.	248	249	250
WHSV, h^{-1}	1.0	1.0	1.0
Temp. of FT reactor, ^{o}C	250	250	250
Temp. of HZSM-5 reactor, ^{o}C	350	375	400
Time-on-stream, h	5.0	6.5	8.0
Pressure, MPa	2.0	2.0	2.0
CO Conversion, %	17.2	14.6	49.0
Hydrocarbon Distribution, wt%			
C_1	64.8	68.1	70.5
C_2	16.5	17.4	18.1
C_3	7.8	7.6	8.1
C_4	4.0	3.5	2.1
C_5+ (Includes Aromatics)	6.9	3.4	1.2
A_6	0.0	0.0	0.0
A_7	0.0	0.0	0.0
A_8	0.0	0.0	0.0
A_9	0.0	0.0	0.0
Total Aromatics, wt%			
$C_2^{=}$ /total C_2, wt%	4.1	2.4	5.4
$C_3^{=}$ /total C_3, wt%	0.0	0.0	0.0
iC_4/total C_4, wt%	61.8	63.3	64.7

Table 17. Operating Conditions (251-281)

FT Catalyst	:	10% Co/base (mixed with 1% graphite & 1% stearic acid)
Wt of FT Catalyst	:	2.9998 g
Particle size of FT catalyst	:	-10+20 mesh
Wt. of HZSM-5	:	12.0020 g
Particle size of HZSM-5	:	-12+24 mesh
Feed Composition	:	47.5% CO, 47.5% H_2, 5% Ar
Temp. of FT Reactor	:	250°C
Temp. of HZSM-5 reactor	:	350°C
WHSV	:	0.16 h^{-1}
Pressure	:	1 atm (0.101 MPa)

Table 17a. Results of GC/MS Analysis for 10% Co/base + HZSM-5 Experiment Condensate from Liquid Nitrogen + Hexane Trap

Wt. of Condensate = 5.3180 g.

(i) Lighter Components

Carbon No.	Major Compounds	Approximate Area %
C_7	3 - methyl hexane heptane 4,4 - dimethyl - 2 - pentene	22.0
C_9	2,2,3,4 - tetramethyl-pentane 2,2,3 - trimethyl hexane 2,3,5 - trimethyl hexane 2,3,4 - trimethyl hexane 4 - ethyl - 2 - methyl hexane	21.1
C_{10}	2,3,6 - trimethyl heptane 2,3,5 - trimethyl heptane	0.7
A_8	ethyl benzene 1,2 - dimethyl benzene 1,4 - dimethyl benzene 1 - ethenyl - 3 - methylene cyclopentane	51.1
A_9	1 - methyl ethyl benzene 1 - ethyl - 2 - methyl benzene 1 - ethyl - 4 - methyl benzene 1,2,4 - trimethyl benzene 1,2,3 - trimethyl benzene 1,3,5 - trimethyl benzene	0.4
C_{11}	3 - methyl decane 4 - undecene 5 - undecene 2 - methyl - 4 - undecene 4,5 - dimethyl nonane 2,4,6 - trimethyl octane	3.1
A_{10}	1,2,3,5 - tetramethyl benzene 1,2,3,4 - tetramethyl benzene 1,2,4,5 - tetramethyl benzene 2 - ethyl - 1,4 - dimethyl benzene naphthalene	1.3
		100.0

Table 17a continued

(ii) Heavier Components

Carbon No.	Major Compounds	Approximate Area %
C_{13}	4,7 - dimethyl undecane 2,9 - dimethyl undecane 3,9 - dimethyl undecane 4,6 - dimethyl undecane 3 - ethyl undecane 4 - ethyl undecane	91.6
	2,4,6 - trimethyl decane 2,6,8 - trimethyl decane 3,3,8 - trimethyl decane 3,3,6 - trimethyl decane 2,3,5 - trimethyl decane 2,3,7 - trimethyl decane 6 - ethyl - 2 - methyl decane 3 - methyl dodecane 5 - (1 - methyl propyl) nonane	
A_{12}	2,3 - dimethyl naphthalene 1,3 - dimethyl naphthalene 1,2 - dimethyl naphthalene 1,5 - dimethyl naphthalene	4.6
C_{14}	6 - methyl tridecane tetradecane	3.8
		100.0

Table 18. Analysis of Fresh and Used Catalysts

Analysis, wt%	FT (10% Co/base)		HZSM-5	
	Fresh	Used	Fresh	Used
C	1.48	6.82	0.03	0.14

Table 19. Product Distribution as a Function of Time-on-Stream
(see Table 17 for operating conditions)

Run No.	251	252	253	258	259	260	265	266	267	272	273	274	279	280	281
WHSV, h^{-1}	0.16	0.16	0.16	0.16	0.16	0.16	0.16	0.16	0.16	0.16	0.16	0.16	0.16	0.16	0.16
Temp. of FT reactor, ^{o}C	250	250	250	250	250	250	250	250	250	250	250	250	250	250	250
Temp. of HZSM-5 reactor, ^{o}C	350	350	350	350	350	350	350	350	350	350	350	350	350	350	350
Time-on-stream, h	2	4	6	24	27	30	48	51	54	72	75	78	96	99	100
CO Conversion,%	44.1	41.0	40.6	33.3	32.4	31.5	27.1	30.4	29.2	26.4	25.9	27.9	26.4	25.1	27.2
Hydrocarbon Distribution, wt%															
C_1	32.2	30.5	31.9	30.8	25.6	31.5	28.8	32.1	31.7	31.6	32.3	35.2	33.6	32.6	34.5
C_2	8.0	7.3	6.6	6.0	5.2	6.1	5.8	6.2	6.3	6.7	6.7	7.0	7.0	6.9	6.9
C_3	23.9	21.4	18.4	17.6	18.2	16.2	15.7	16.4	15.5	15.3	15.7	15.7	15.5	15.7	15.0
C_4	24.6	23.0	22.6	21.8	25.0	20.8	20.7	20.7	19.5	19.5	19.5	19.8	19.1	19.7	19.0
C_5+	11.3	17.8	20.5	23.8	26.0	25.4	29.0	24.6	27.0	26.9	25.8	22.3	24.8	25.1	24.6
(Includes Aromatics)															
A_6	1.7	2.5	2.0	2.2	1.5	2.2	2.3	2.0	2.1	1.9	2.0	1.8	1.8	2.1	1.9
A_7	0.0	6.1	8.1	7.6	6.6	6.8	6.2	7.0	9.1	7.2	9.4	6.2	5.8	7.0	7.6
A_8	0.0	0.0	1.6	3.8	5.2	6.4	5.8	5.3	6.1	4.5	4.7	4.8	4.6	5.7	6.3
A_9	0.0	0.0	0.0	0.0	0.0	0.0	0.0	0.0	0.0	0.0	0.0	0.0	0.0	0.0	0.0
Total Aromatics, wt%	1.7	8.6	11.7	13.6	13.3	15.4	14.3	14.3	17.3	13.6	16.1	12.8	12.2	14.8	15.8
$C_2^{=}$ /total C_2 wt%	15.2	18.2	18.4	25.6	30.0	27.3	40.2	25.1	29.2	30.0	28.6	25.5	37.4	29.7	26.5
$C_3^{=}$ /total C_3 wt%	6.2	7.5	7.9	10.5	11.4	12.0	14.3	11.0	14.0	14.9	13.9	13.4	14.8	14.6	14.1
iC_4/total C_4 wt%	63.0	63.9	53.5	66.4	65.1	66.3	66.2	67.3	66.9	66.5	68.3	66.3	66.2	66.4	66.6

Table 20. Operating conditions (Runs 283-287)

HZSM-5/FT	:	1
FT Catalyst	:	2% Ni-5% Co/base (Mixed with 1% graphite & 1% stearic acid)
Wt of FT Catalyst	:	2.9999 g
Particle size of FT catalyst	:	-10+20 mesh
Wt. of HZSM-5	:	3.0001 g
Particle size of HZSM-5	:	-12+24 mesh
Feed Composition	:	47.5% CO, 47.5% H_2, 5% Ar
Temp. of FT Reactor	:	250^{o}C
Temp. of HZSM-5 reactor	:	350, 375, 400^{o}C
WHSV	:	1.0 h^{-1}
Pressure	:	0.101, 1, 2 MPa

Table 21. Effect of the HZSM-5 Reactor Temperature on the Product Distribution at 0.101 MPa (HZSM-5/FT Ratio = 1)

Run No.	283	287	288	189
WHSV, h^{-1}	1.0	1.0	1.0	1.0
Temp. of FT reactor, ^{o}C	250	250	250	250
Temp. of HZSM-5 reactor, ^{o}C	325	350	375	400
Time-on-stream, h	5.0	6.5	8.0	9.5
Pressure, MPa	0.101	0.101	0.101	0.101
CO conversion, %	24.0	23.8	21.8	22.8
Hydrocarbon Distribution, wt%				
C_1	7.8	9.7	7.7	10.8
C_2	3.8	5.7	7.0	10.0
C_3	10.2	14.2	16.2	19.0
C_4	16.0	18.5	16.0	14.4
C_5+ (incl. arom.)	62.2	51.9	53.1	45.8
A_6	0.3	0.4	0.9	0.8
A_7	2.2	2.9	2.6	2.2
A_8	6.7	5.1	6.8	5.3
A_9	6.6	3.7	3.8	4.5
Total aromatics, wt%	15.8	12.1	14.1	12.8
$C_2^{=}$ /total C_2, wt%	56.6	64.6	76.8	76.6
$C_3^{=}$ /total C_3, wt%	63.1	64.1	70.4	76.4
iC_4/total C_4, wt%	36.0	35.6	29.6	21.8

Table 22. Effect of the HZSM-5 Reactor Temperature on the Product Distribution at 1 MPa (HZSM-5/FT Ratio = 1)

Run No.	291	292	293
WHSV, h^{-1}	1.0	1.0	1.0
Temp. of FT reactor, ^{o}C	250	250	250
Temp. of HZSM-5 reactor, ^{o}C	350	375	400
Time-on-stream, h	5.0	6.5	8.0
Pressure, MPa	1.0	1.0	1.0
CO conversion, %	50.9	51.9	50.5
Hydrocarbon Distribution, wt%			
C_1	29.5	17.9	15.7
C_2	10.7	8.6	7.1
C_3	33.8	42.6	40.1
C_4	20.7	24.5	27.8
C_5+ (incl. arom.)	5.3	6.4	9.3
A_6	0.0	0.0	0.0
A_7	0.0	0.0	0.0
A_8	0.0	0.0	0.0
A_9	0.0	0.0	0.0
Total aromatics, wt%	0.0	0.0	0.0
$C_2^=$ /total C_2, wt%	1.5	5.2	5.4
$C_3^=$ /total C_3, wt%	0.9	1.2	1.4
iC_4/total C_4, wt%	47.2	47.6	46.1

Table 23. Effect of the HZSM-5 Reactor Temperature on the Product Distribution at 2 MPa (HZSM-5/FT Ratio = 1)

Run No.	295	296	297
WHSV, h^{-1}	1.0	1.0	1.0
Temp. of FT reactor, ^{o}C	250	250	250
Temp. of HZSM-5 reactor, ^{o}C	350	375	400
Time-on-stream, h	5.0	6.5	8.0
Pressure, MPa	2.0	2.0	2.0
CO conversion, %	39.3	44.3	43.0
Hydrocarbon Distribution, wt%			
C_1	54.4	47.2	56.9
C_2	16.1	17.0	17.1
C_3	11.6	20.1	12.4
C_4	5.8	8.7	6.3
C_5+ (incl. arom.)	12.1	7.0	7.3
A_6	0.0	0.0	0.0
A_7	0.0	0.0	0.0
A_8	0.0	0.0	0.0
A_9	0.0	0.0	0.0
Total aromatics, wt%	0.0	0.0	0.0
$C_2^=$ /total C_2, wt%	2.4	2.1	2.2
$C_3^=$ /total C_3, wt%	4.0	3.4	6.4
iC_4/total C_4, wt%	48.3	49.4	47.0

Table 24. Operating Conditions (Runs 298-307)

HZSM-5/FT	:	2.5
FT Catalyst	:	2% Ni-5% Co/base (mixed with 1% graphite & 1% stearic acid)
Wt of FT Catalyst	:	3.0090 g
Particle size of FT catalyst	:	-10+20 mesh
Wt. of HZSM-5	:	7.5034 g
Particle size of HZSM-5	:	-12+24 mesh
Feed Composition	:	47.5% CO, 47.5% H_2, 5% Ar
Temp. of FT Reactor	:	250^{o}C
Temp. of HZSM-5 reactor	:	350, 375, 400^{o}C
WHSV	:	1.0 h^{-1}
Pressure	:	0.101, 1, 2 MPa

Table 25. Effect of the HZSM-5 Reactor Temperature on the Product Distribution at 0.101 MPa (HZSM-5/FT Ratio = 2.5)

Run No.	298	299	300	301
WHSV, h^{-1}	1.0	1.0	1.0	1.0
Temp. of FT reactor, ^{o}C	250	250	250	250
Temp. of HZSM-5 reactor, ^{o}C	325	350	375	400
Time-on-stream, h	5.0	6.5	8.0	9.5
Pressure, MPa	0.101	0.101	0.101	0.101
CO conversion, %	26.0	24.6	23.5	21.2
Hydrocarbon Distribution, wt%				
C_1	12.0	11.5	10.9	10.4
C_2	4.9	6.0	7.9	10.3
C_3	12.7	16.3	19.2	22.2
C_4	23.0	23.5	20.9	19.4
C_5+ (incl. arom.)	47.4	42.7	41.1	37.7
A_6	1.1	1.6	1.9	2.0
A_7	6.8	7.3	8.2	7.1
A_8	10.5	8.9	9.4	8.8
A_9	0.5	1.5	2.1	2.6
Total aromatics, wt%	18.9	19.3	21.6	20.5
$C_2^=$ /total C_2, wt%	40.3	50.9	59.4	62.8
$C_3^=$ /total C_3, wt%	24.6	27.3	33.0	37.2
iC_4/total C_4, wt%	59.9	58.3	53.6	49.2

Table 26. Effect of the HZSM-5 Reactor Temperature on the Product Distribution at 1 MPa (HZSM-5/FT Ratio = 2.5)

Run No.	302	303	304
WHSV, h^{-1}	1.0	1.0	1.0
Temp. of FT reactor, ^{o}C	250	250	250
Temp. of HZSM-5 reactor, ^{o}C	350	375	400
Time-on-stream, h	5.0	6.5	8.0
Pressure, MPa	1.0	1.0	1.0
CO conversion, %	61.5	65.8	61.5
Hydrocarbon Distribution, wt%			
C_1	26.7	27.3	18.8
C_2	12.7	11.2	10.0
C_3	40.3	42.2	53.7
C_4	13.0	14.4	13.6
C_5+ (incl. arom.)	7.3	4.9	3.9
A_6	0.1	0.1	0.1
A_7	0.1	0.1	0.1
A_8	0.0	0.0	0.0
A_9	0.0	0.0	0.0
Total aromatics, wt%	0.2	0.2	0.2
$C_2^=$ /total C_2, wt%	1.0	1.0	1.2
$C_3^=$ /total C_3, wt%	0.0	0.0	0.0
iC_4/total C_4, wt%	55.4	63.8	66.5

Table 27. Effect of the HZSM-5 Reactor Temperature on the Product Distribution at 2 MPa (HZSM-5/FT Ratio = 2.5)

Run No.	305	306	307
WHSV, h^{-1}	1.0	1.0	1.0
Temp. of FT reactor, ^{o}C	250	250	250
Temp. of HZSM-5 reactor, ^{o}C	350	375	400
Time-on-stream, h	5.0	6.5	8.0
Pressure, MPa	2.0	2.0	2.0
CO conversion, %	21.4	24.1	26.8
Hydrocarbon Distribution, wt%			
C_1	43.7	41.2	41.4
C_2	19.9	20.4	20.4
C_3	16.6	18.3	19.5
C_4	6.4	7.7	8.4
C_5+ (incl. arom.)	13.4	12.4	10.3
A_6	0.0	0.0	0.0
A_7	0.2	0.1	0.1
A_8	0.0	0.0	0.0
A_9	0.0	0.0	0.0
Total aromatics, wt%	0.2	0.1	0.1
$C_2^{=}$ /total C_2, wt%	3.8	3.1	2.7
$C_3^{=}$ /total C_3, wt%	4.9	4.1	3.1
iC_4/total C_4, wt%	69.6	69.5	70.4

Table 28. Operating Conditions (Runs 308-317)

HZSM-5/FT	:	4
FT Catalyst	:	2% Ni-5% Co/base (Mixed with 1% graphite & 1% stearic acid)
Wt of FT Catalyst	:	3.0000 g
Particle size of FT catalyst	:	-10+20 mesh
Wt. of HZSM-5	:	12.0070 g
Particle size of HZSM-5	:	-12+24 mesh
Feed Composition	:	47.5% CO, 47.5% H_2, 5% Ar
Temp. of FT Reactor	:	250°C
Temp. of HZSM-5 reactor	:	350, 375, 400°C
WHSV	:	1.0 h^{-1}
Pressure	:	0.101, 1, 2 MPa

Table 29. Effect of the HZSM-5 Reactor Temperature on the Product Distribution at 0.101 MPa (HZSM-5/FT Ratio = 4)

Run No.	308	309	310	311
WHSV, h^{-1}	1.0	1.0	1.0	1.0
Temp. of FT reactor, ^{o}C	250	250	250	250
Temp. of HZSM-5 reactor, ^{o}C	325	350	375	400
Time-on-stream, h	5.0	6.5	8.0	9.5
Pressure, MPa	0.101	0.101	0.101	0.101
CO conversion, %	27.5	26.7	25.2	25.0
Hydrocarbon Distribution, wt%				
C_1	12.3	12.1	13.0	14.7
C_2	5.2	7.4	9.2	14.1
C_3	14.2	19.3	19.3	21.1
C_4	24.0	23.0	20.8	17.0
C_5+ (incl. arom.)	44.3	38.2	37.7	33.1
A_6	1.4	1.8	2.5	2.3
A_7	9.0	9.0	8.3	7.7
A_8	11.9	11.5	12.5	11.0
A_9	0.0	0.6	1.3	1.7
Total aromatics, wt%	22.3	22.9	24.6	22.7
$C_2^=$ /total C_2, wt%	17.4	42.2	20.9	19.3
$C_3^=$ /total C_3, wt%	11.3	20.6	14.6	15.4
iC_4/total C_4, wt%	63.8	63.1	60.2	58.1

Table 30. Effect of the HZSM-5 Reactor Temperature on the Product Distribution at 1 MPa (HZSM-5/FT Ratio = 4)

Run No.	312	313	314
WHSV, h^{-1}	1.0	1.0	1.0
Temp. of FT reactor, ^{o}C	250	250	250
Temp. of HZSM-5 reactor, ^{o}C	350	375	400
Time-on-stream, h	5.0	6.5	8.0
Pressure, MPa	1.0	1.0	1.0
CO conversion, %	66.9	64.2	57.5
Hydrocarbon Distribution, wt%			
C_1	31.4	22.3	13.3
C_2	14.7	10.3	7.1
C_3	44.1	54.3	62.7
C_4	6.8	10.4	14.8
C_5+ (incl. arom.)	3.0	2.7	2.1
A_6	0.0	0.0	0.0
A_7	0.3	0.2	0.1
A_8	0.1	0.1	0.0
A_9	0.0	0.0	0.0
Total aromatics, wt%	0.4	0.3	0.1
$C_2^{=}$ /total C_2, wt%	0.7	0.8	1.4
$C_3^{=}$ /total C_3, wt%	0.0	0.0	0.0
iC_4/total C_4, wt%	70.4	67.9	75.0

Table 31. Effect of the HZSM-5 Reactor Temperature on the Product Distribution at 2 MPa (HZSM-5/FT Ratio = 4)

Run No.	315	316	317
WHSV, h^{-1}	1.0	1.0	1.0
Temp. of FT reactor, ^{o}C	250	250	250
Temp. of HZSM-5 reactor, ^{o}C	350	375	400
Time-on-stream, h	5.0	6.5	8.0
Pressure, MPa	2.0	2.0	2.0
CO conversion, %	46.2	47.6	45.6
Hydrocarbon Distribution, wt%			
C_1	34.1	27.9	19.4
C_2	16.7	13.4	10.5
C_3	35.7	40.0	49.2
C_4	9.3	16.4	18.6
C_5+ (incl. arom.)	4.2	2.3	2.3
A_6	0.0	0.0	0.0
A_7	0.0	0.0	0.0
A_8	0.4	0.2	0.1
A_9	0.0	0.0	0.0
Total aromatics, wt%	0.4	0.2	0.1
$C_2^=$ /total C_2, wt%	0.7	0.4	0.9
$C_3^=$ /total C_3, wt%	0.0	0.0	0.0
iC_4/total C_4, wt%	80.8	67.3	66.8

Table 32. Operating Conditions (Runs 318-332)

FT Catalyst	:	2% Ni-5% Co/base (Mixed with 1% graphite & 1% stearic acid)
Wt of FT Catalyst	:	3.0000 g
Particle size of FT catalyst	:	-10+20 mesh
Wt. of HZSM-5	:	12.0070 g
Particle size of HZSM-5	:	-12+24 mesh
Feed Composition	:	47.5% CO, 47.5% H_2, 5% Ar
Temp. of FT Reactor	:	250°C
Temp. of HZSM-5 reactor	:	350°C
WHSV	:	0.16 h^{-1}
Pressure	:	1 atm (0.101 MPa)

Table 32a. Results of GC/MS Analysis for 2% Ni-5% Co/base + HZSM-5 Experiment,Condensate from Liquid Nitrogen + Hexane Trap

Wt. of Condensate = 3.9715 g.

Carbon No.	Major Compounds	Approximate Area %
A_7	methyl benzene	32.8
A_8	ethyl benzene 1,3 - dimethyl benzene	61.4
A_9	propyl benzene 1 - ethyl - 2 - methyl benzene 1 - ethyl - 3 - methyl benzene 1,2,3 - trimethyl benzene 1,2,4 - trimethyl benzene	5.3
A_{10}	naphthalene	0.2
A_{11}	1 - methyl naphthalene	0.3
		100.0

Table 33. Analysis of Fresh and Used Catalysts

Analysis, wt%	FT (2% Ni-5% Co/base)		HZSM-5	
	Fresh	Used	Fresh	Used
C	1.52	6.70	0.03	0.12

Table 34. Product Distribution as a Function of Time-on-Stream

Run No.	318	319	320	321	322	323	324	326	327	328	329	330	331	332
WHSV, h^{-1}	0.16	0.16	0.16	0.16	0.16	0.16	0.16	0.16	0.16	0.16	0.16	0.16	0.16	0.16
Temp. of FT reactor, °C	250	250	250	250	250	250	250	250	250	250	250	250	250	250
Temp. of HZSM-5 reactor, °C	350	350	350	350	350	350	350	350	350	350	350	350	350	350
Time-on-stream, h	1	3	6	9	27	30	33	54	57	75	78	81	99	100
CO Conversion, %	44.5	53.8	40.6	38.7	35.4	35.3	33.9	33.9	31.1	26.1	26.8	24.5	22.6	22.1
Hydrocarbon Distribution, wt%														
C_1	20.3	16.4	14.6	13.7	12.4	14.1	14.2	16.4	13.3	14.1	16.5	15.7	15.9	16.0
C_2	7.8	6.3	5.8	5.3	4.7	5.8	5.7	6.0	5.2	5.4	6.0	5.7	6.1	6.4
C_3	23.6	22.6	20.0	21.2	18.3	18.2	17.0	18.1	19.2	17.0	17.3	17.0	16.2	17.0
C_4	26.9	28.7	27.9	29.3	26.6	26.7	25.0	26.8	28.3	23.6	23.3	23.8	21.6	22.8
C_5+ (incl. arom.)	21.4	26.0	31.7	30.5	38.0	35.2	38.1	32.7	34.0	39.9	36.9	37.8	40.2	37.8
A_6	1.3	2.7	2.4	2.6	2.3	1.8	2.8	2.3	2.5	1.8	2.2	1.9	2.0	2.1
A_7	0.2	4.4	10.5	7.7	6.6	6.8	9.4	7.2	7.7	8.4	7.7	8.8	5.0	8.8
A_8	1.9	0.7	0.8	2.2	10.3	6.0	5.4	5.2	4.9	12.4	5.1	5.0	13.7	7.9
A_9	0.2	0.3	1.3	1.0	1.5	1.7	1.1	1.3	1.0	1.7	2.2	1.5	1.9	1.7
Total aromatics, wt%	3.6	8.1	15.0	13.5	20.7	16.3	18.7	16.0	16.1	24.3	17.2	17.2	22.6	20.5
$C_2^=$ /total C_2, wt%	20.3	21.0	25.0	13.5	31.0	30.9	31.5	28.7	31.3	29.9	29.8	29.6	29.6	28.9
$C_3^=$ /total C_3, wt%	8.8	8.7	10.1	27.8	11.5	11.9	14.0	12.6	12.5	12.8	13.6	13.7	15.2	14.7
iC_4/total C_4, wt%	68.1	66.9	66.3	68.8	68.5	68.2	68.3	67.0	67.3	65.9	65.9	66.8	64.9	66.4

Table 35. Operating Conditions for Regeneration Studies (Runs 1-38)

Catalyst	:	10% Co/base
Wt of FT Catalyst	:	0.1018 g
Feed Composition	:	40% CO, 40% H_2, 20% Ar
WHSV	:	3.5 h^{-1}
Temp. of FT reactor	:	250°C
Pressure	:	1 atm (0.101 MPa)

Table 36. Product Distribution as a Function of Time-on-Stream for the Regeneration Experiments (see Table 35 for operating conditions)

Run No.	1	2	3	4	5	6	7	8	13	14	15	16	17	18	19	25	26	27	28	29	30	36	37	38
WHSV, h^{-1}	3.5	3.5	3.5	3.5	3.5	3.5	3.5	3.5	3.5	3.5	3.5	3.5	3.5	3.5	3.5	3.5	3.5	3.5	3.5	3.5	3.5	3.5	3.5	3.5
Temp. of FT reactor, ^{o}C	250	250	250	250	250	250	250	250	250	250	250	250	250	250	250	250	250	250	250	250	250	250	250	250
Time-on-stream, h	1.25	3.25	20.5	22.75	25.25	27.5	1.0	3.5	22.5	25.25	27.75	1.0	2.0	3.25	6.0	23.75	26.5	30.0	1.0	2.0	4.5	21.5	24.0	27.5
CO conversion, %	12.3	7.7	6.3	3.7	3.0	3.2	9.5	12.7	3.2	3.5	3.6	11.1	7.8	7.7	7.2	2.8	3.8	2.2	11.1	6.7	6.5	3.4	3.5	3.3
Hydrocarbon Distribution, wt%																								
C_1+C_2	27.0	28.2	30.7	30.2	30.7	30.4	27.7	28.8	35.6	34.1	35.8	26.9	28.8	29.4	29.5	36.6	36.2	36.1	28.3	32.1	30.2	35.0	34.4	35.0
C_3	11.3	10.4	10.0	8.5	8.5	9.9	11.8	11.1	9.6	9.1	9.4	11.2	11.2	10.7	9.7	8.0	7.9	7.7	10.1	10.6	8.8	8.0	7.7	7.8
C_4	11.6	10.1	6.5	7.9	7.8	9.0	12.2	11.0	8.7	8.1	8.4	11.6	11.1	10.3	9.2	7.4	7.1	6.9	10.3	10.6	8.5	7.3	7.1	7.0
C_5+	50.1	51.3	52.8	53.4	53.0	50.7	48.3	49.1	46.1	48.7	46.4	50.3	48.9	49.6	51.6	48.0	48.8	49.3	51.3	46.7	52.5	49.7	50.8	50.2
$C_2^=$ /total C_2, wt%	27.6	42.3	66.3	67.1	68.3	69.6	28.5	43.2	69.6	70.2	70.5	27.3	40.2	48.6	54.6	70.1	71.6	71.1	27.5	34.3	45.0	66.7	67.4	67.4
$C_3^=$ /total C_3, wt%	81.0	87.1	88.8	92.1	92.2	91.3	79.1	88.0	92.2	100.0	100.0	77.2	81.3	88.9	90.6	96.2	100.0	100.0	78.2	82.6	86.9	92.1	94.2	100.0

TABLE 37.
Summary of Experimental Runs for Task 3

Ranges of Operating Conditions								Analysis of a Typical Run											
								Operating Conditions				H.C. Analysis, wt%							
Run No.	FT-Catalyst	CO/H_2	WHSV, h^{-1}	HISM-5/FT Ratio	Pressure, MPa	Temp, °C FT	Temp, °C HISM-5	Typical Run No.	WHSV, h^{-1}	Pressure, MPa	Temp, °C FT	Temp, °C HISM-5	CO Conv.%	C_1	C_2	C_3	C_4	C_5^+ (incl. Arom.)	Total Aromatics
1-38	10% Co/base	1.0	3.5	-	0.101	250	-	1	3.5	0.101	250	-	12.3	22.7	4.3	11.3	11.6	50.1*	-
209-232	10% Co/base	1.0	1.0	1.0	0.101,1,2	250	350-400	211	1.0	0.101	250	350	17.4	19.7	9.3	15.4	18.9	36.7	15.1
233-241	10% Co/base	1.0	1.0	2.5	0.101,1,2	250	350-400	233	1.0	0.101	250	350	22.3	21.4	5.6	16.9	22.2	33.9	18.5
242-250	10% Co/base	1.0	1.0	4.0	0.101,1,2	250	350-400	242	1.0	0.101	250	350	21.2	20.3	5.0	16.5	20.3	37.9	22.0
251-281	10% Co/base	1.0	0.16	4.0	0.101	250	350	258	0.16	0.101	250	350	33.3	30.8	6.0	17.6	21.8	23.8	13.6
283-297	2%Ni-5%Co/base	1.0	1.0	1.0	0.101,1,2	250	350-400	287	1.0	0.101	250	350	23.8	9.7	5.7	14.2	18.5	51.9	12.1
298-307	2%Ni-5%Co/base	1.0	1.0	2.5	0.101,1,2	250	350-400	299	1.0	0.101	250	350	24.6	11.5	6.0	16.3	23.5	42.7	19.3
308-317	2%Ni-5%Co/base	1.0	1.0	4.0	0.101,1,2	250	350-400	309	1.0	0.101	250	350	26.7	12.1	7.4	19.3	23.0	38.2	22.9
318-332	2%Ni-5%Co/base	1.0	0.16	4.0	0.101	250	350	322	0.16	0.101	250	350	35.4	12.4	4.7	18.3	26.6	38.0	20.7

*C_5^+ Aliphatics

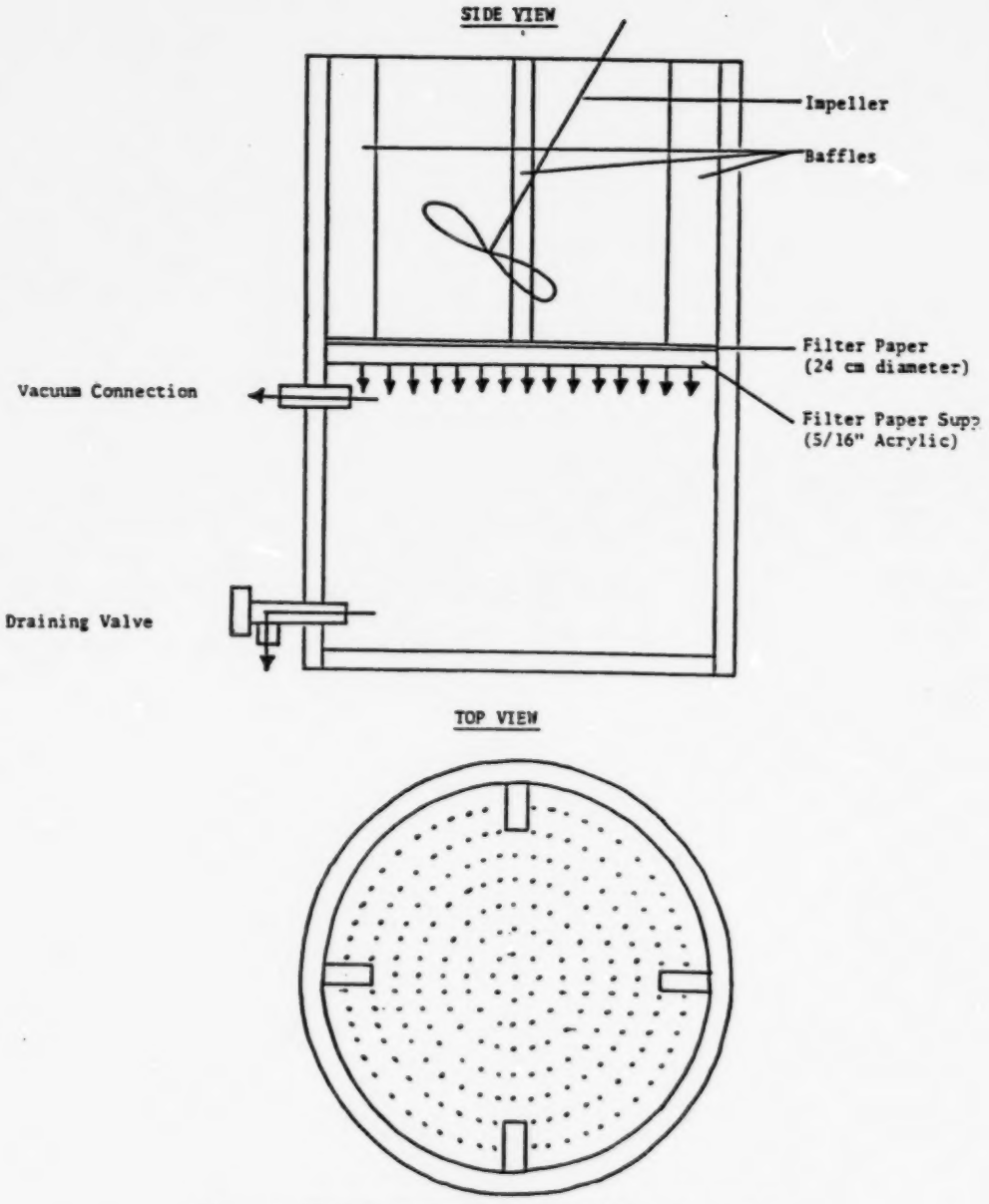

Figure 1: Diagram of the filtration/washing unit used in preparing 5%Ni/Zirconia (Base Catalyst)

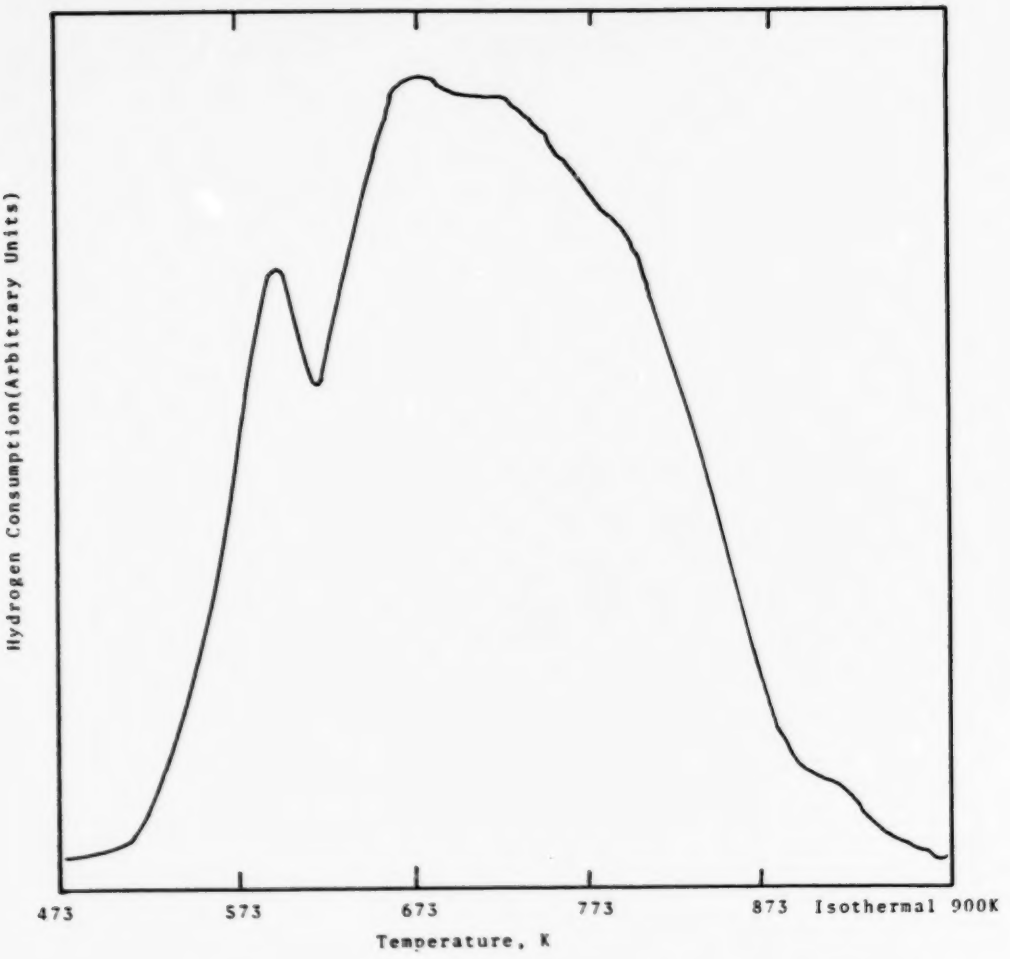

Figure 2. TPR of nickel-cobalt-zirconia catalyst(10% Co/base)

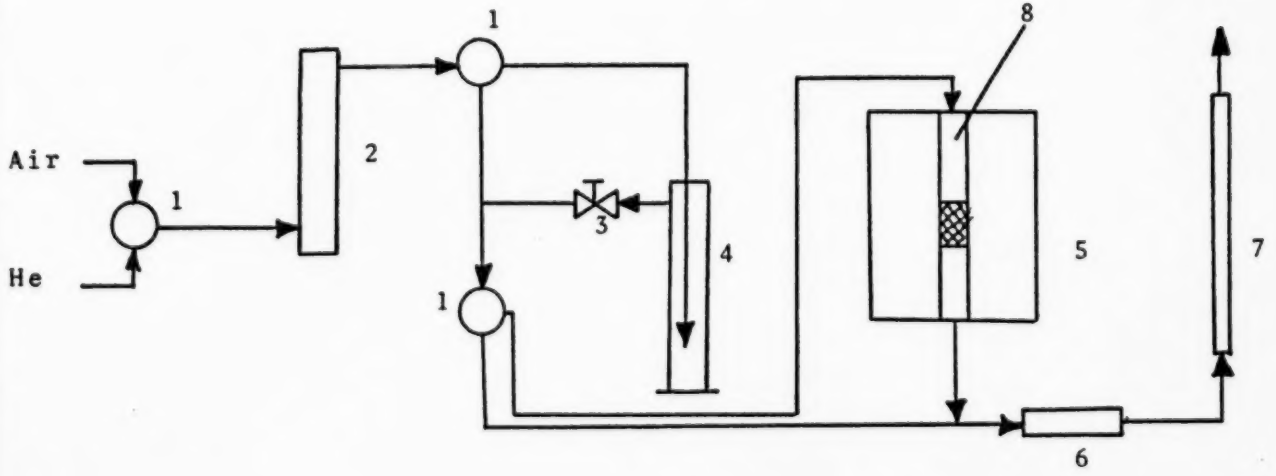

Figure 3. Schematic Diagram of the Apparatus used in Determining the Constraint Index (C.I.) of the Catalyst. 1-3 Way Valve; 2-Rotameter; 3-On/Off Valve; 4-Bubbler; 5-Furnace; 6-Gas Trap; 7-Bubble Flow Meter; 8-Reactor

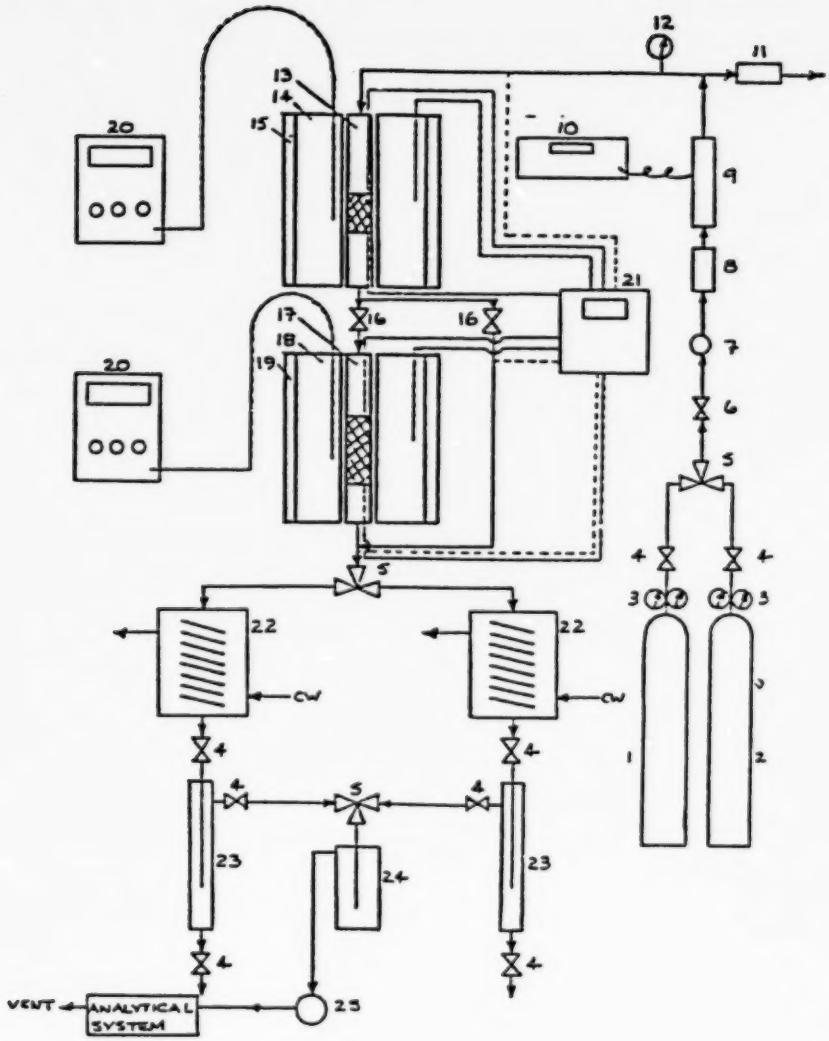

Figure 4. Schematic Diagram of High Pressure Reactor System.(1-feed cylinder; 2-H_2 cylinder; 3-pressure regulator; 4-on/off valve; 5-3-way valve; 6-needle valve; 7-micrometering valve; 8-in-line filter; 9-mass flow transducer; 10-mass flow indicator; 11-relief valve (150 to 350 PSI); 12-pressure guage (0 to 600 PSIG); 13-FT reactor; 14-heating block; 15-heating refractories; 16-on/off valve; 17-HZSM-5 reactor; 18-heating block; 19-heating rafractories; 20-temp. controller; 21-temp. indicator; 22-condensers (water cooled); 23-condensate trap; 24-knock-out drum; 25-back pressure regulator (0 to 500PSIG))

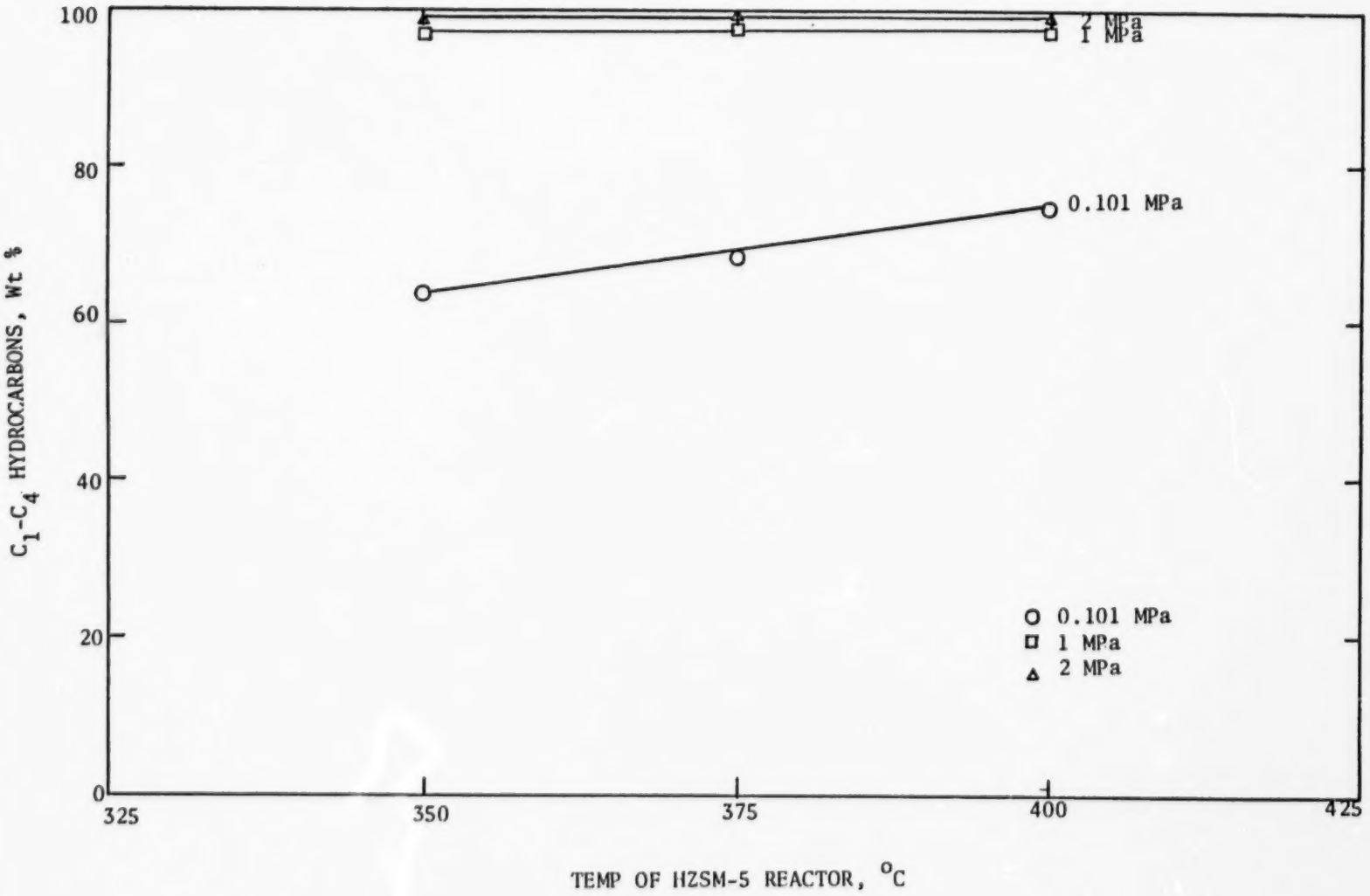

Figure 5 Variation of C_1-C_4 Hydrocarbon Product Distribution with HZSM-5 Bed Temperture (HZSM-5/FT= 1).

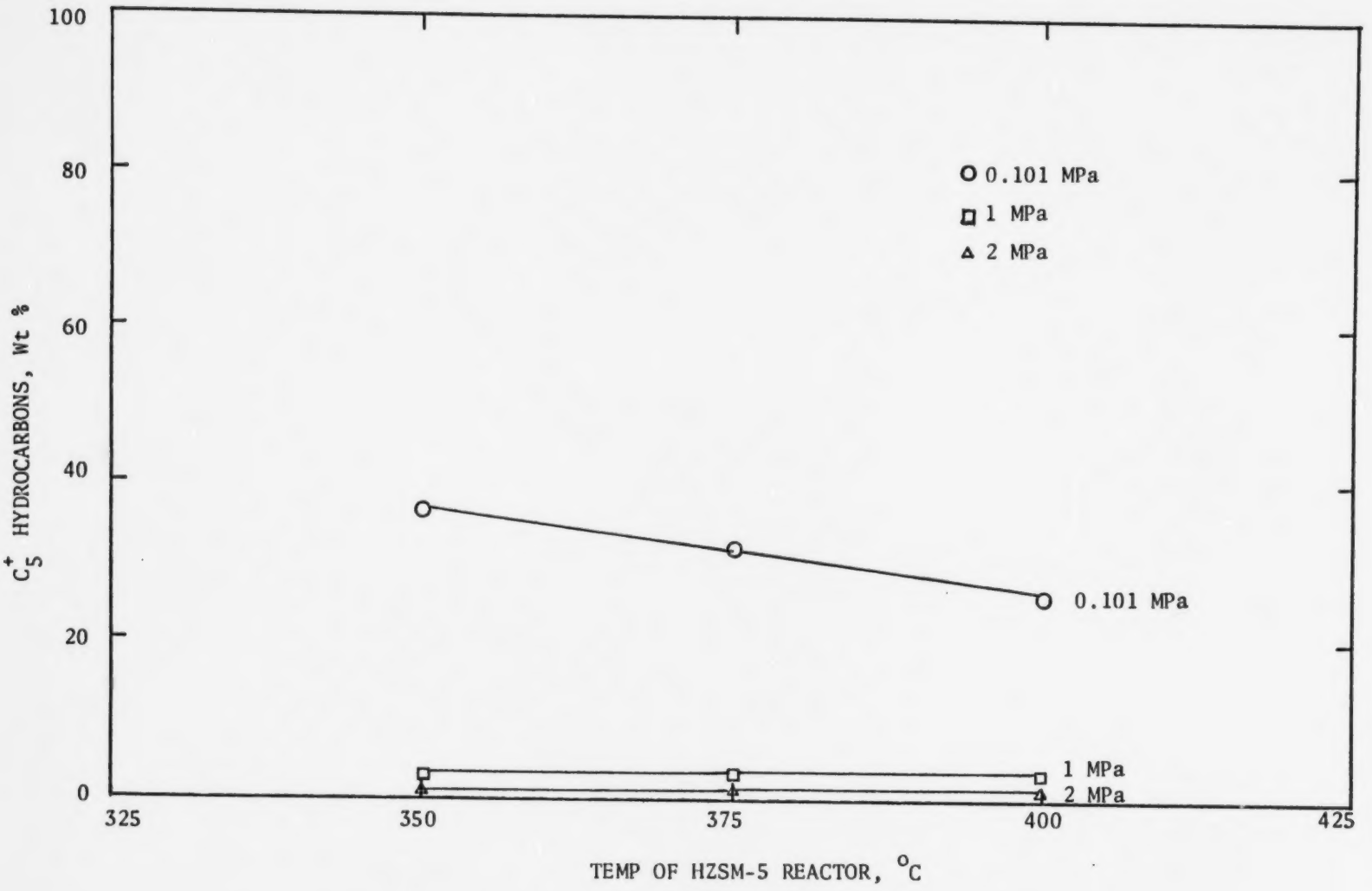

Figure 6: Variation of C_5^+ Hydrocarbons in the Hydrocarbon Product with the HZSM-5 Bed Temperature (HZSM-5/FT =1)

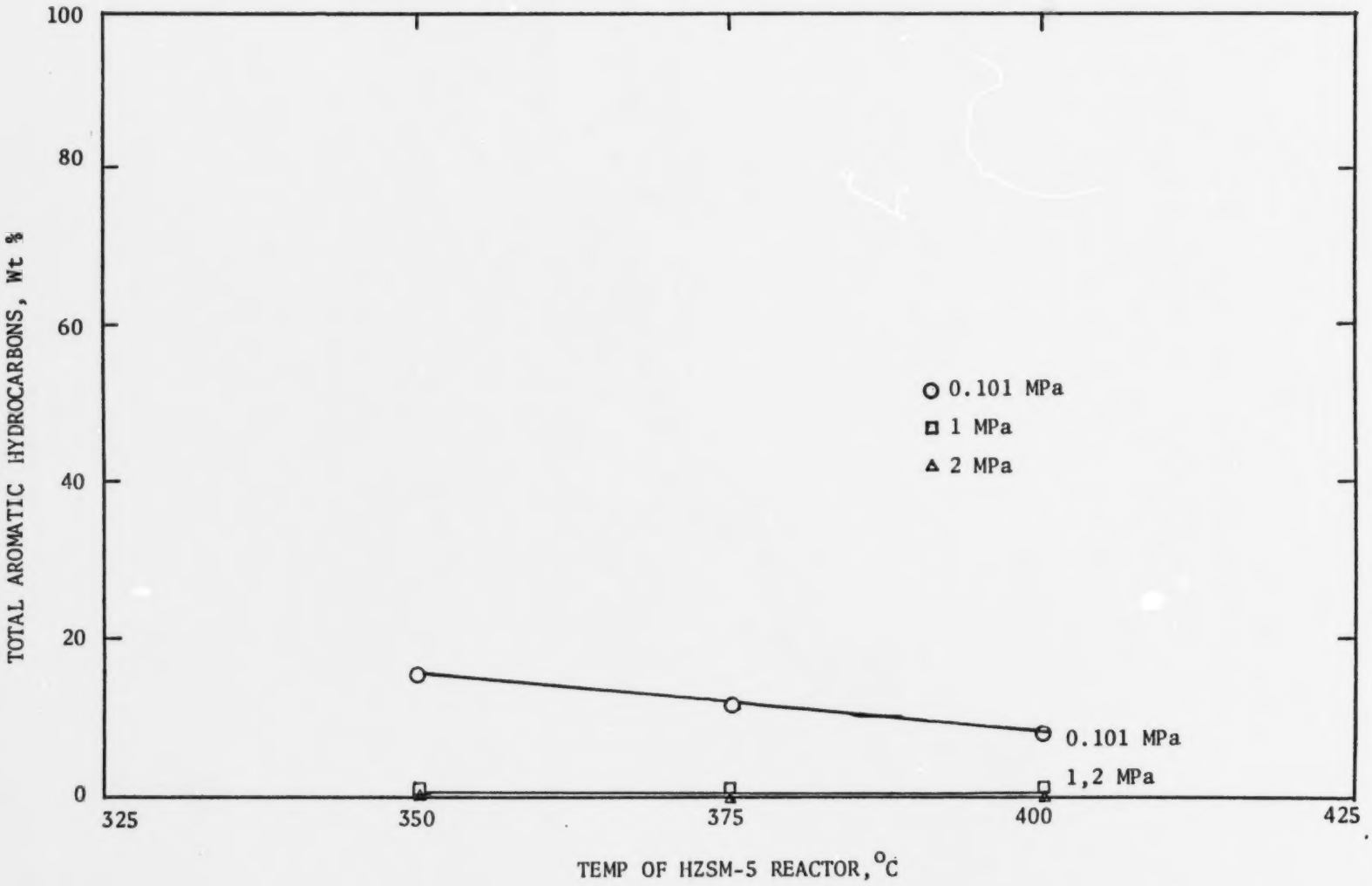

Figure 7: Variations of Total Aromatic Hydrocarbons in the Hydrocarbon Product with the HZSM-5 Bed Temperature (HZSM-5/FT =1)

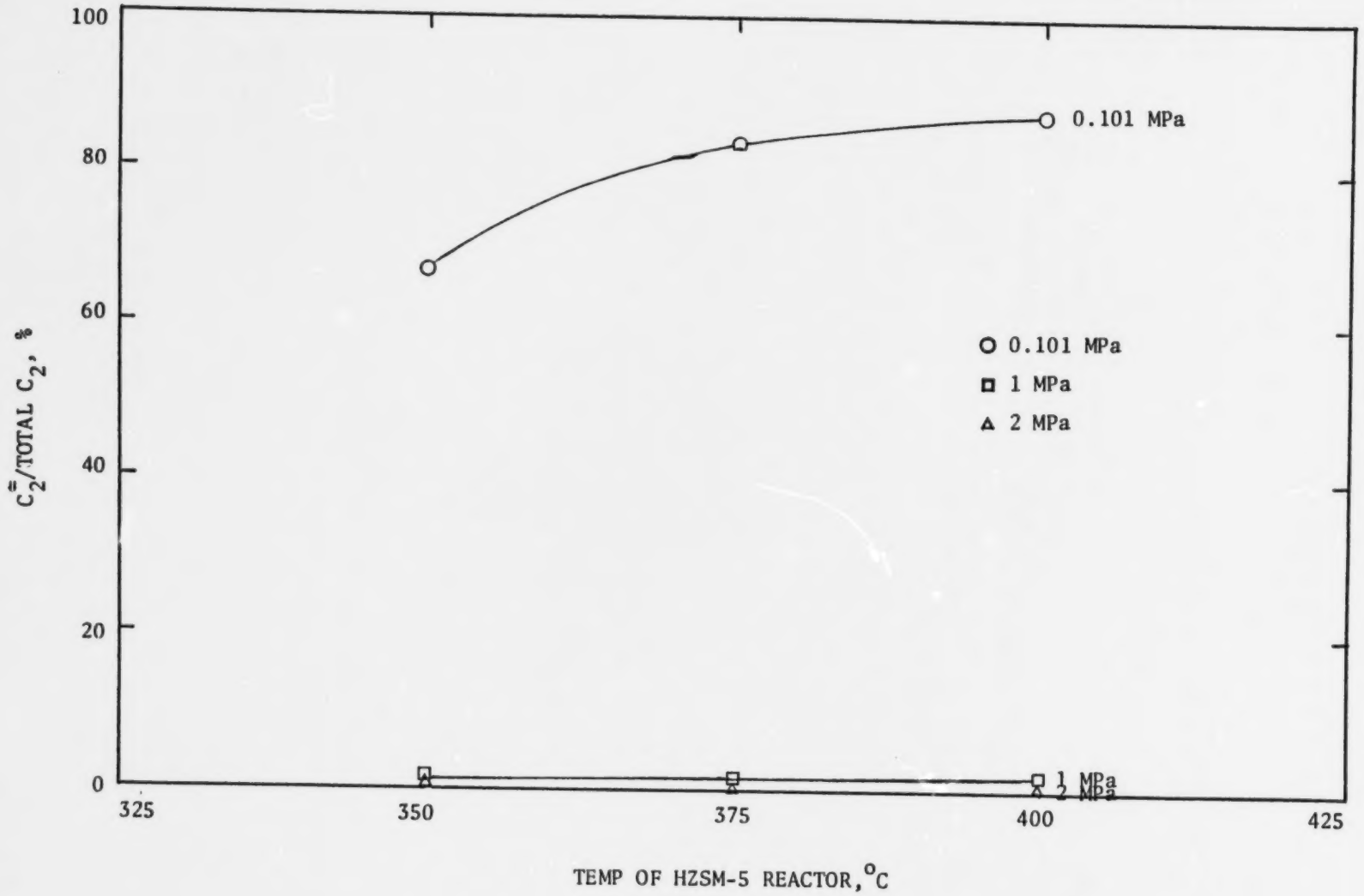

Figure 8: Variation of $C_2^=/C_2$ Fraction in the Hydrocarbon Product with Temperature of the HZSM-5 Bed,(HZSM-5/FT= 1).

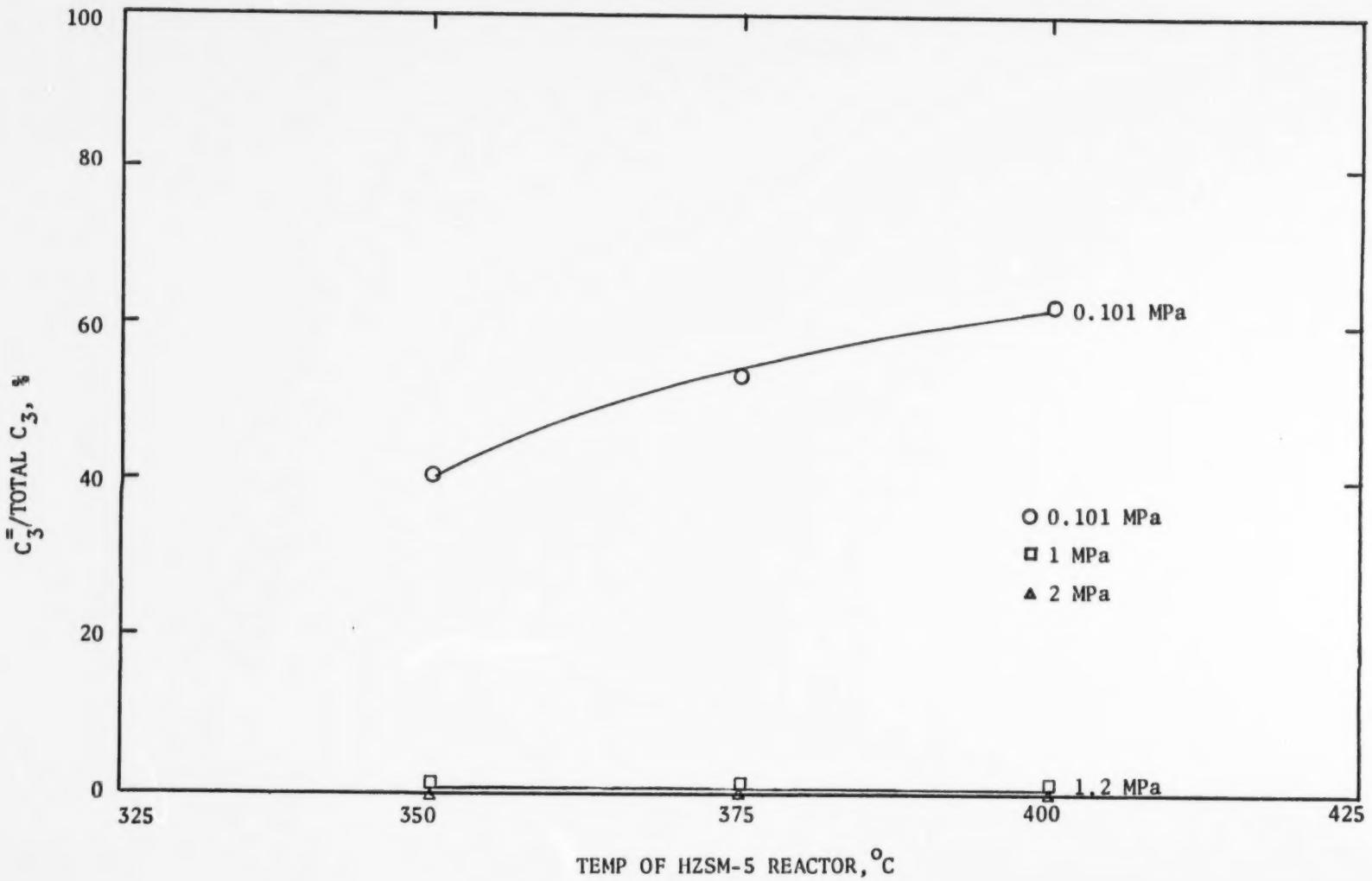

Figure 9: Variation of $C_3^=/C_3$ Fraction in the Hydrocarbon Product with Temperature of the HZSM-5 Bed, (HZSM-5/FT= 1)

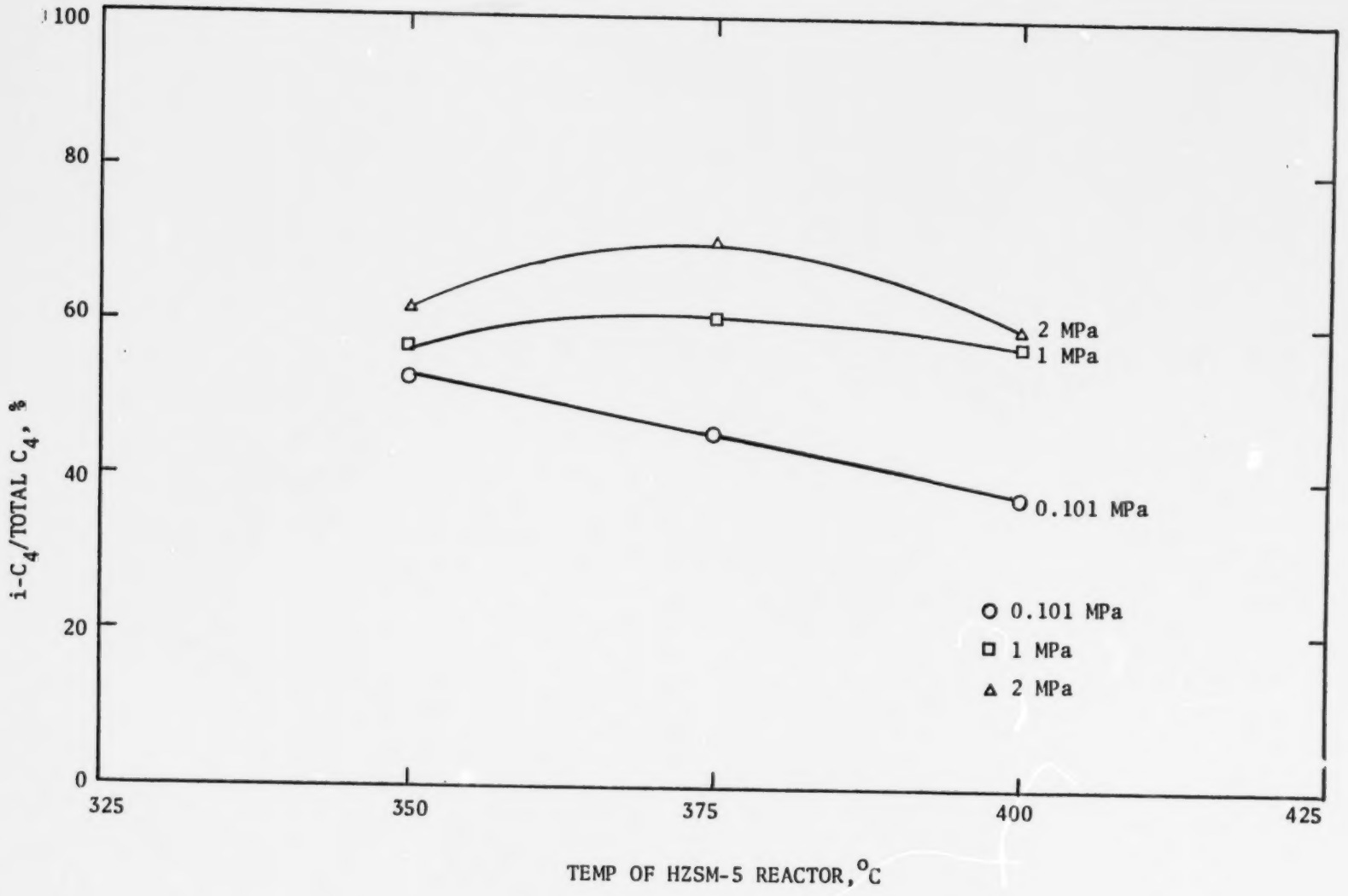

Figure 10: Variation of the i-C_4/C_4 Fraction in the Hydrocarbon Product with the Temperature of the HZSM-5 Bed (HZSM-5/FT = 1)

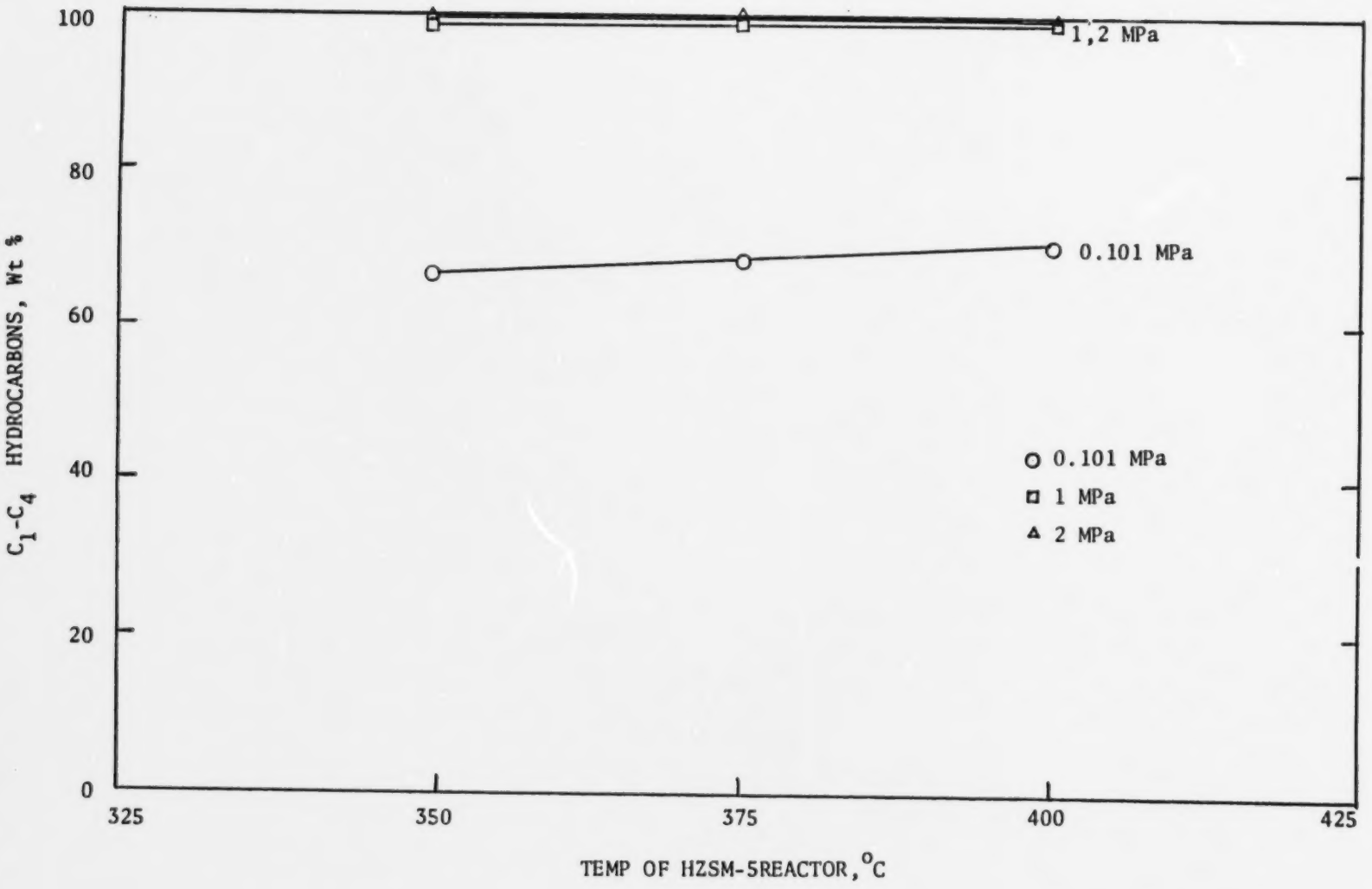

Figure 11 Variation of C_1-C_4 Hydrocarbon Product Distribution with the HZSM-5 Bed Temperature (HZSM-5/FT= 2.5)

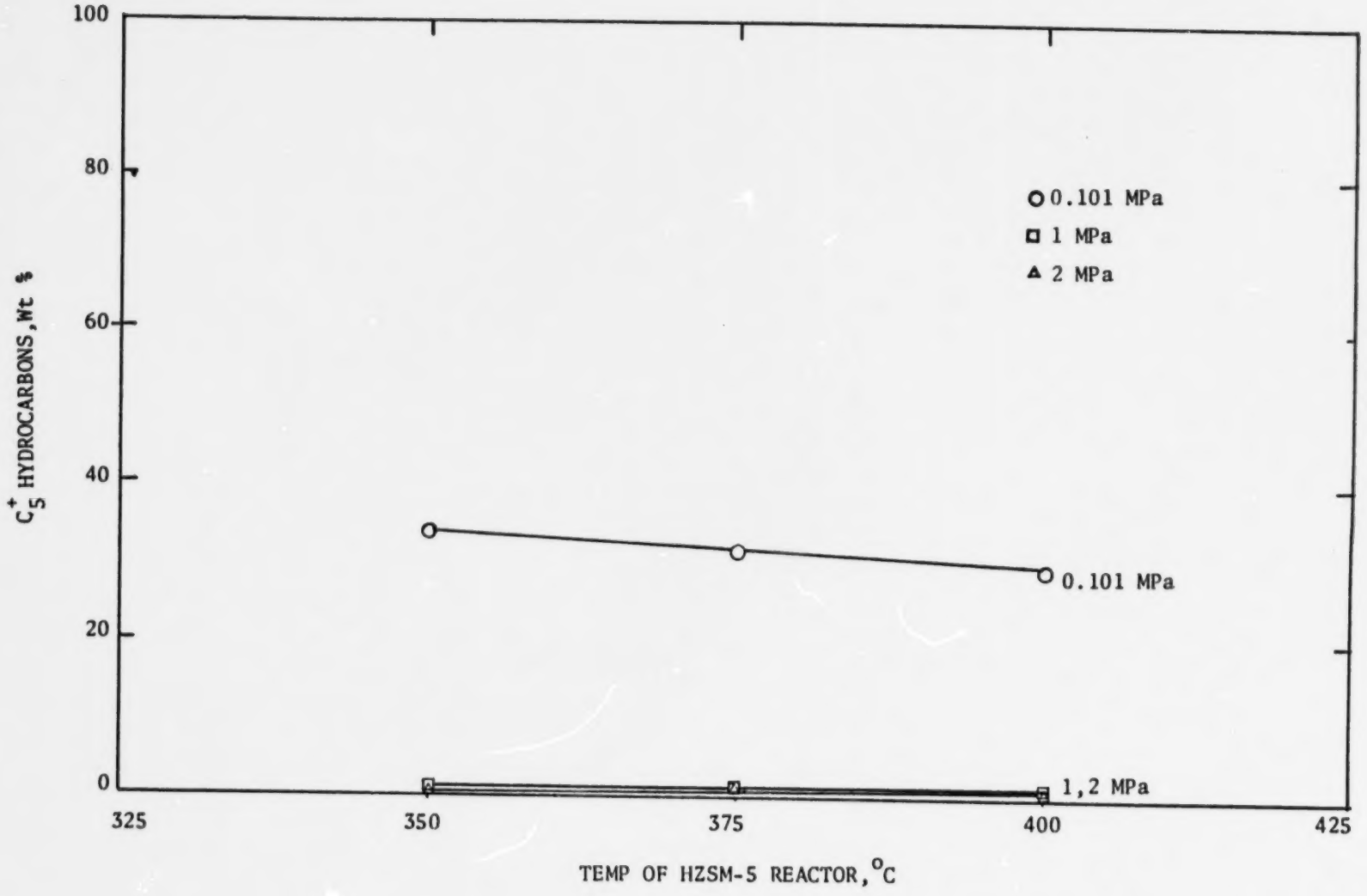

Figure 12: Variation of C_5^+ Hydrocarbons in the Hydrocarbon Product with the HZSM-5 Bed Temperature (HZSM-5/FT = 2.5)

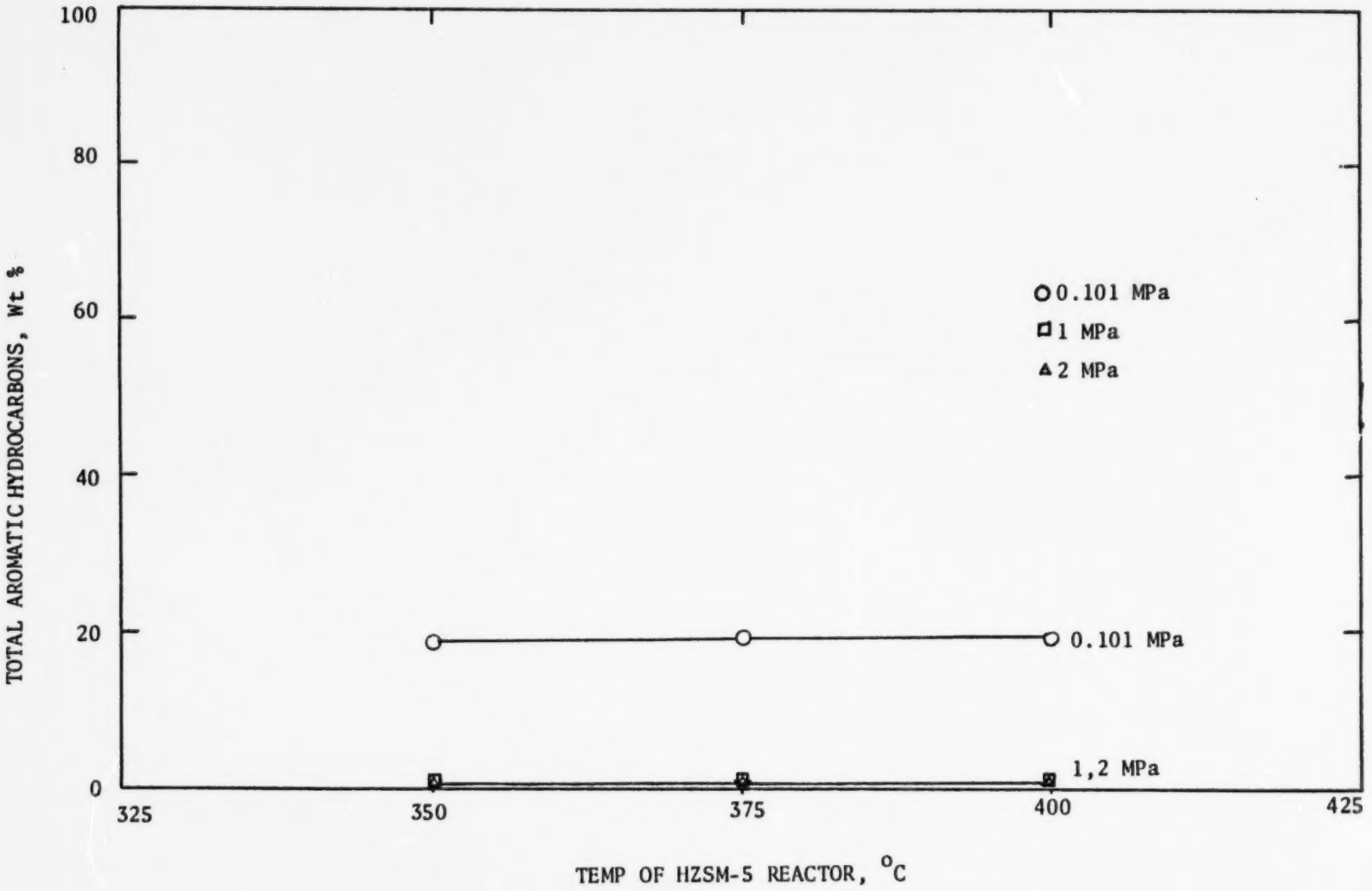

Figure 13 Variations of Total Aromatic Hydrocarbons in the Hydrocarbon Product with the HZSM-5 Bed Temperature (HZSM-5/FT = 2.5)

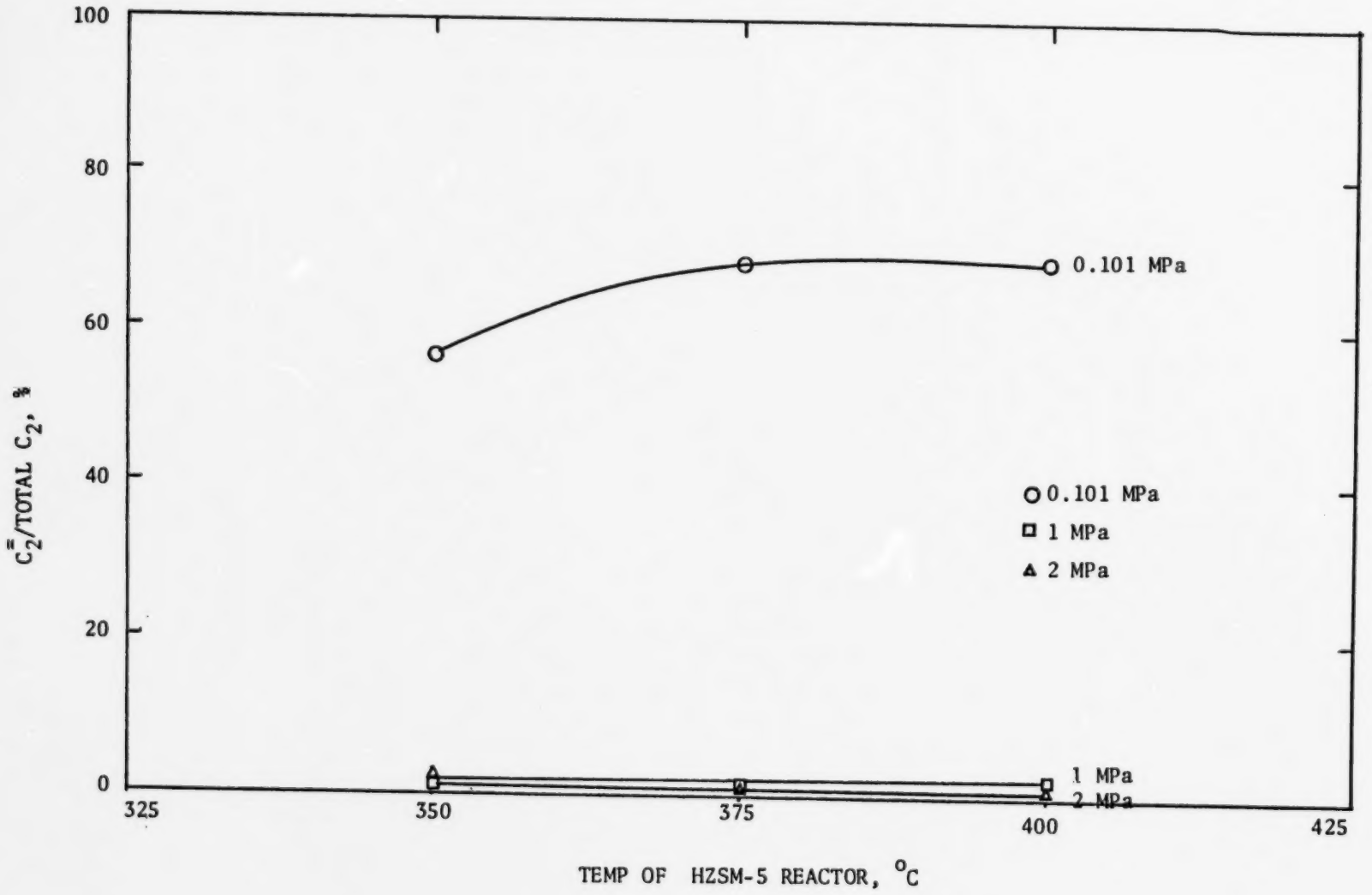

Figure 14 Variation of $C_2^=/C_2$ Fraction in the Hydrocarbon Product with Temperature of the HZSM-5 Bed,(HZSM-5/FT= 2.5).

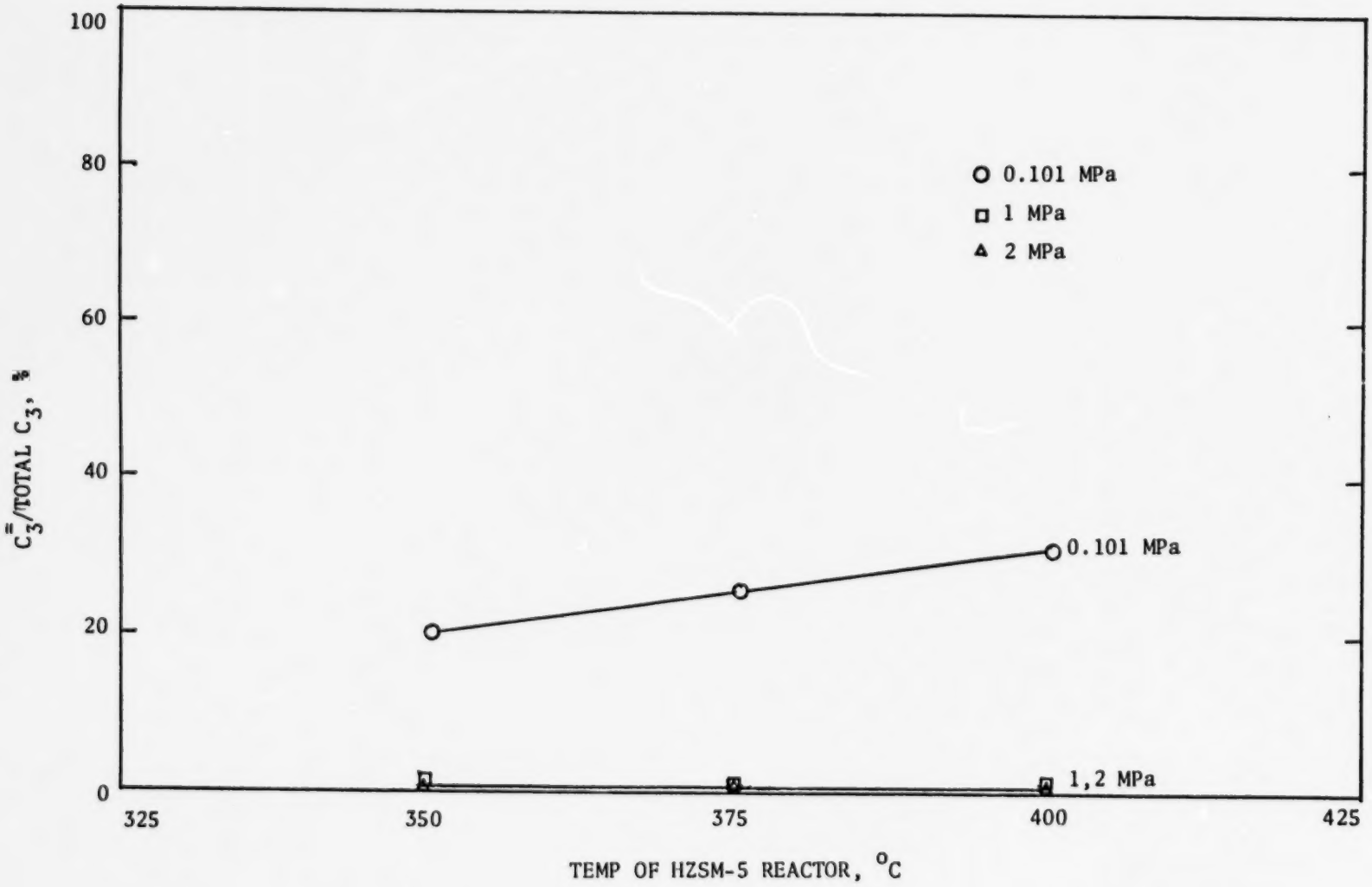

Figure 15 Variation of $C_3^=/C_3$ Fraction in the Hydrocarbon Product with Temperature of the HZSM-5 Bed, (HZSM-5/FT= 2.9.

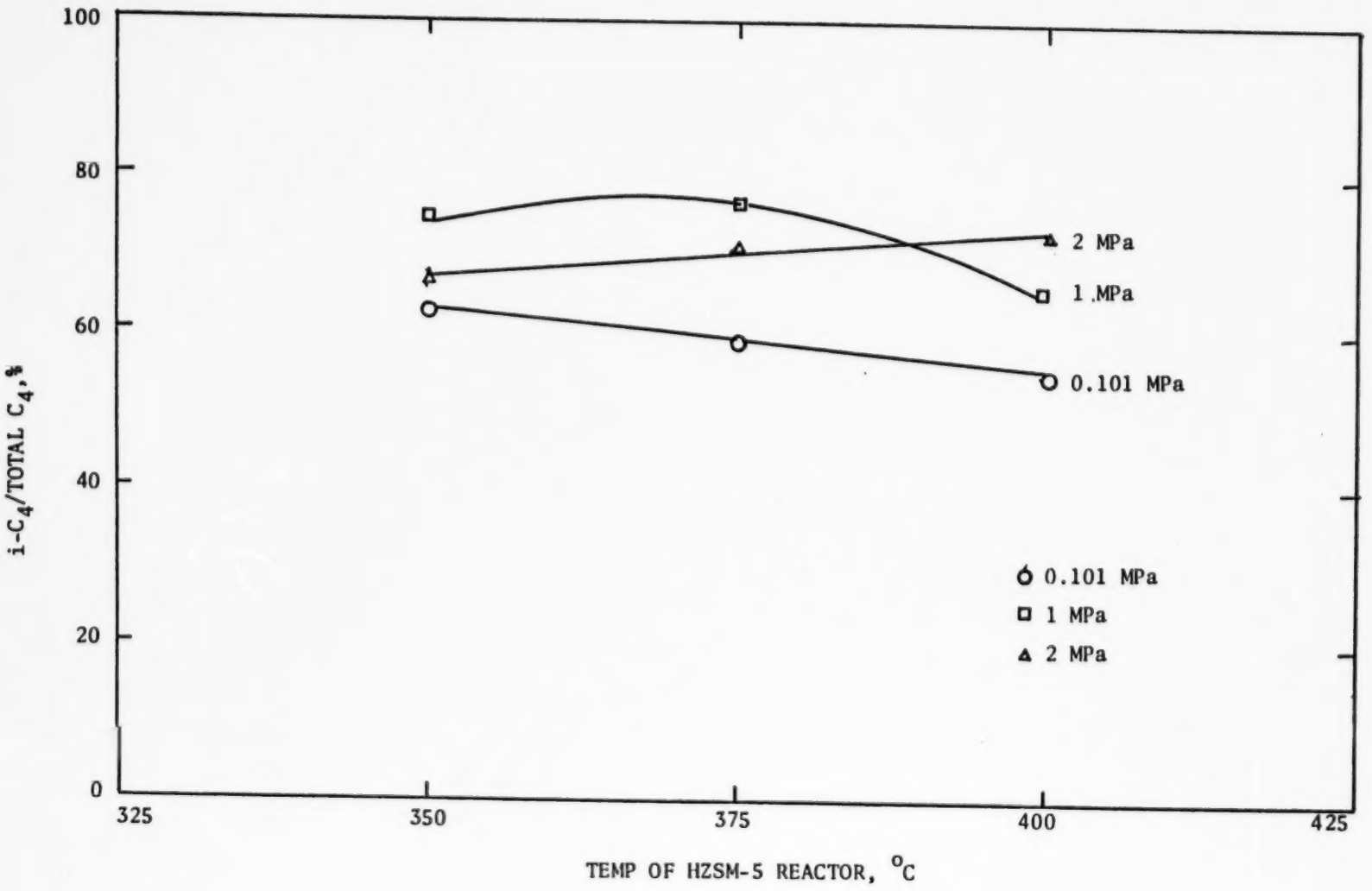

Figure 16 Variation of the i-C_4/C_4 Fraction in the Hydrocarbon Product with the Temperature of the HZSM-5 Bed (HZSM-5/FT = 2.5)

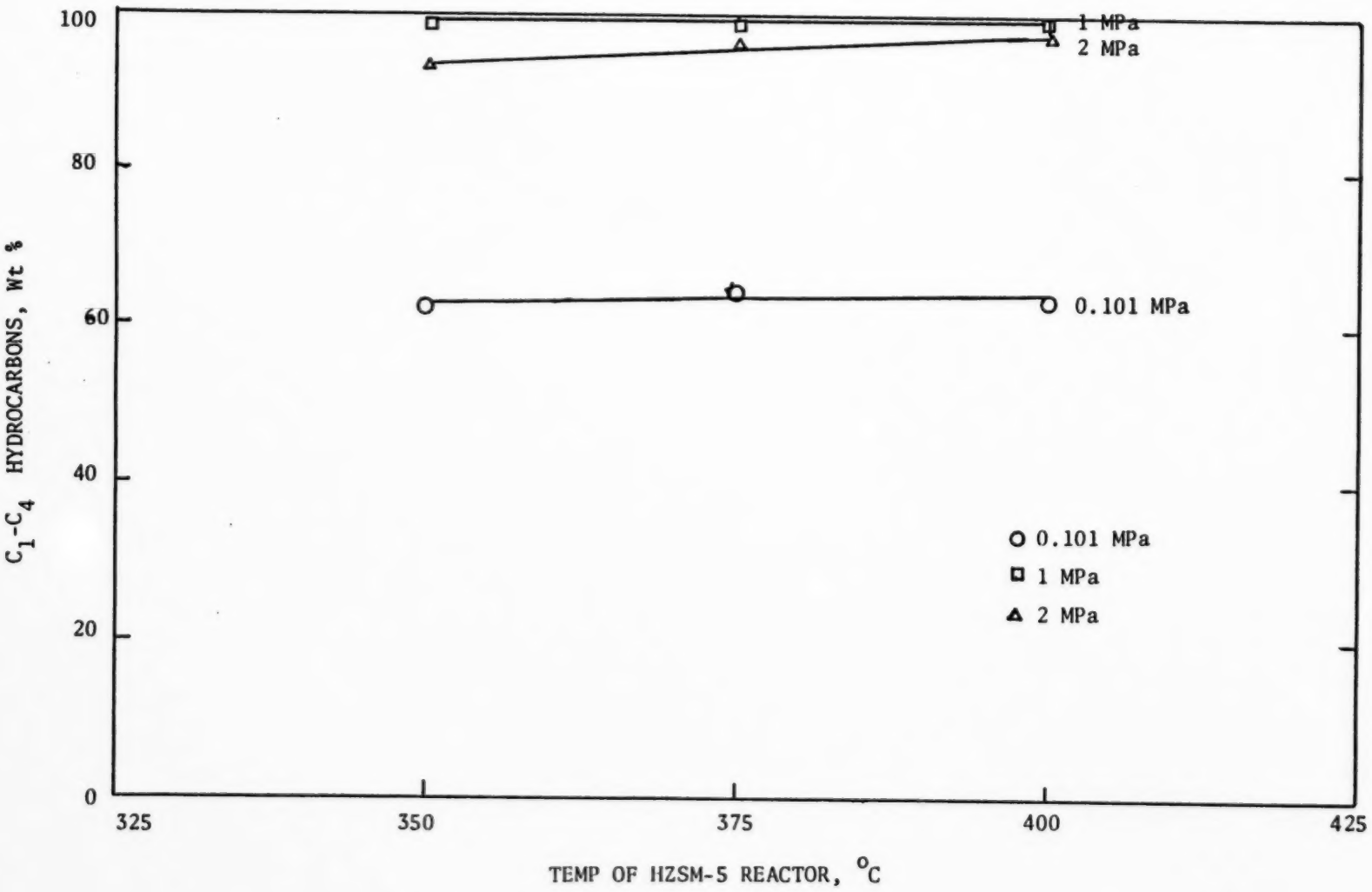

Figure 17 Variation of C_1-C_4 Hydrocarbon Product Distribution with the HZSM-5 Bed Temperature (HZSM-5/FT= 4)

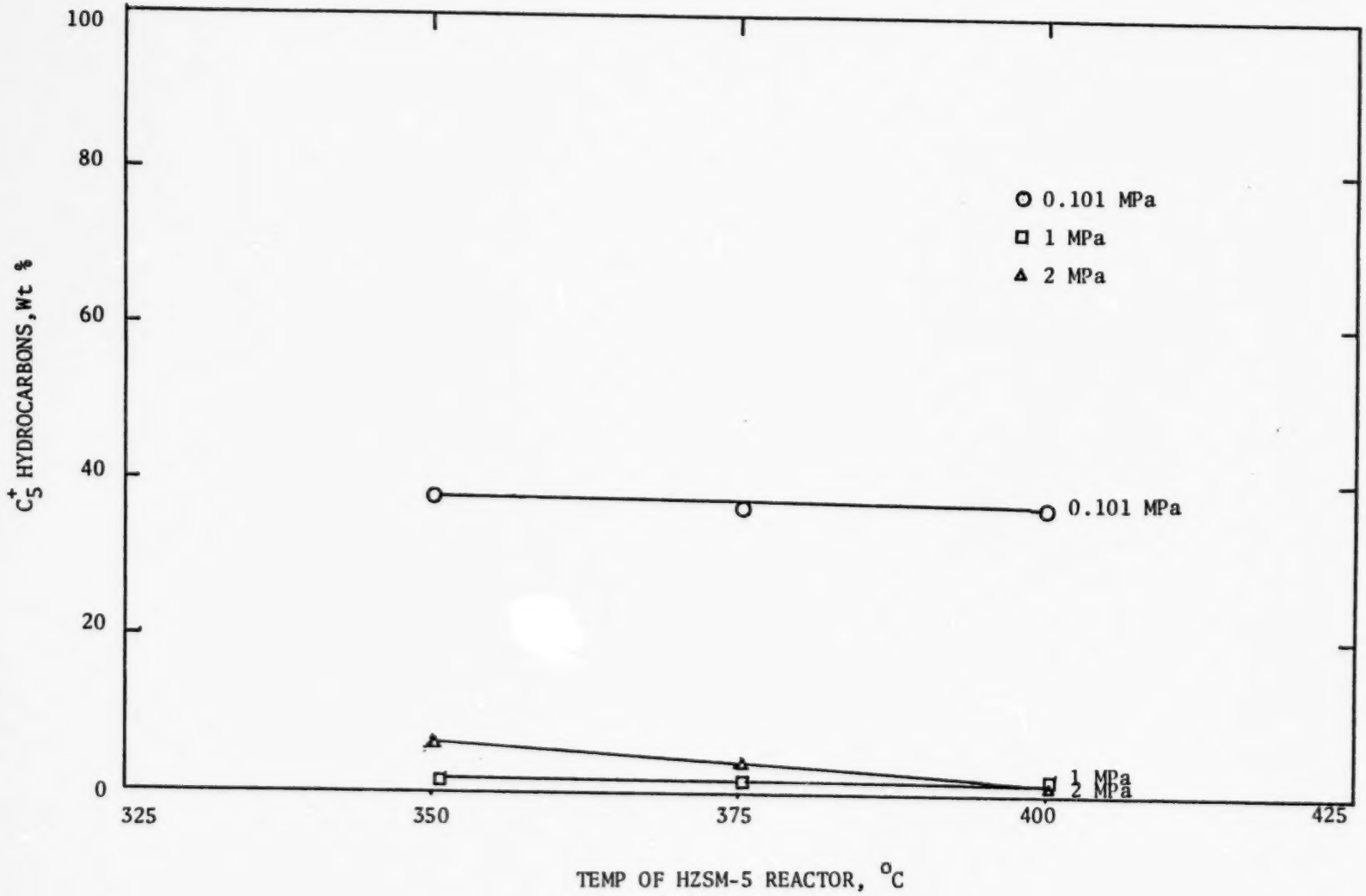

Figure 18 Variation of C_5^+ Hydrocarbons in the Hydrocarbon Product with the HZSM-5 Bed Temperature (HZSM-5/FT = 4)

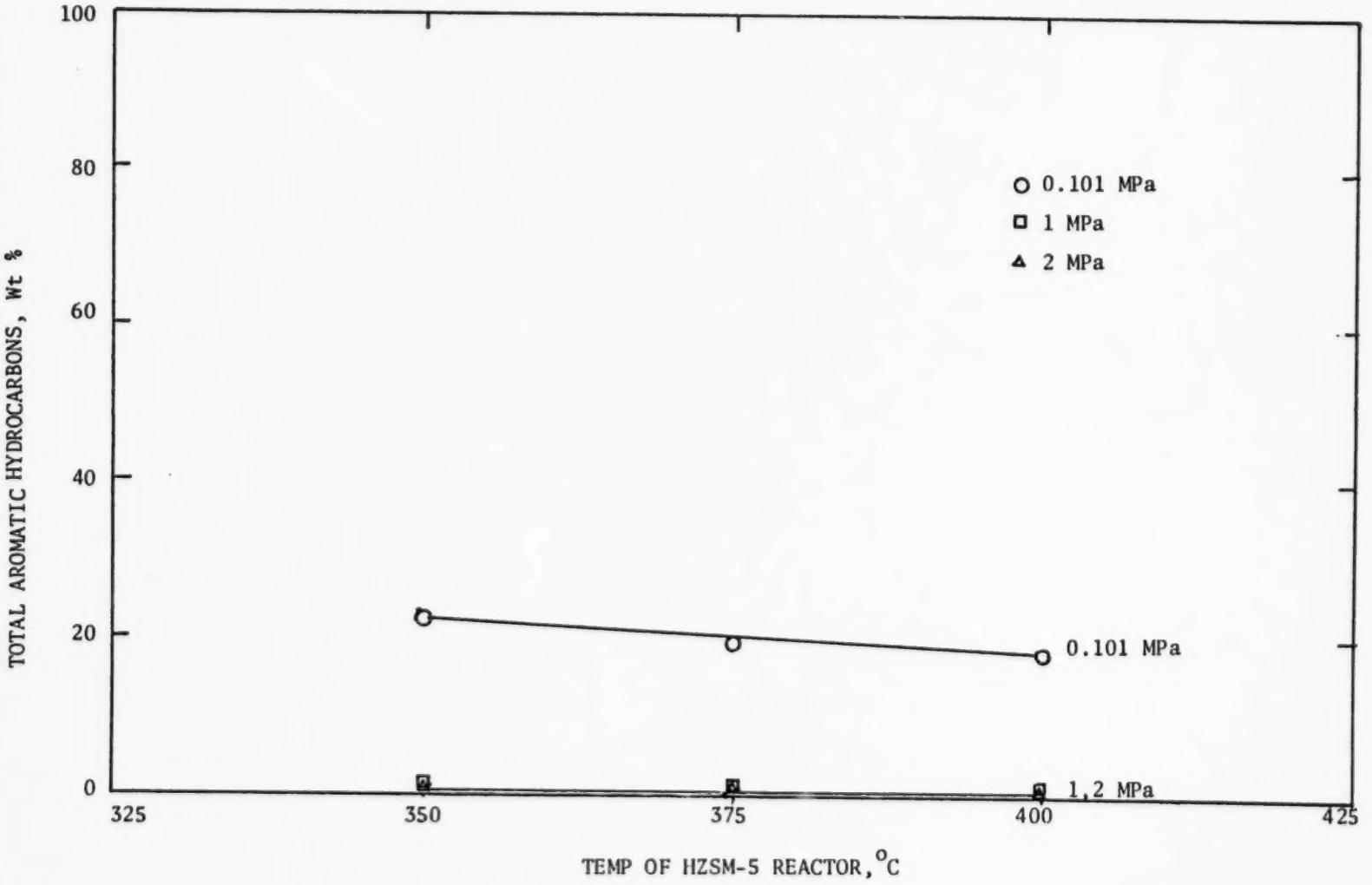

Figure 19 Variations of Total Aromatic Hydrocarbons in the Hydrocarbon Product with the HZSM-5 Bed Temperature (HZSM-5/FT = 4)

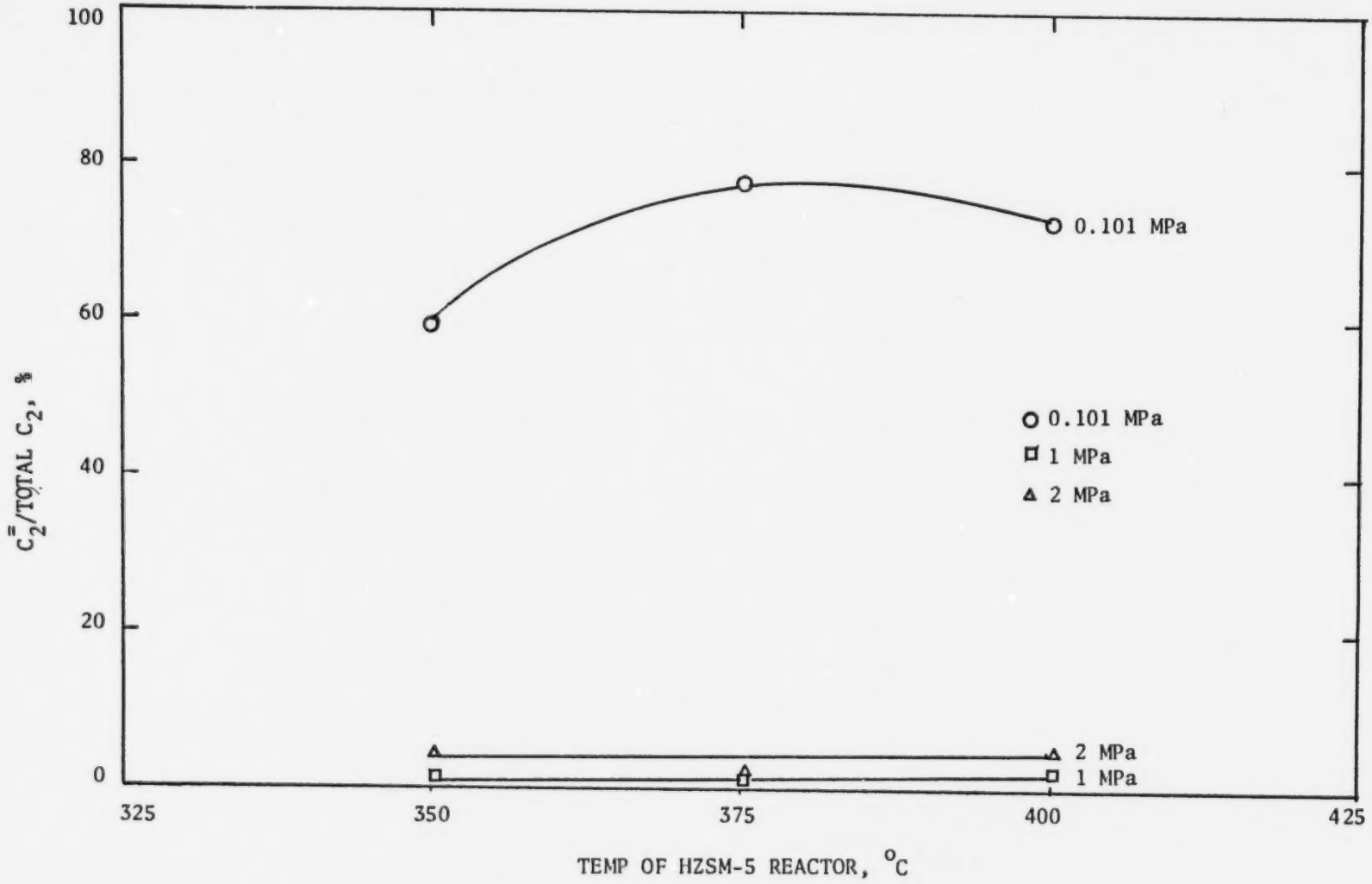

Figure 20 Variation of $C_2^=/C_2$ Fraction in the Hydrocarbon Product with Temperature of the HZSM-5 bed, (HZSM-5/FT= 4).

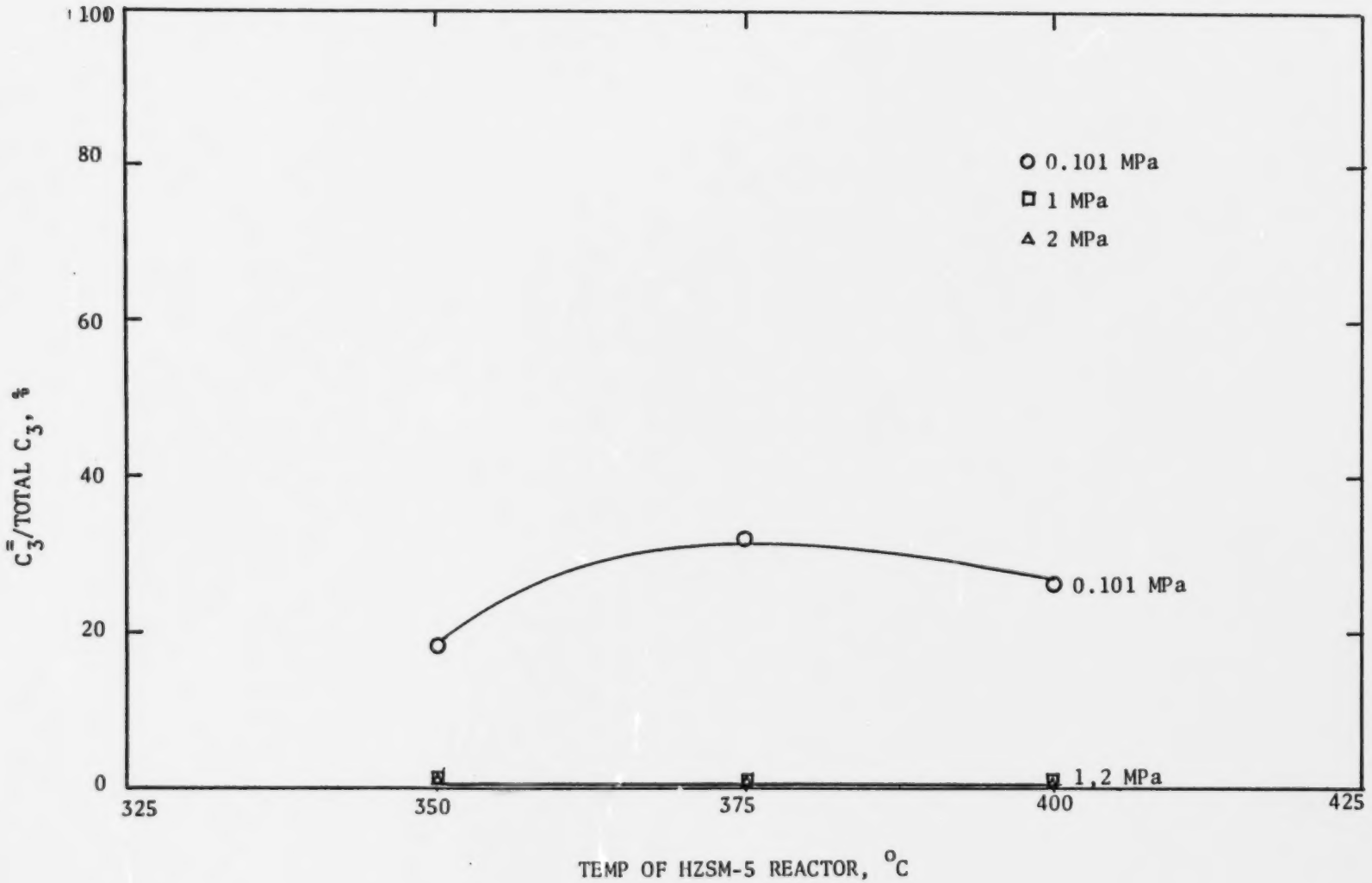

Figure 21 Variation of $C_3^=/C_3$ Fraction in the Hydrocarbon Product with Temperature of the HZSM-5 Bed, (HZSM-5/FT= 4).

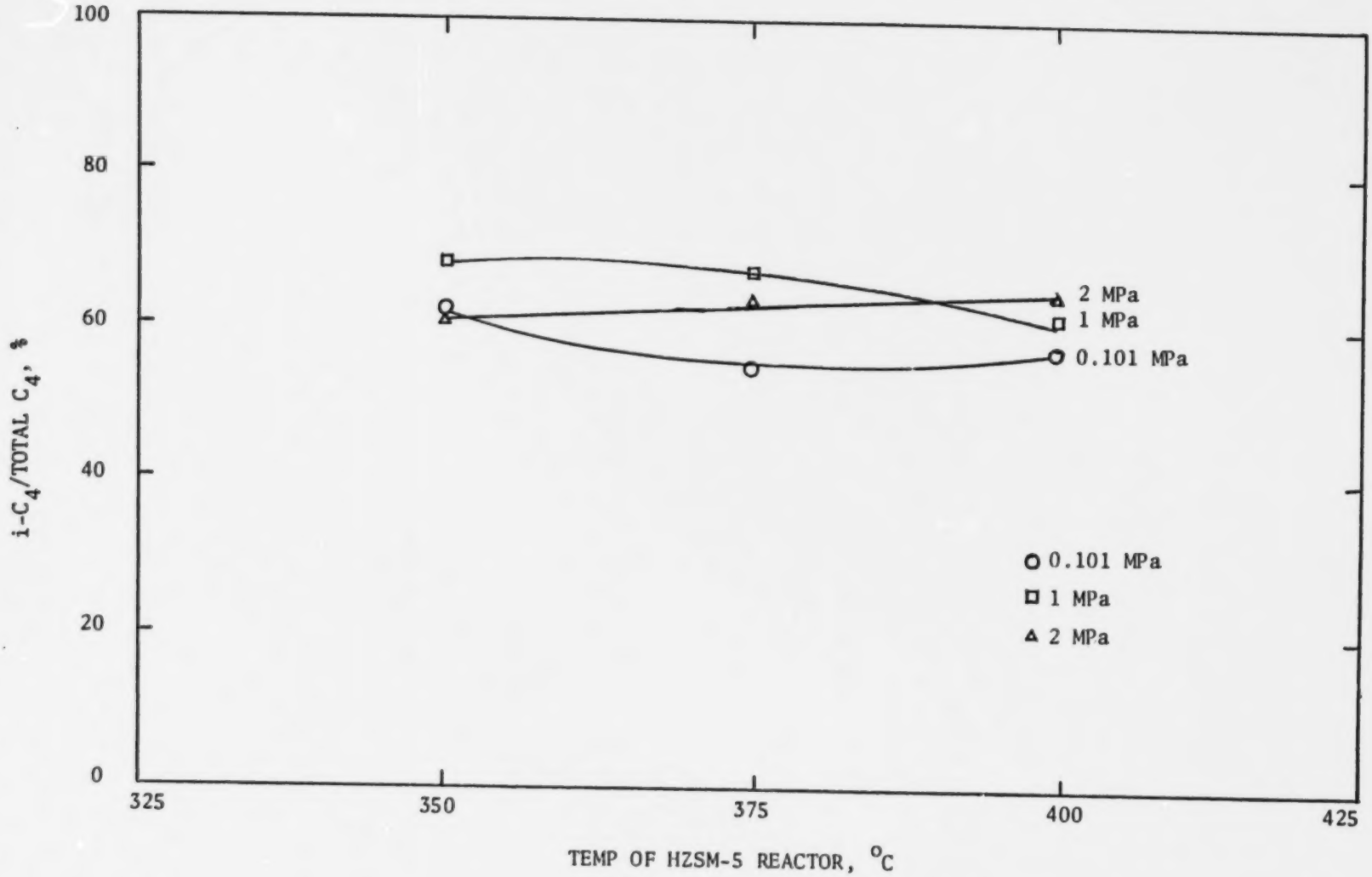

Figure 22 Variation of the i-C_4/C_4 Fraction in the Hydrocarbon Product with the Temperature of the HZSM-5 Bed (HZSM-5/FT = 4)

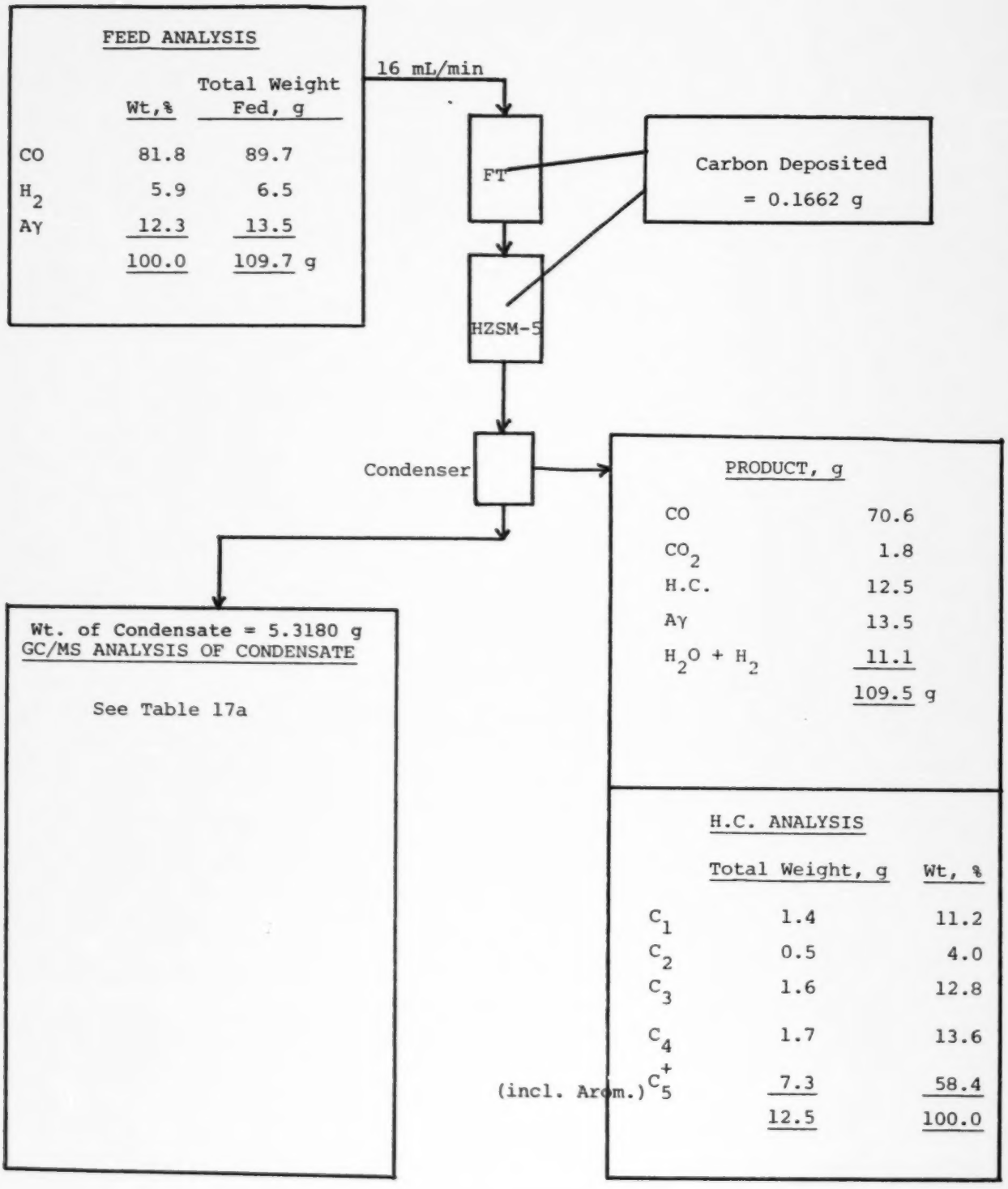

Figure 23. Overall Material Balance (Operating Conditions given in Table 17)

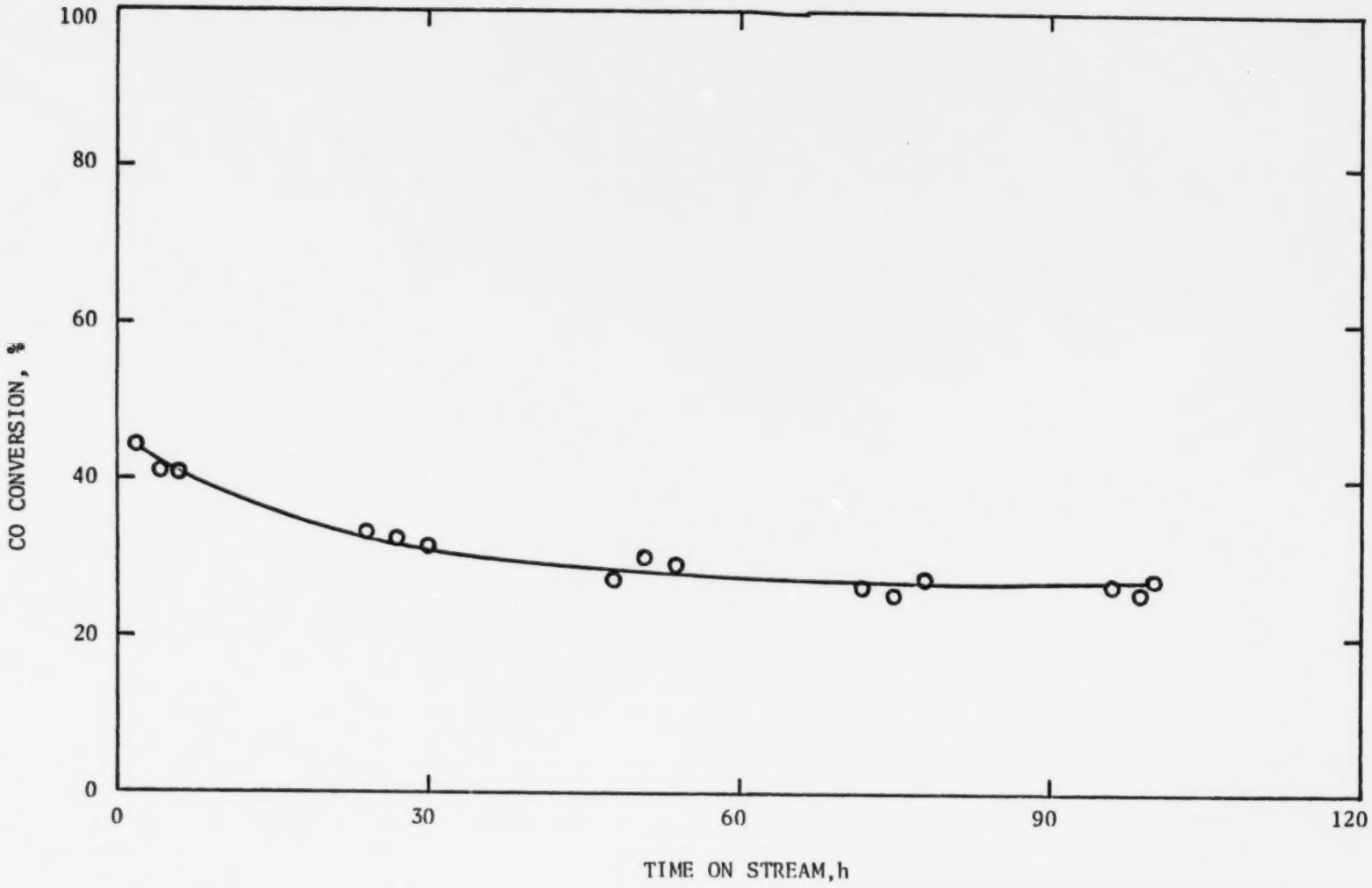

Figure 24 Variation of Carbon Monoxide Conversion with Time-on-Stream

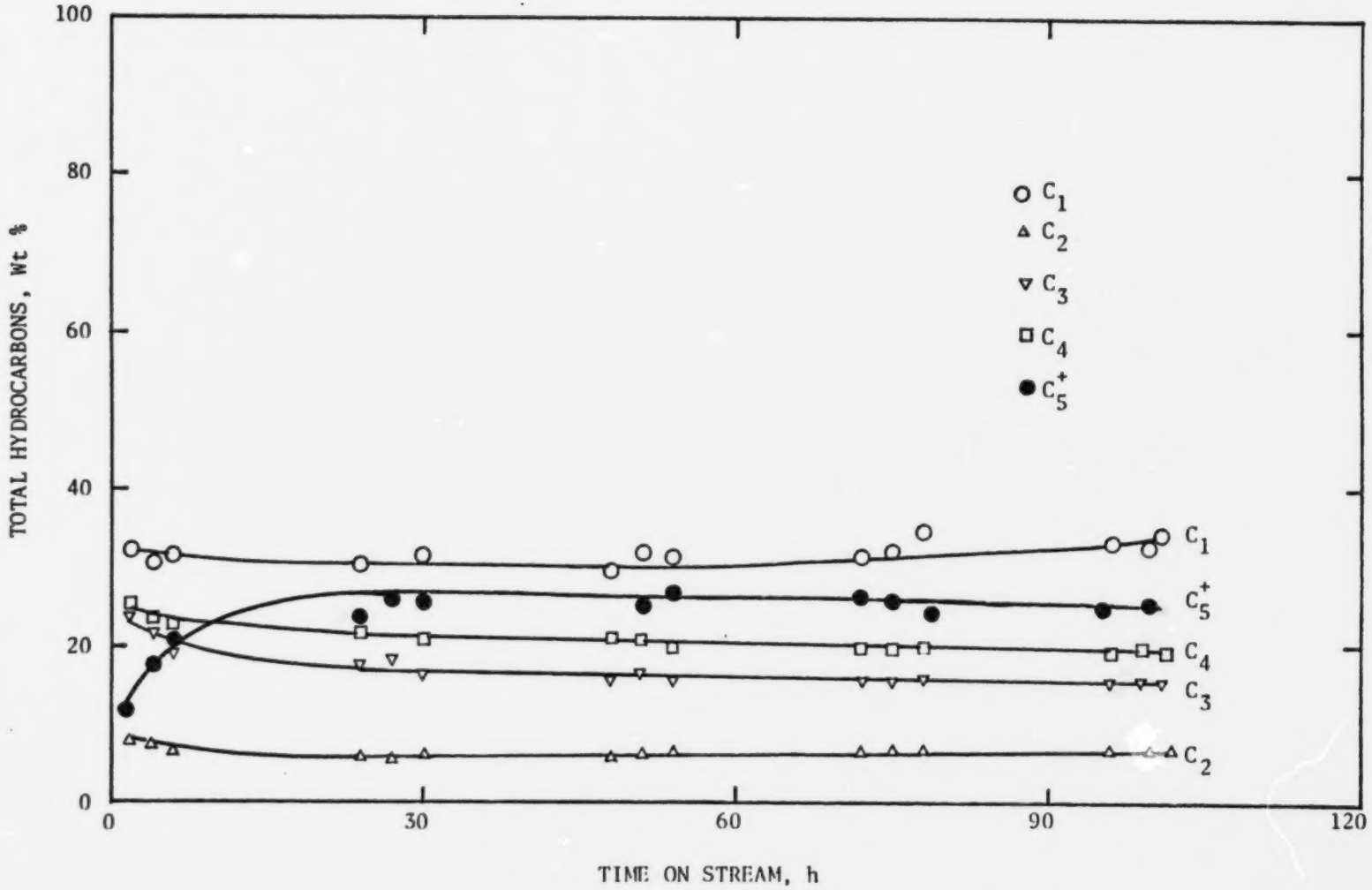

Figure 25 Hydrocarbon Product Distribution with Time-on-Stream

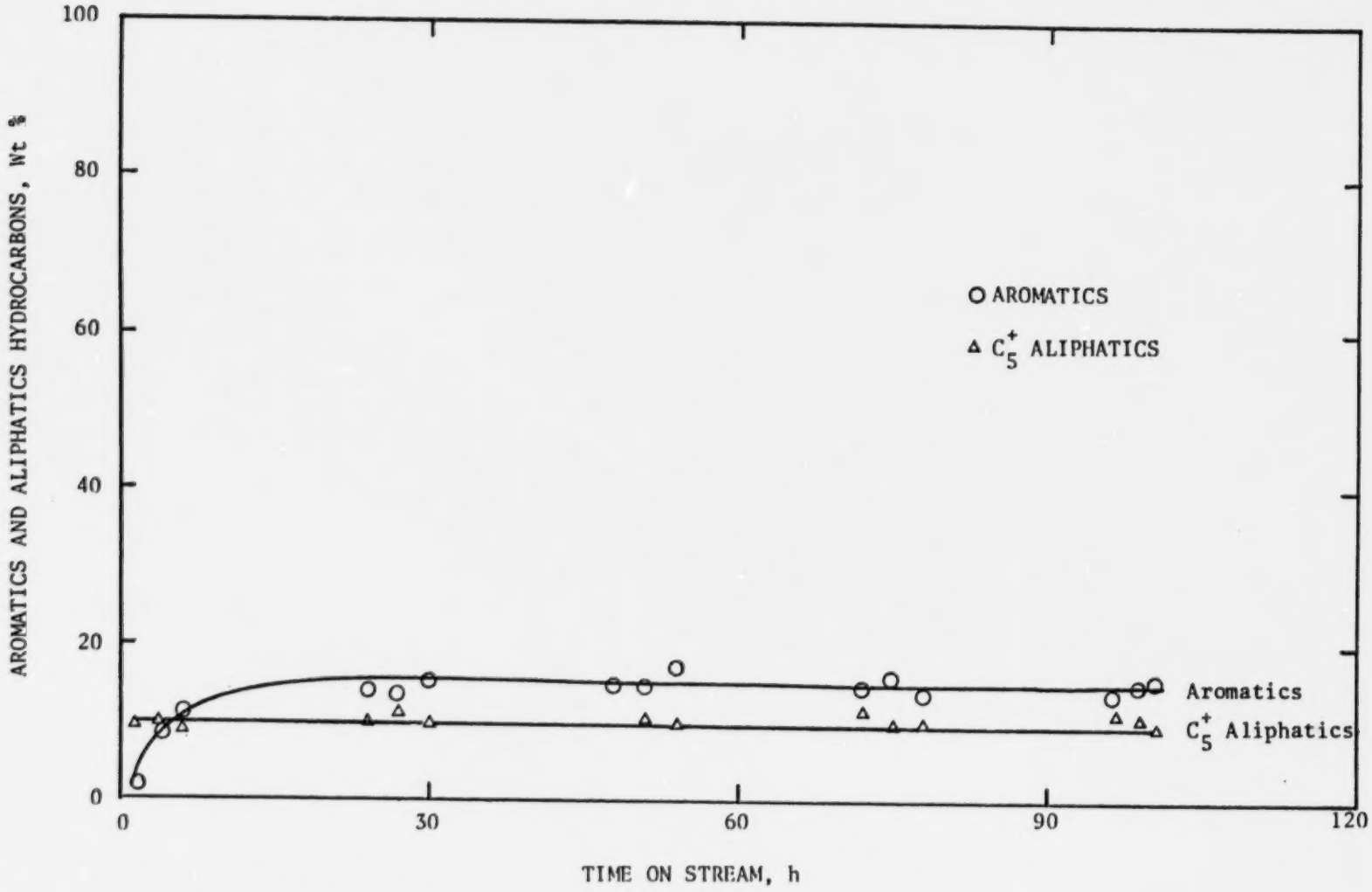

Figure 26 Aromatics and Aliphatics Hydrocarbons in the Hydrocarbon Product with Time-on-Stream

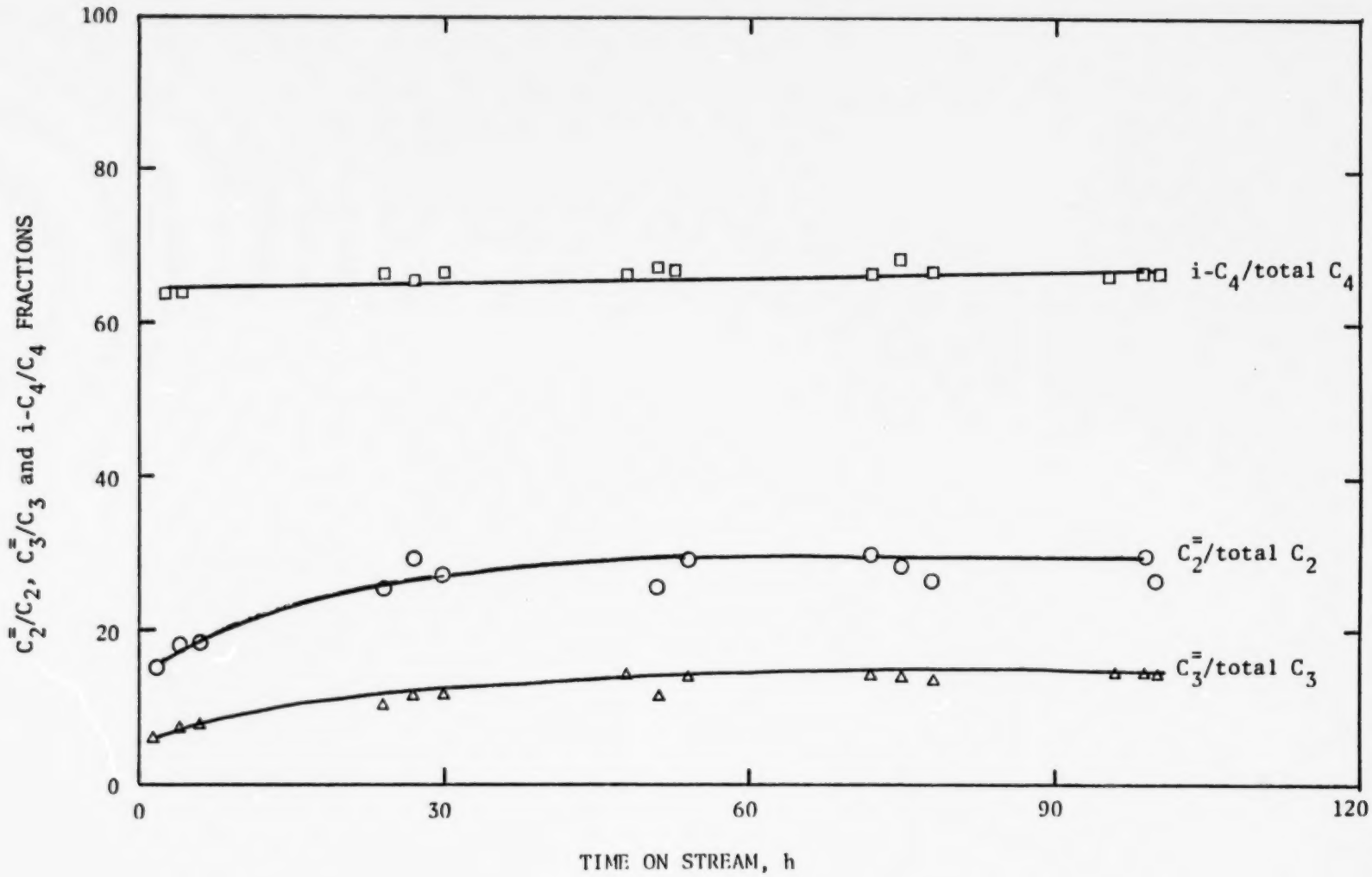

Figure 27 $C_2^=/C_2$, $C_3^=/C_3$ and i-C_4/C_4 Fractions in the Hydrocarbon Product with Time-on-Stream.

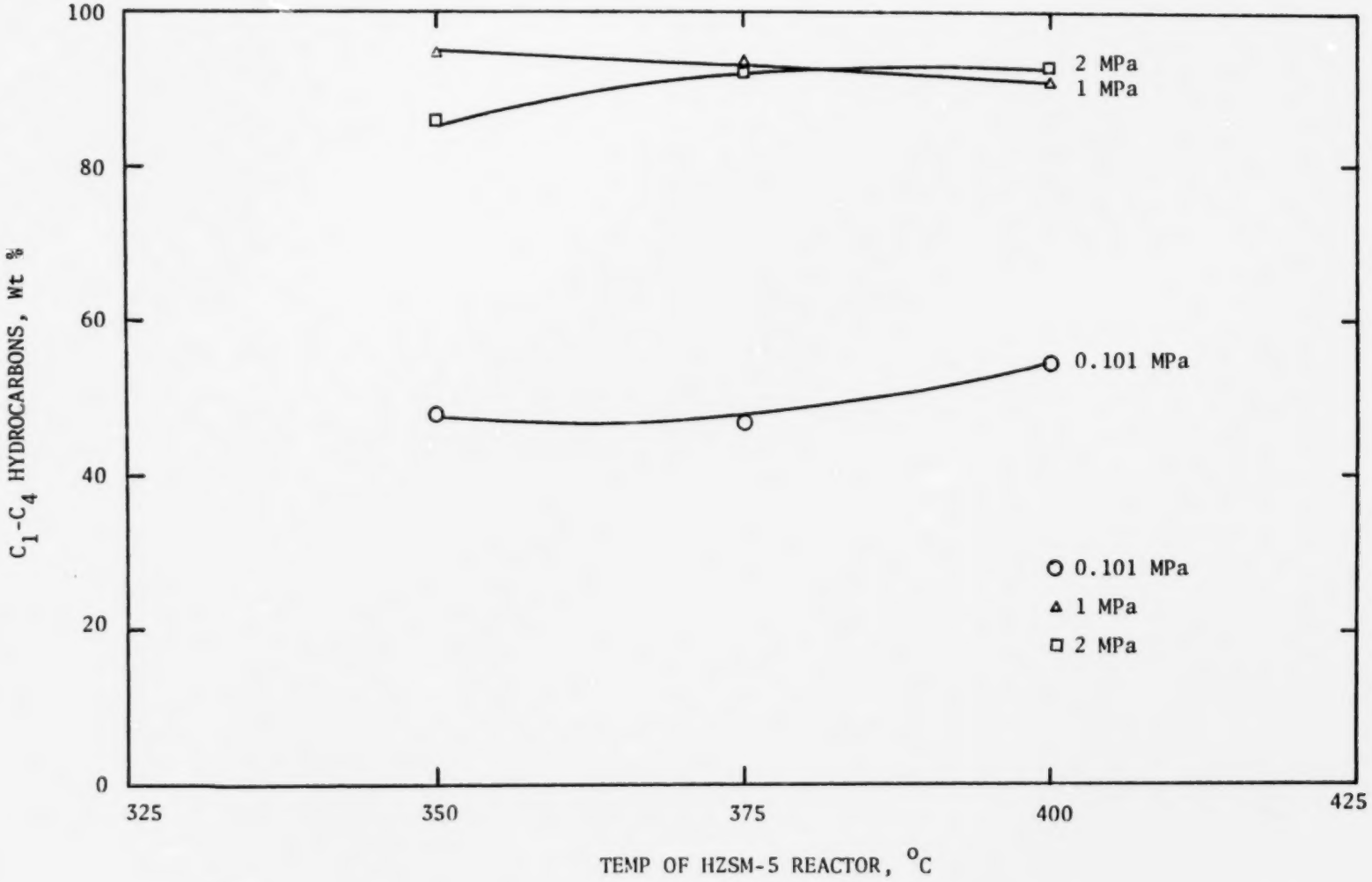

Figure 28 . Variation of C_1-C_4 Hydrocarbon Product Distribution with the HZSM-5 Bed Temperature (HZSM-5/FT=1).

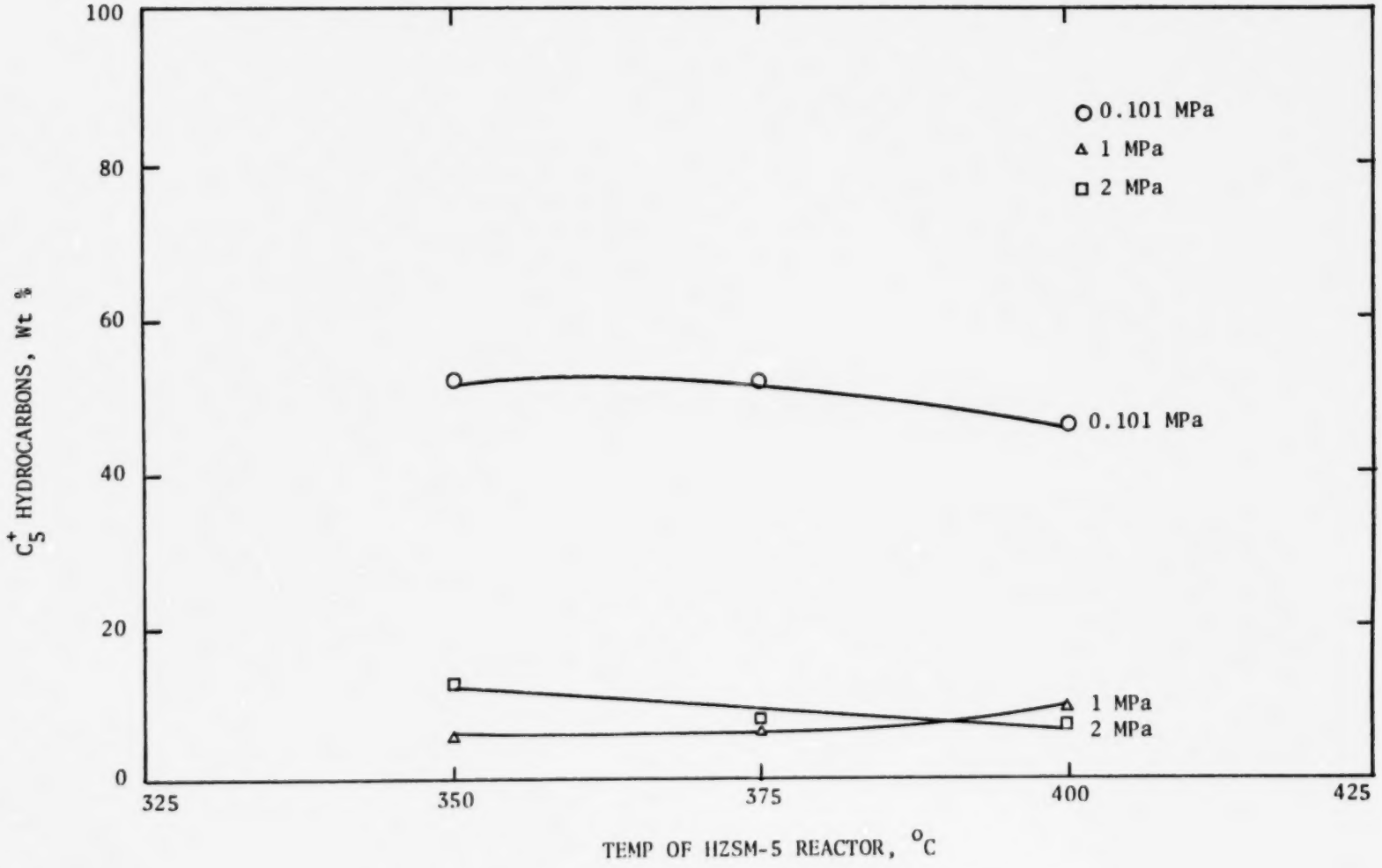

Figure 29 . Variation of C_5^+ Hydrocarbons in the Hydrocarbon Product with the HZSM-5 Bed Temperature (HZSM-5/FT = 1)

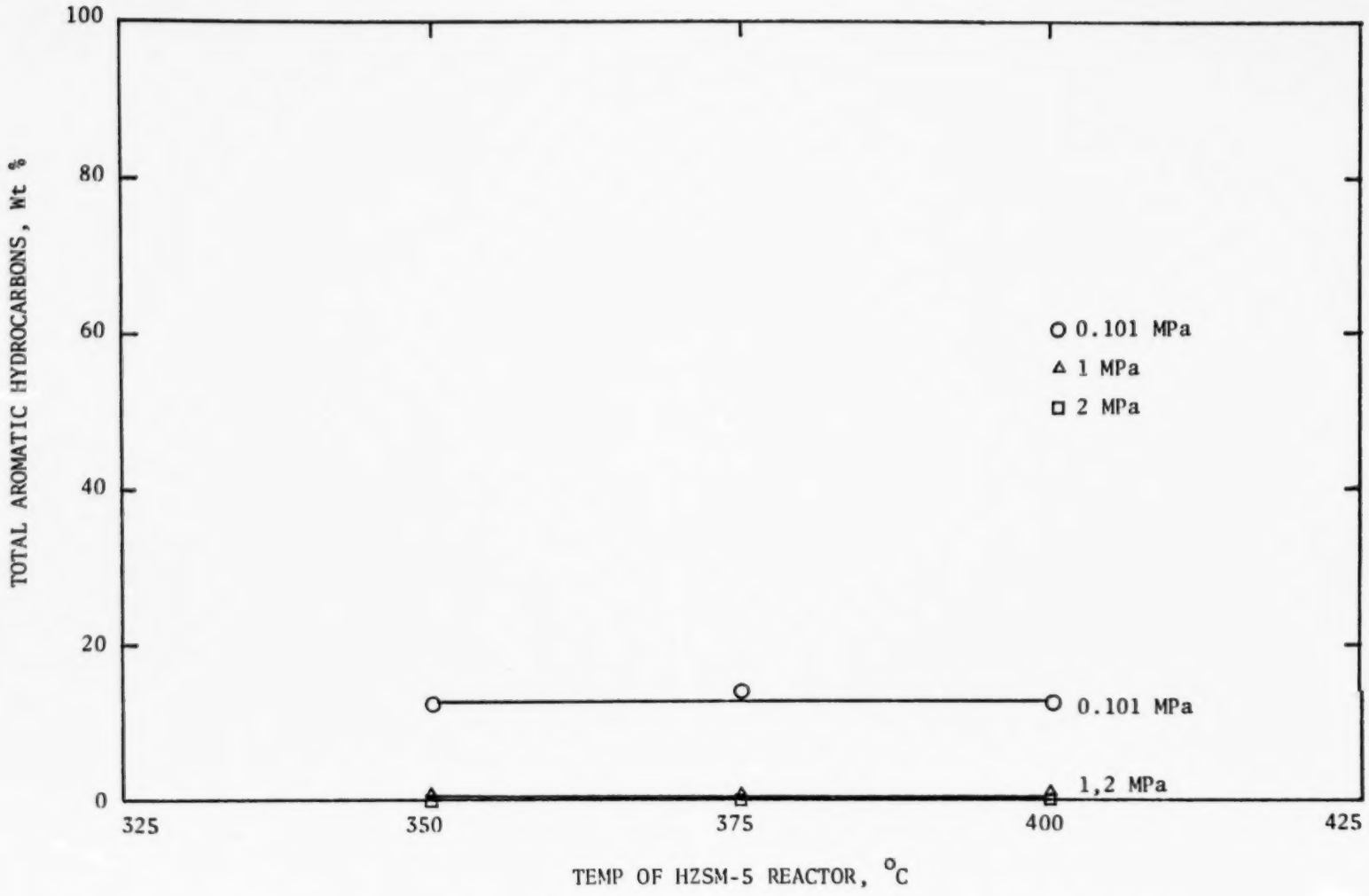

Figure 30. Variations of Total Aromatic Hydrocarbons in the Hydrocarbon Product with the HZSM-5 Bed Temperature (HZSM-5/FT = 1)

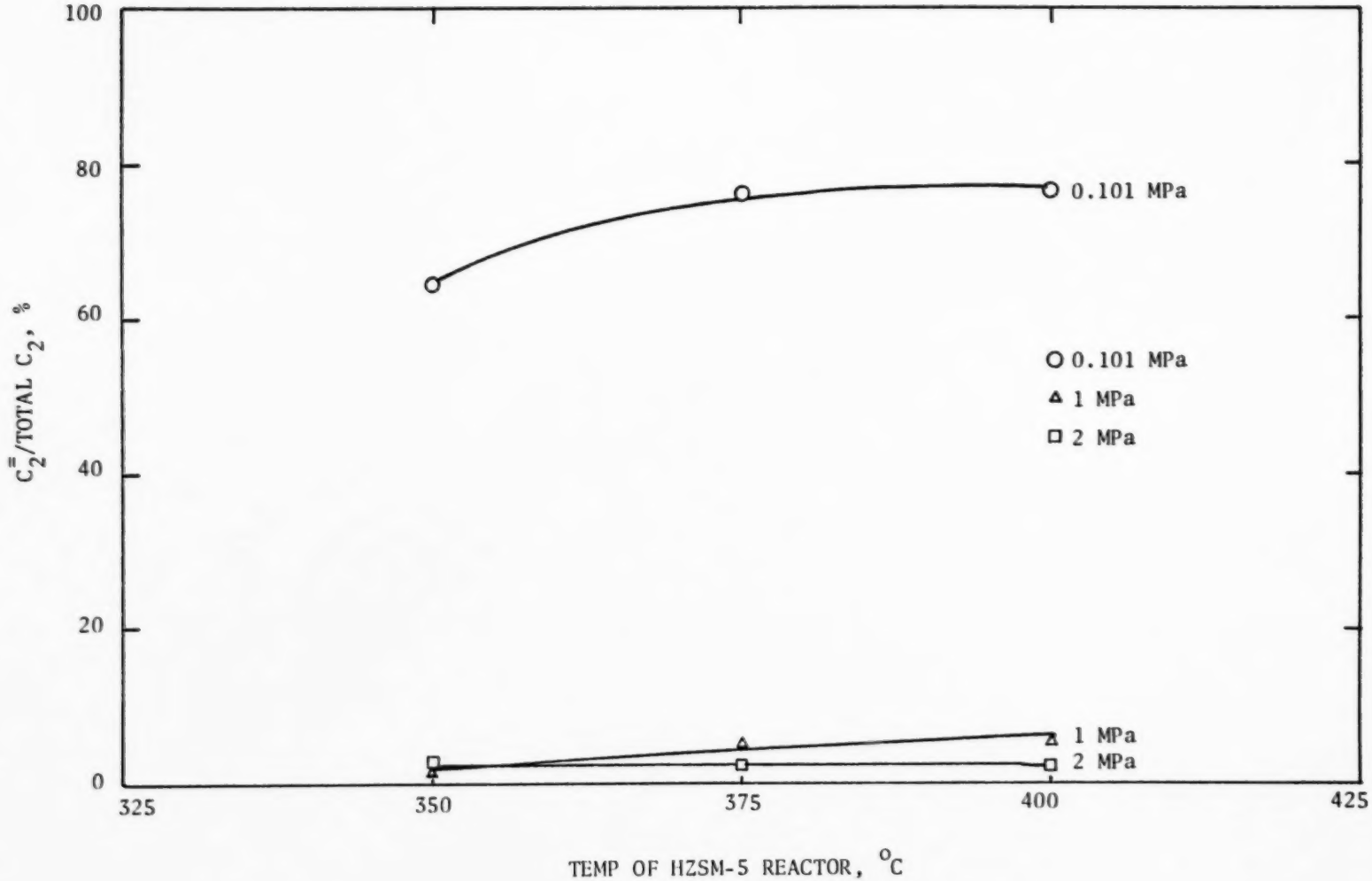

Figure 31. Variation of $C_2^=/C_2$ Fraction in the Hydrocarbon Product with Temperature of the HZSM-5 Bed, (HZSM-5/FT= 1).

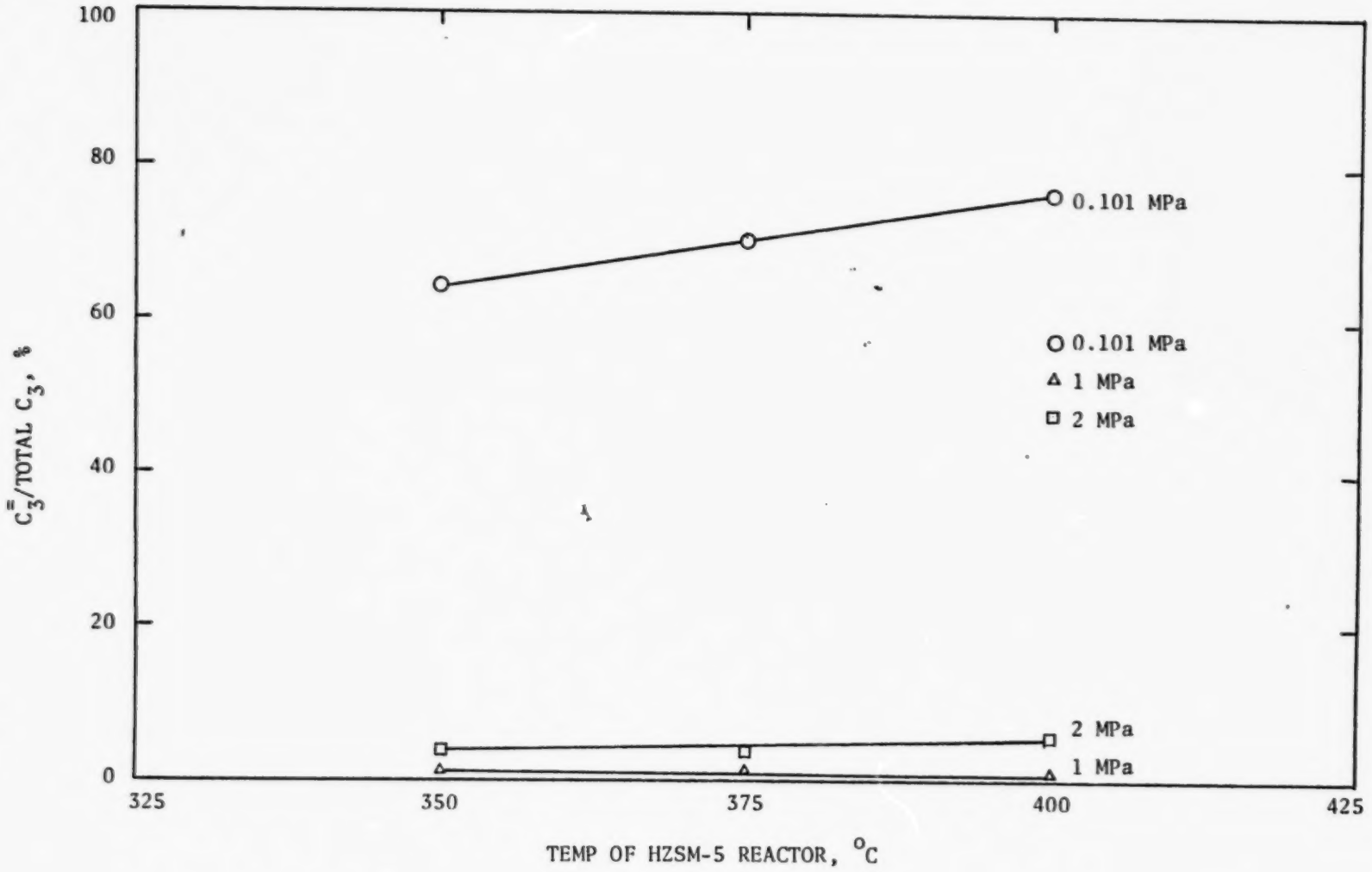

Figure 32 . Variation of $C_3^=/C_3$ Fraction in the Hydrocarbon Product with Temperature of the HZSM-5 Bed, (HZSM-5/FT= 1)

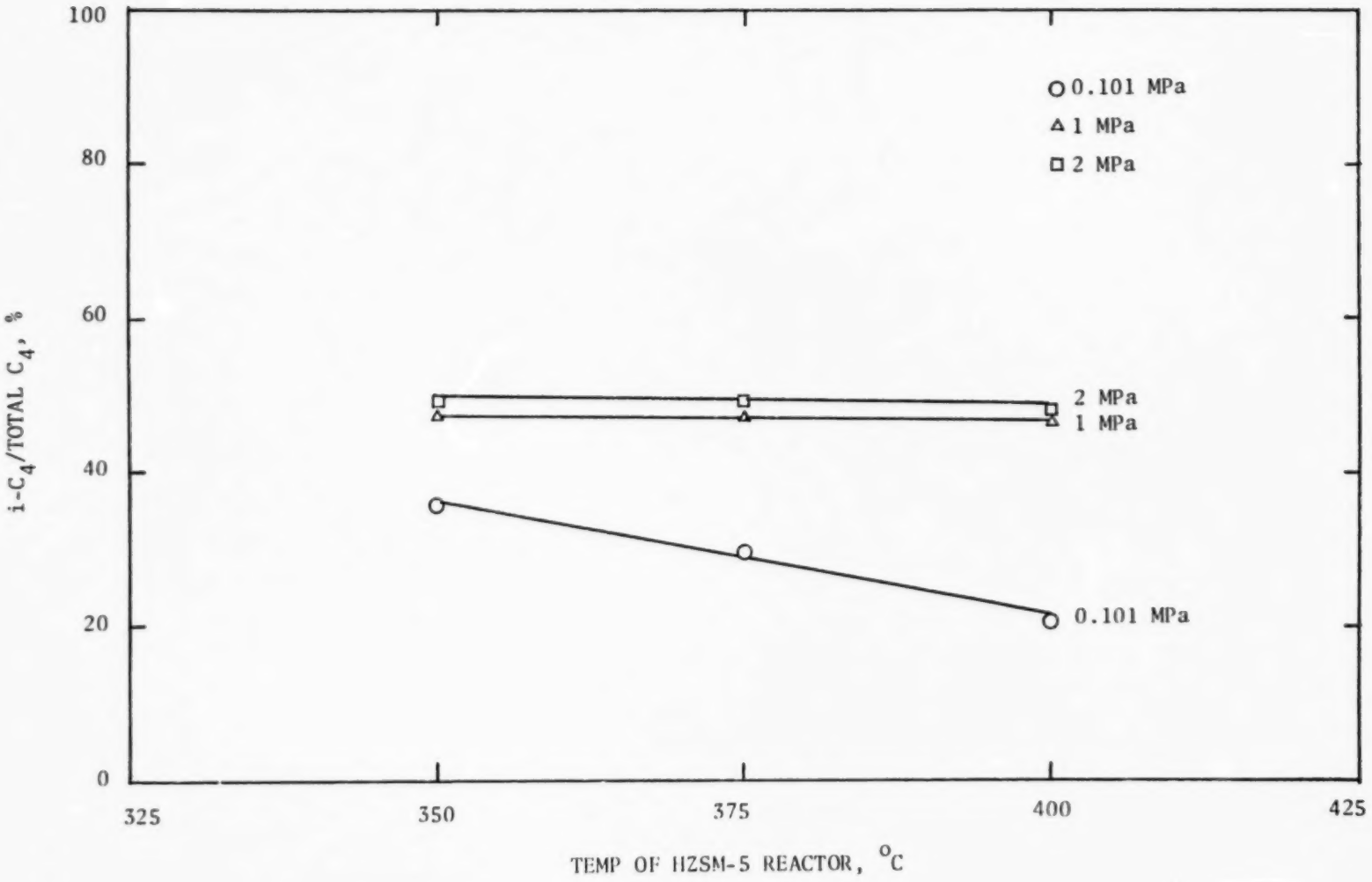

Figure 33 . Variation of the i-C_4/C_4 Fraction in the Hydrocarbon Product with the Temperature of the HZSM-5 Bed (HZSM-5/FT =1)

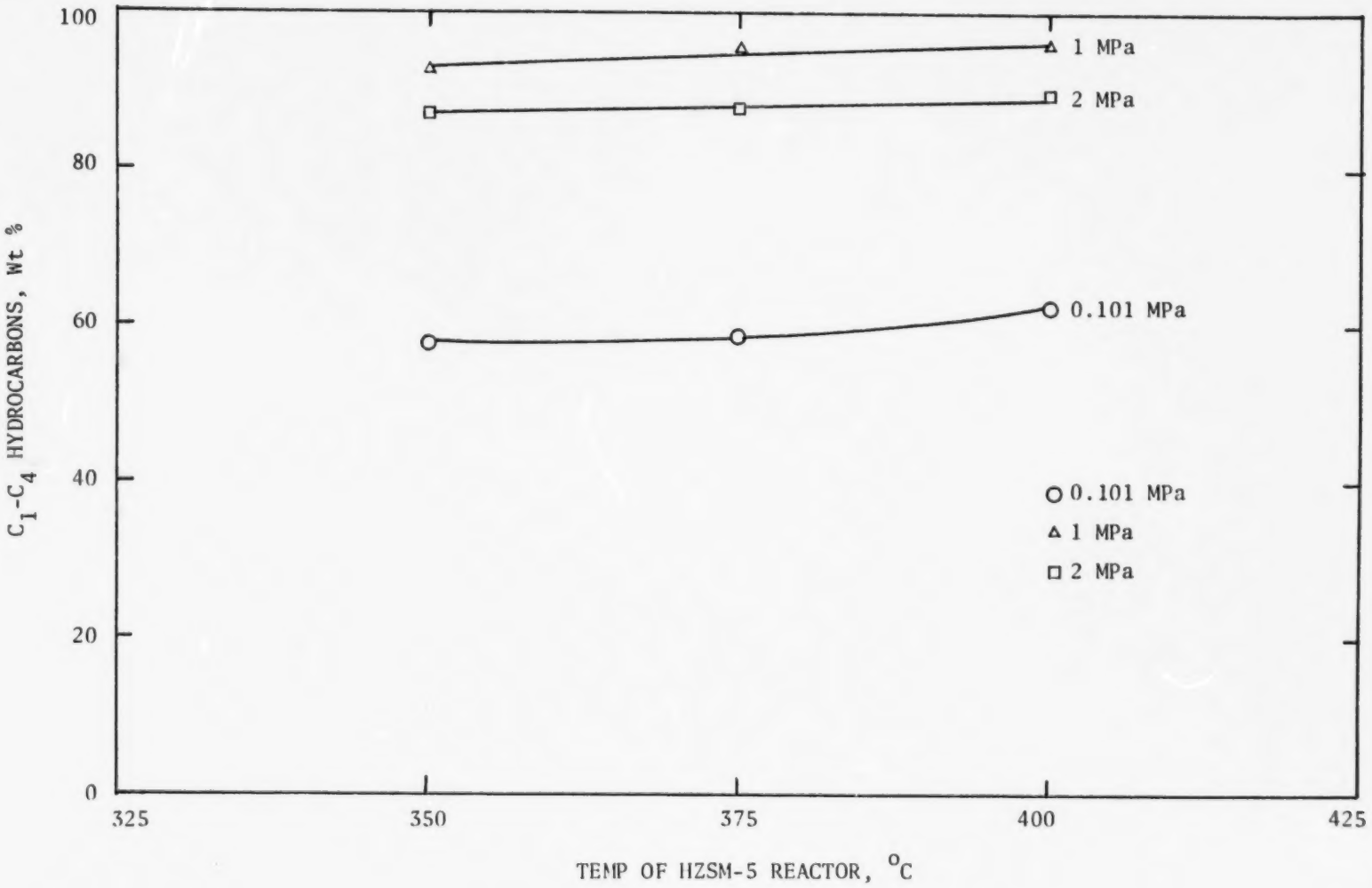

Figure 34 . Variation of C_1-C_4 Hydrocarbon Product Distribution with the HZSM-5 Bed Temperature (HZSM-5/FT= 2.5)

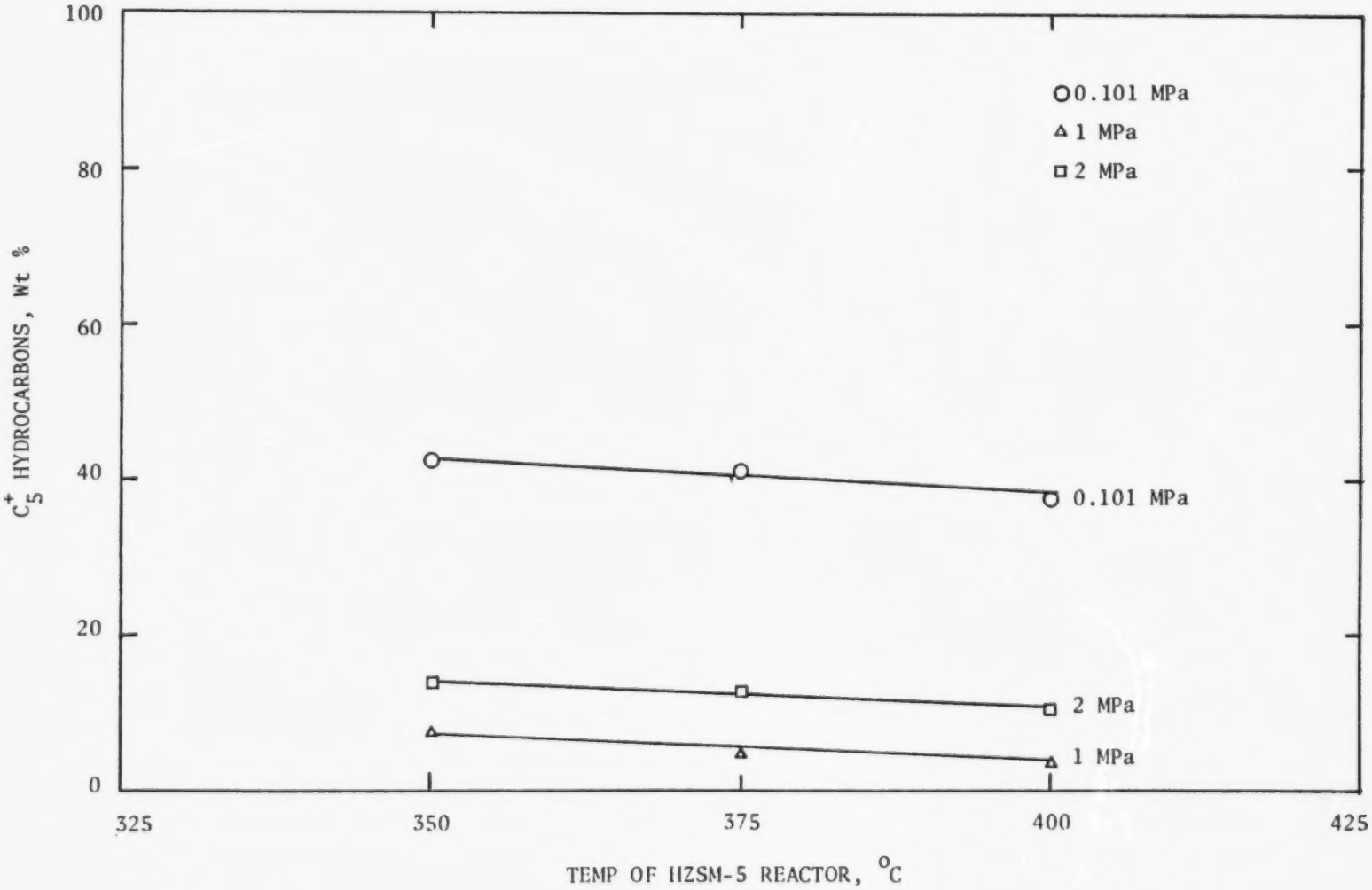

Figure 35. Variation of C_5^+ Hydrocarbon in the Hydrocarbon Product with the HZSM-5 Bed Temperature (HZSM-5/FT = 2.5)

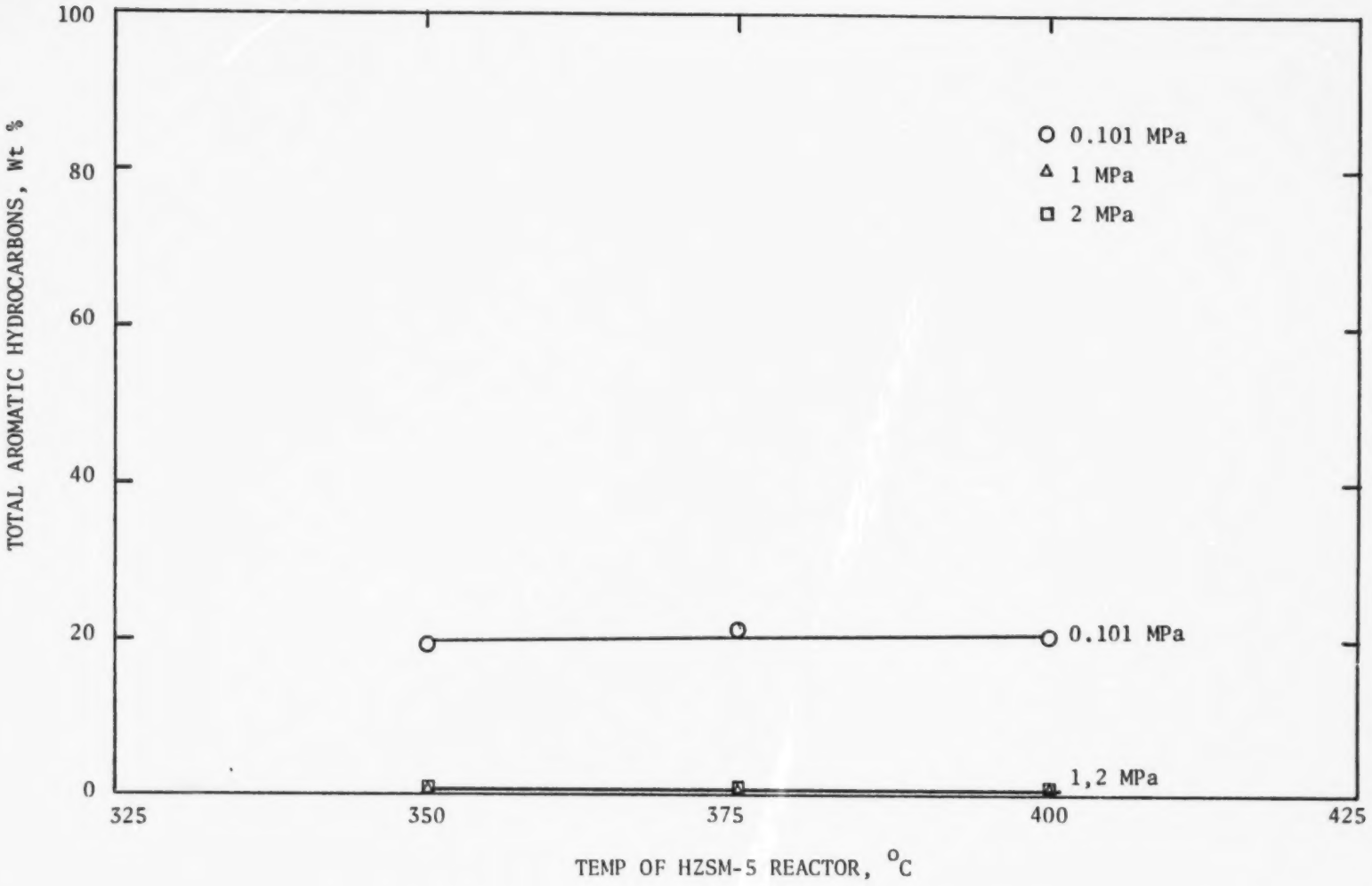

Figure 36 . **Variations of Total Aromatic Hydrocarbons in the Hydrocarbon Product with the HZSM-5 Bed Temperature (HZSM-5/FT = 2.5)**

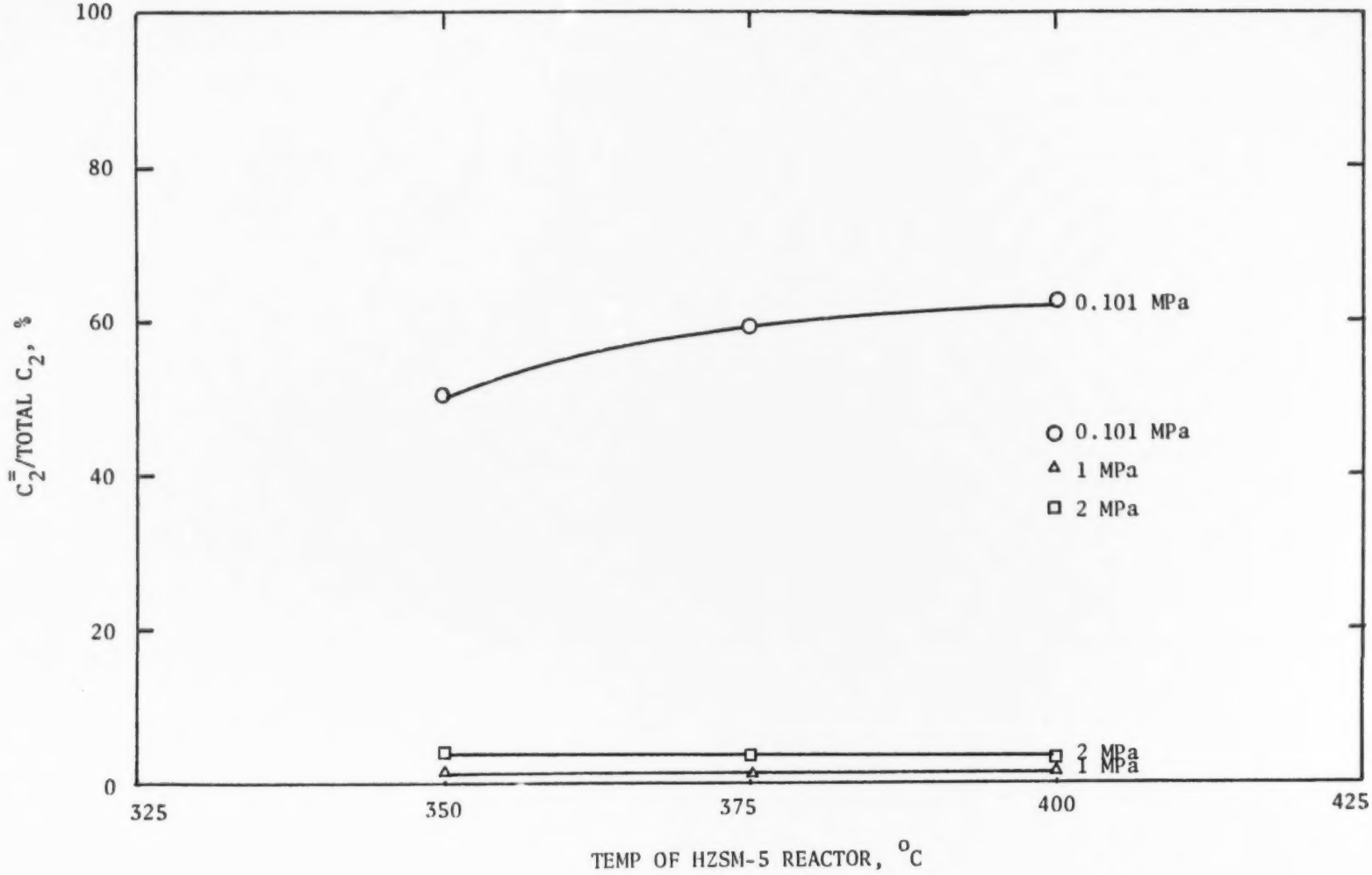

Figure 37 . Variation of $C_2^=/C_2$ Fraction in the Hydrocarbon Product with Temperature of the HZSM-5 Bed,(HZSM-5/FT= 2.5)

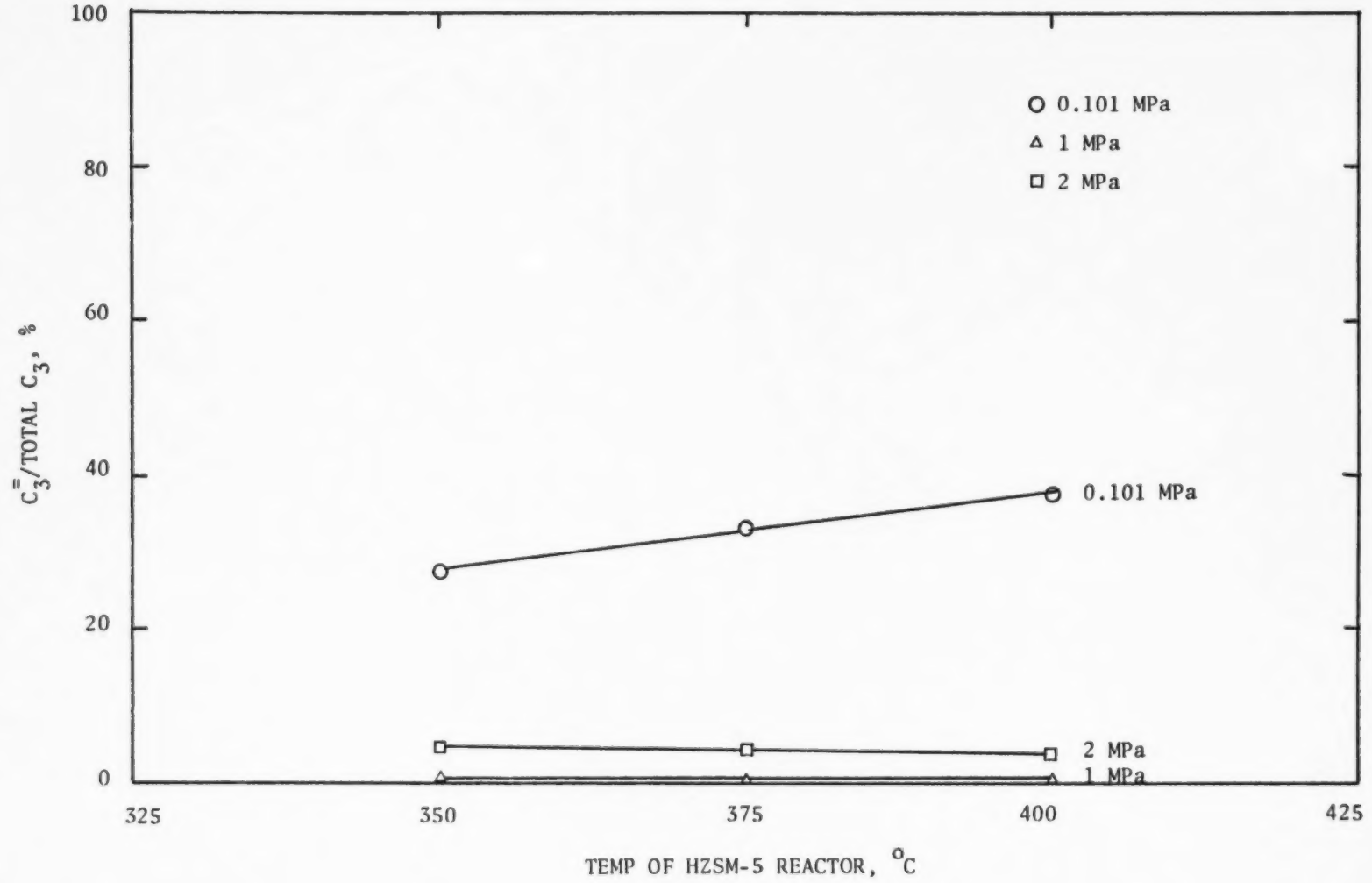

Figure 38 . Variation of $C_3^=/C_3$ Fraction in the Hydrocarbon Product with Temperature of the HZSM-5 Bed,(HZSM-5/FT= 2.5)

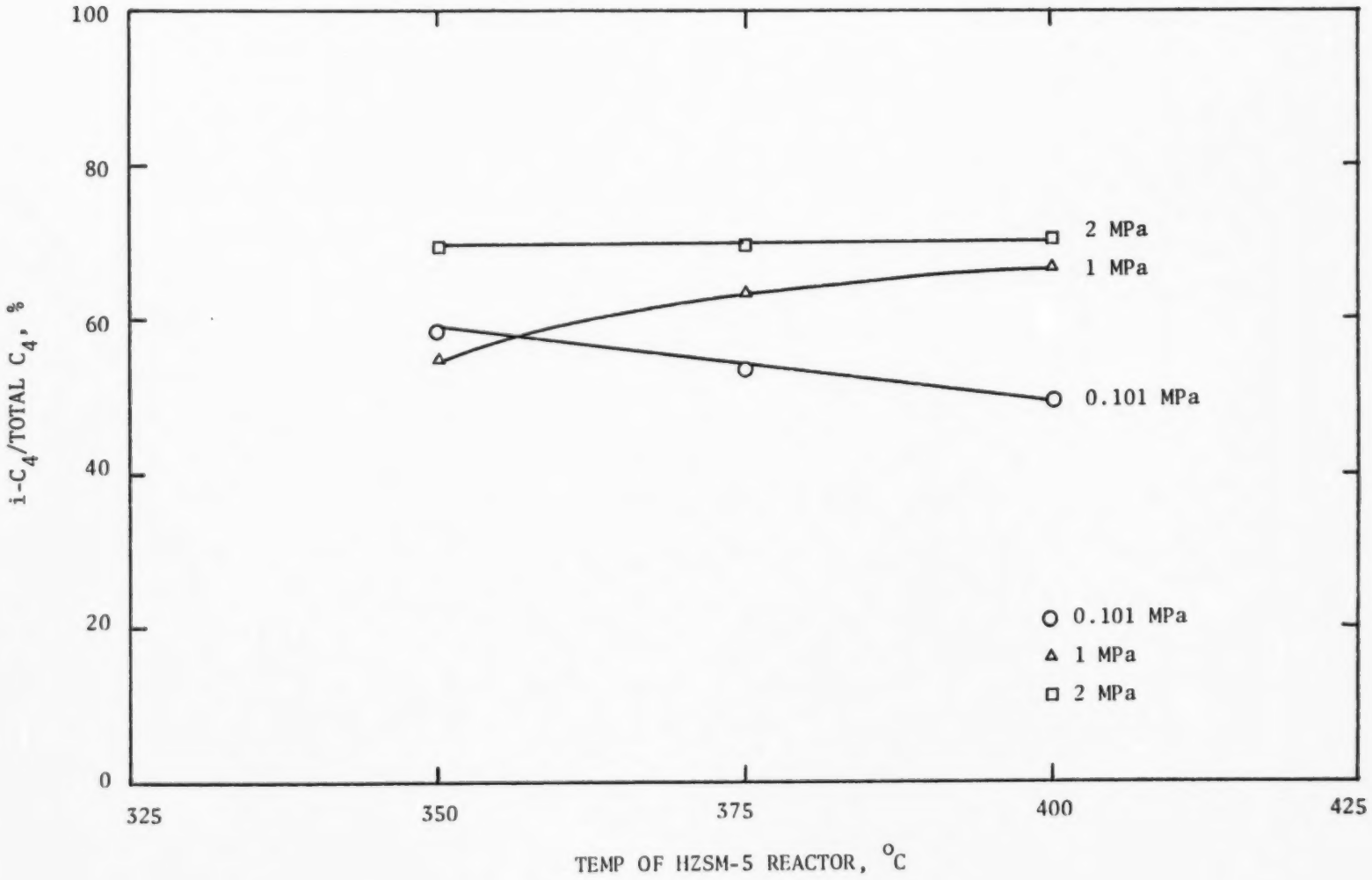

Figure 39. Variation of the iC_4/C_4 Fraction in the Hydrocarbon Product with the Temperature of the HZSM-5 Bed (HZSM-5/FT = 2.5)

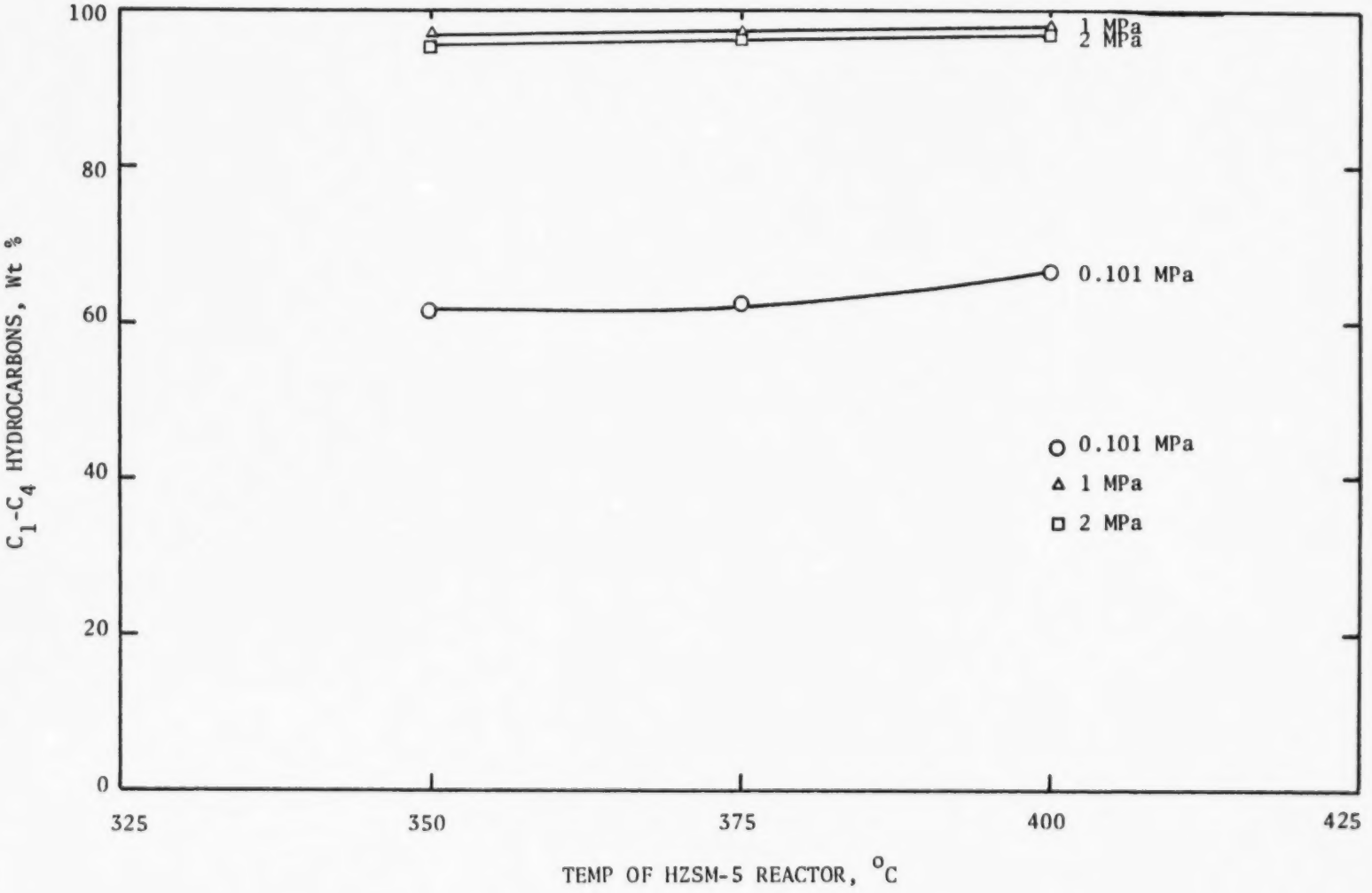

Figure 40 . Variation of C_1-C_4 Hydrocarbon Product Distribution with the HZSM-5 Bed Temperature (HZSM-5/FT= 4).

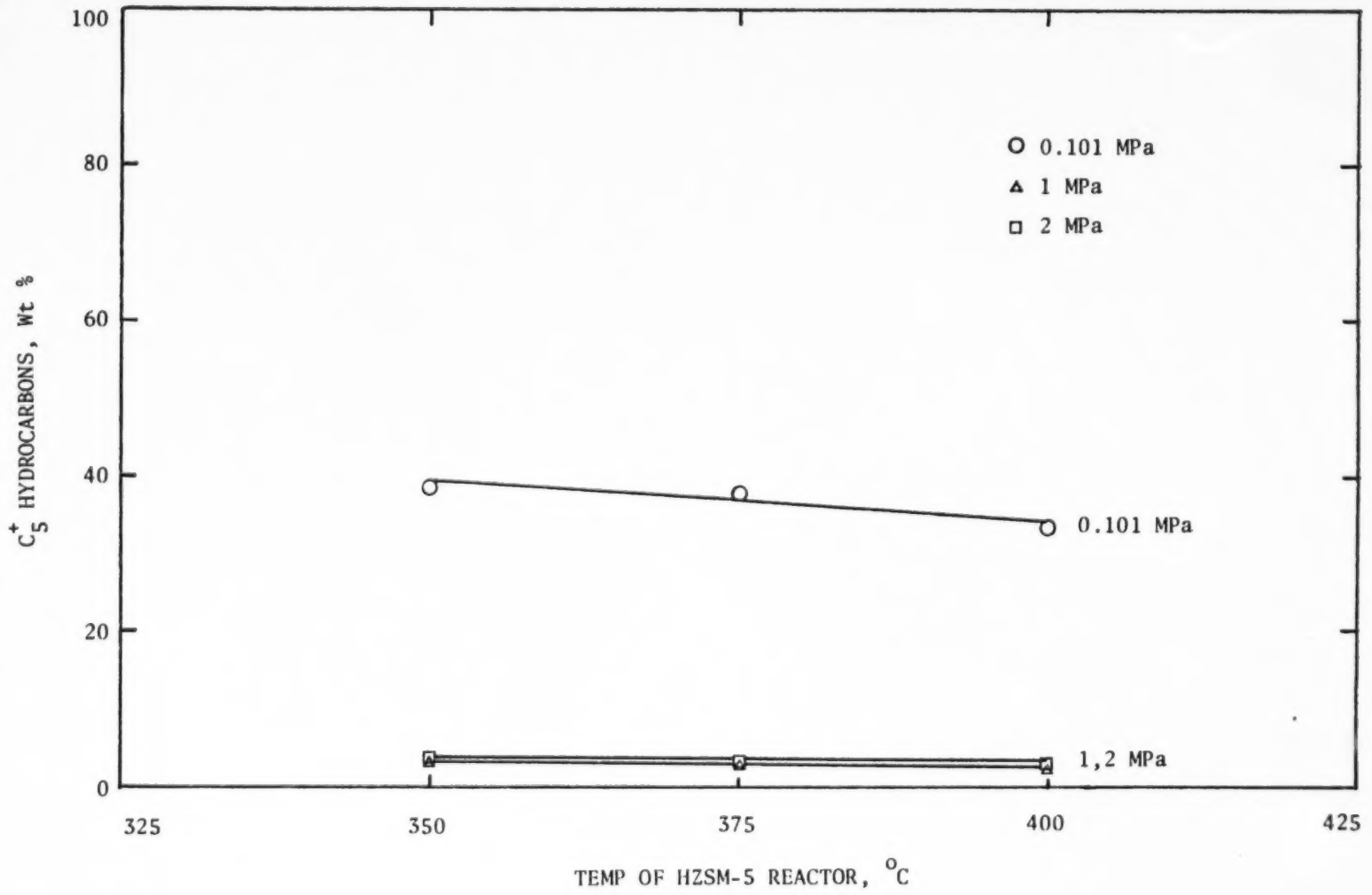

Figure 41 . Variation of C_5^+ Hydrocarbons in the Hydrocarbon Product with the HZSM-5 Bed Temperature (HZSM-5/FT = 4)

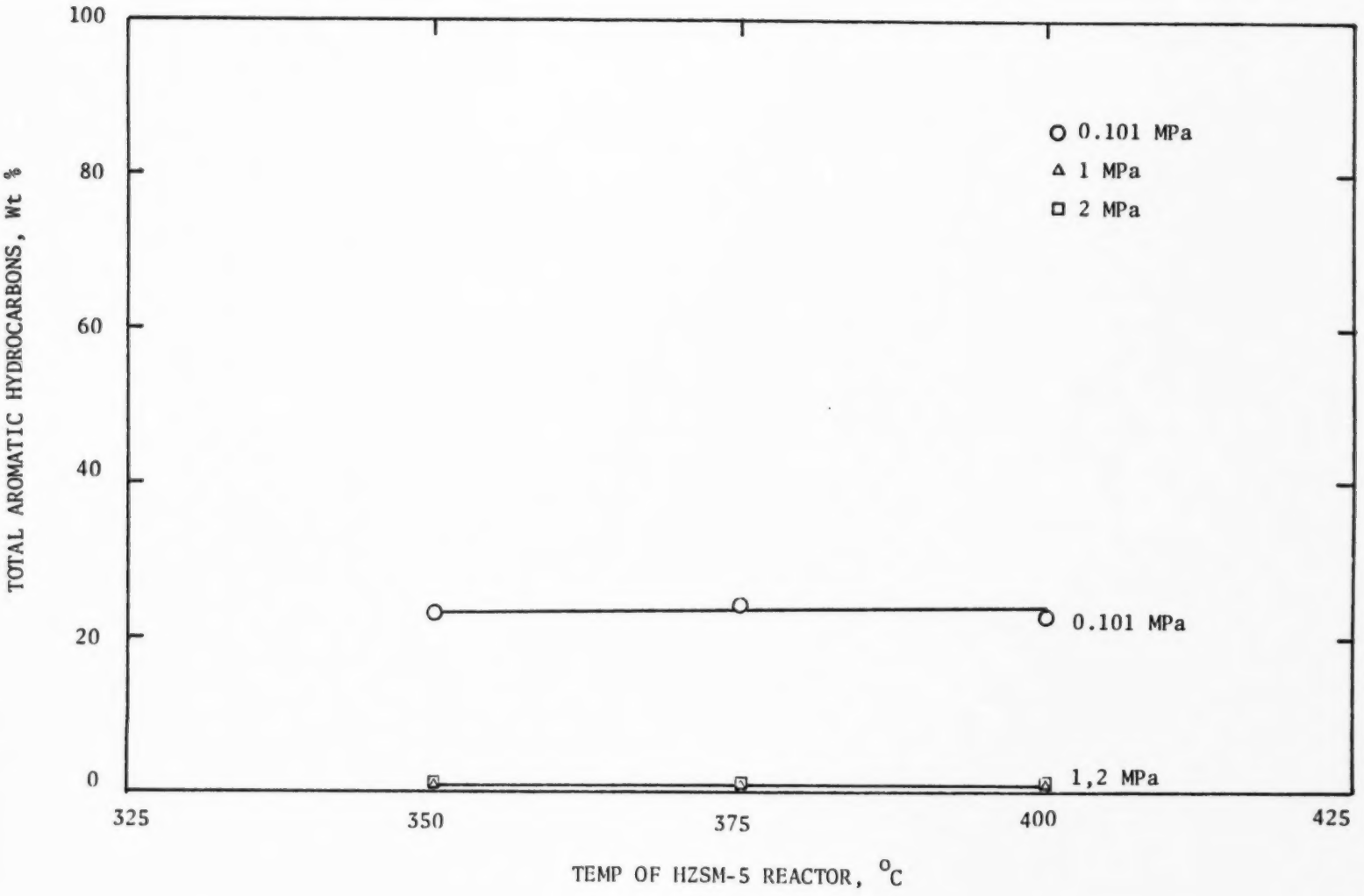

Figure 42. **Variations of Total Aromatic Hydrocarbons in the Hydrocarbon Product with the HZSM-5 Bed Temperature (HZSM-5/FT =4)**

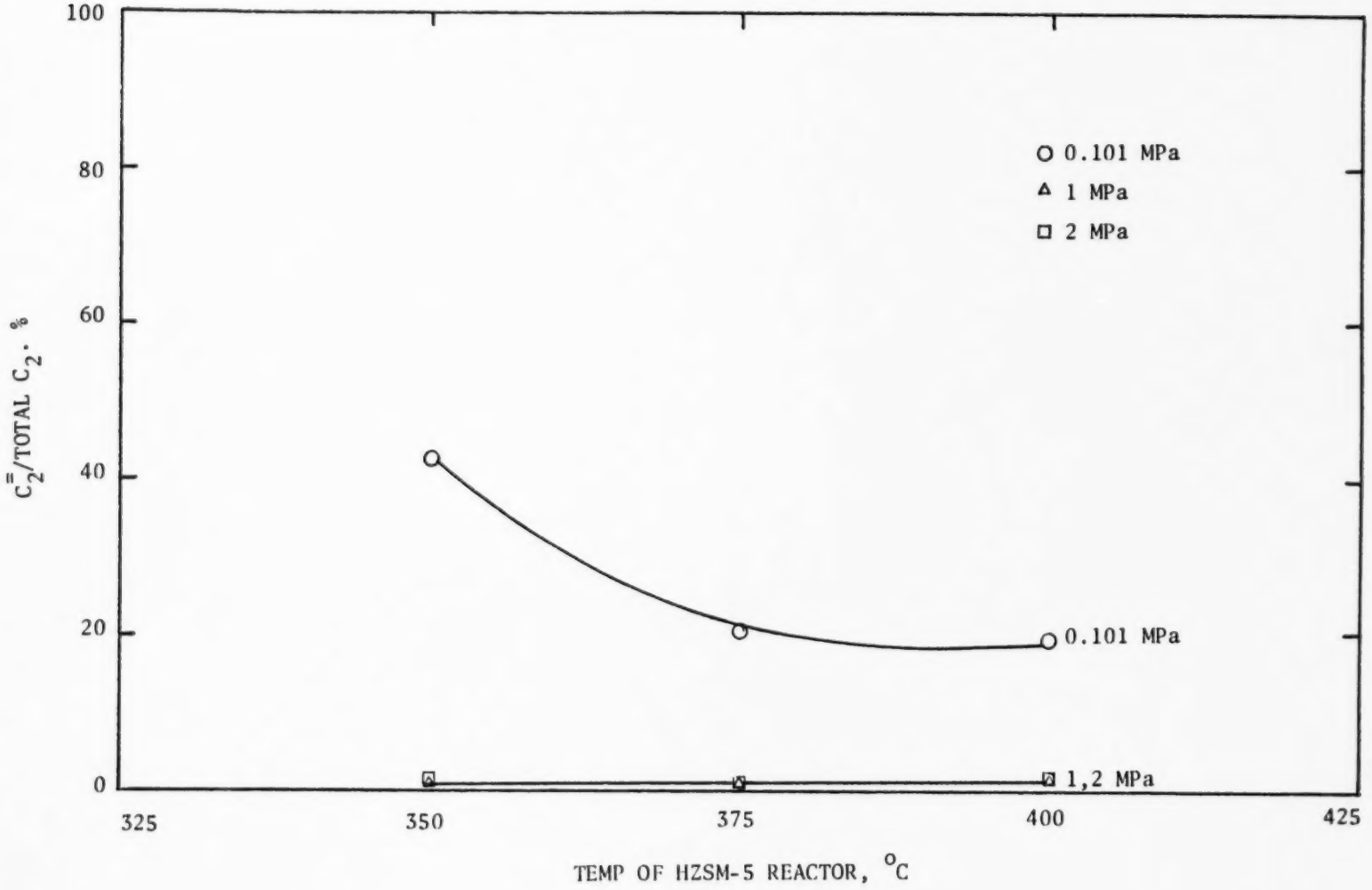

Figure 43 . Variation of $C_2^=/C_2$ Fraction in the Hydrocarbon Product with Temperature of the HZSM-5 Bed,(HZSM-5/FT= 4)

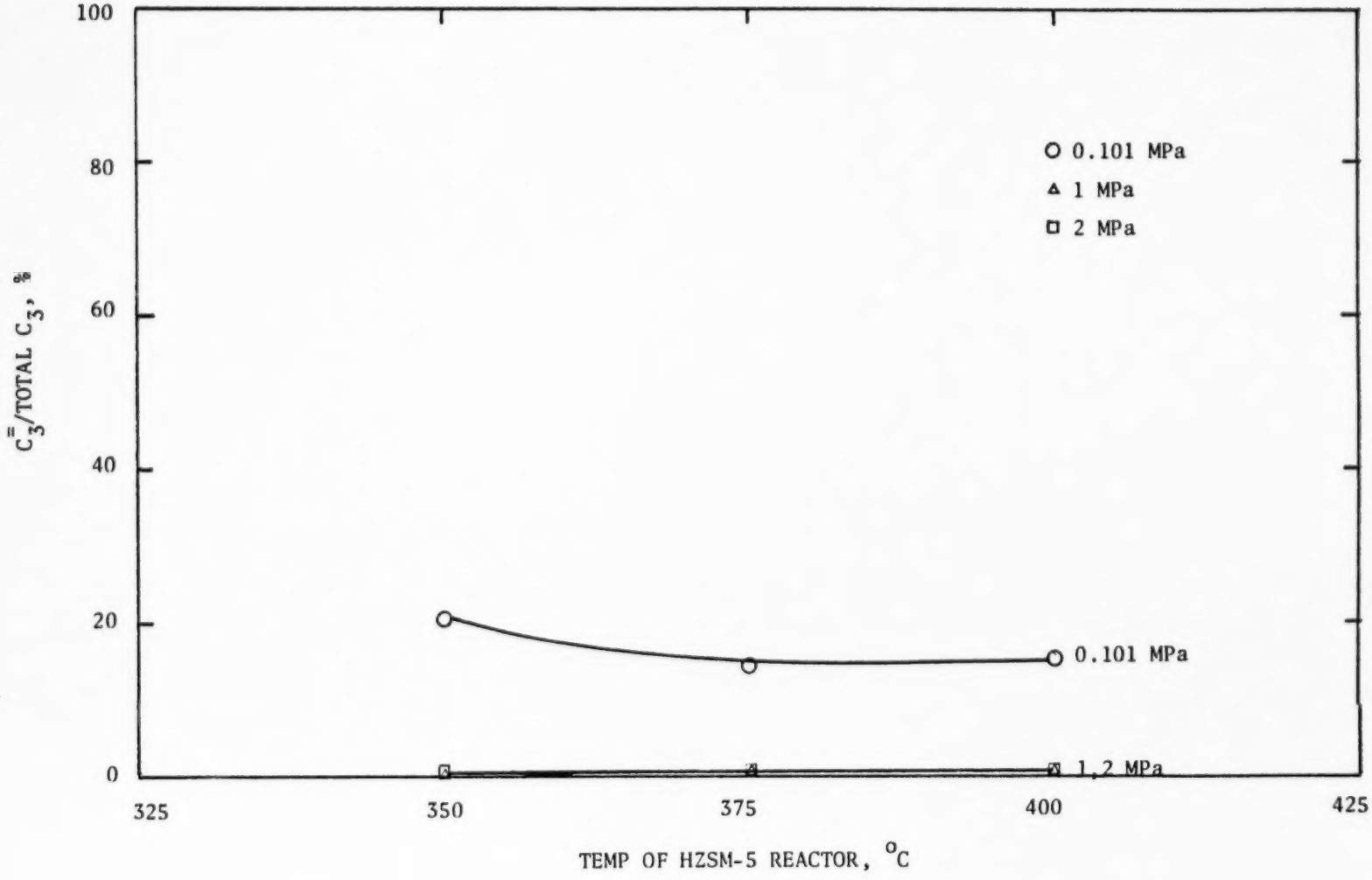

Figure 44 . Variation of $C_3^=/C_3$ Fraction in the Hydrocarbon Product with Temperature of the HZSM-5 Bed,(HZSM-5/FT= 4).

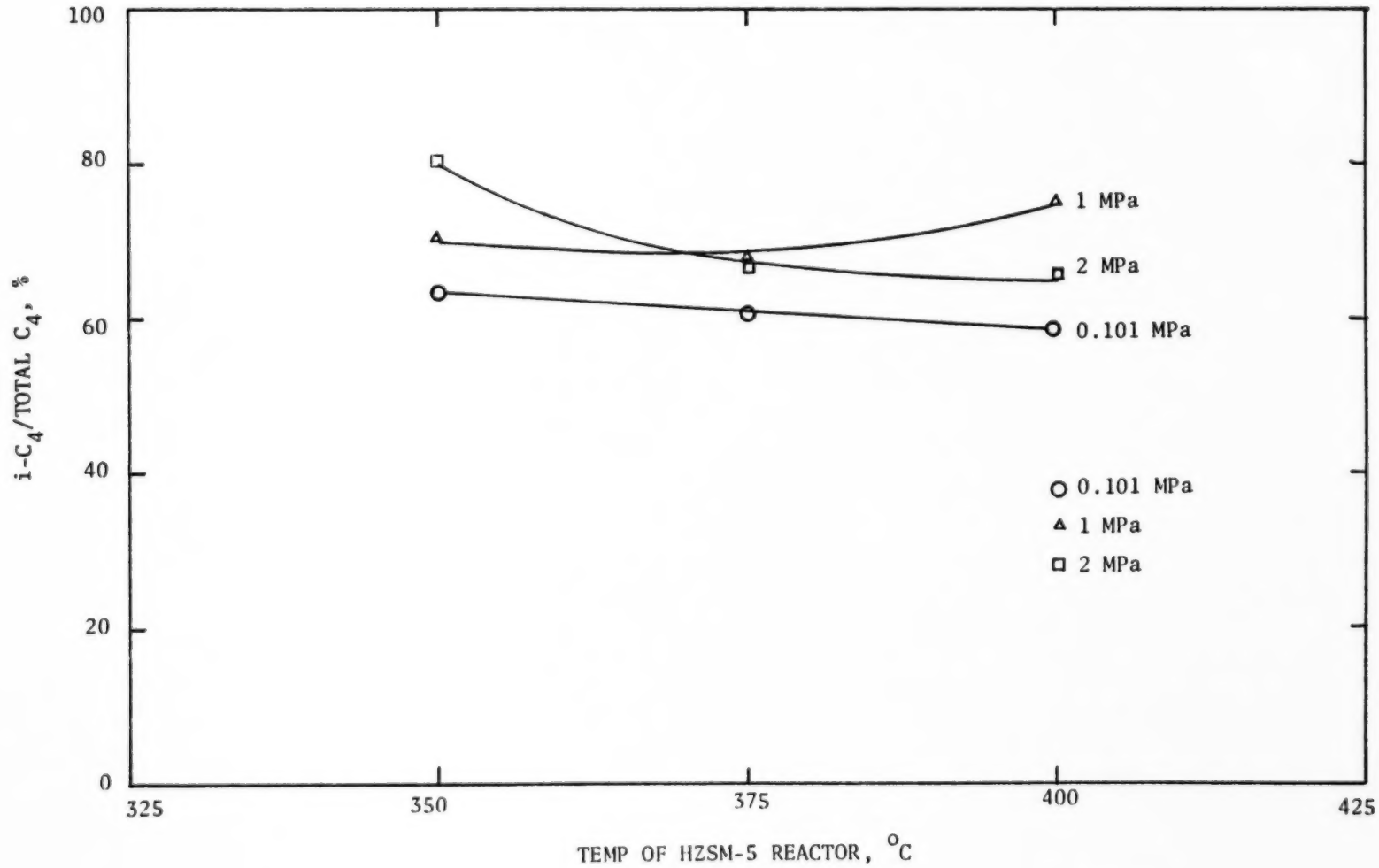

Figure 45 . Variation of the i-C_4/C_4 Fraction in the Hydrocarbon Product with the Temperature of the HZSM-5 Bed (HZSM-5/FT = 4)

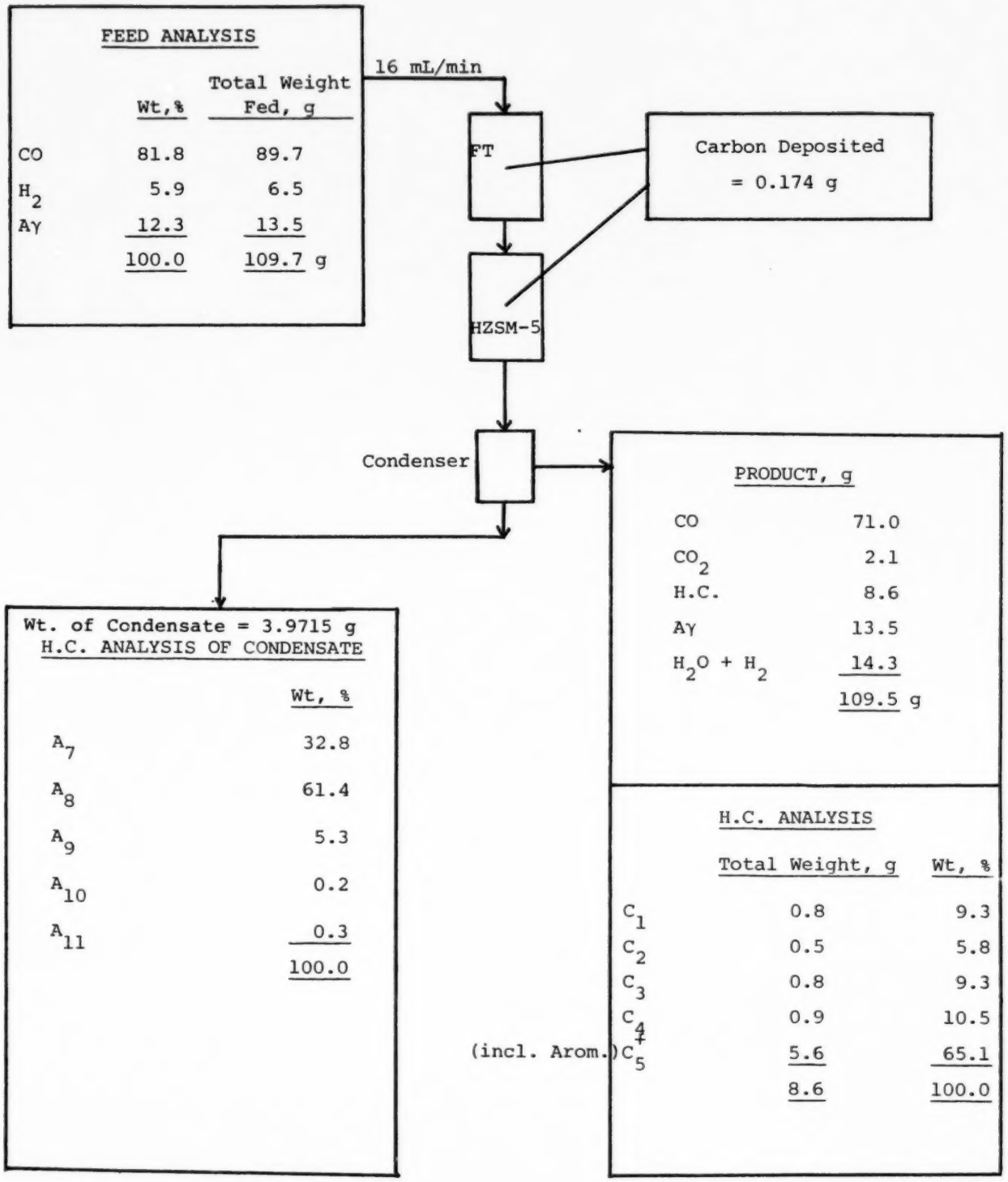

Figure 46. Overall Material Balance
(See Table 32 for Operating Conditions)

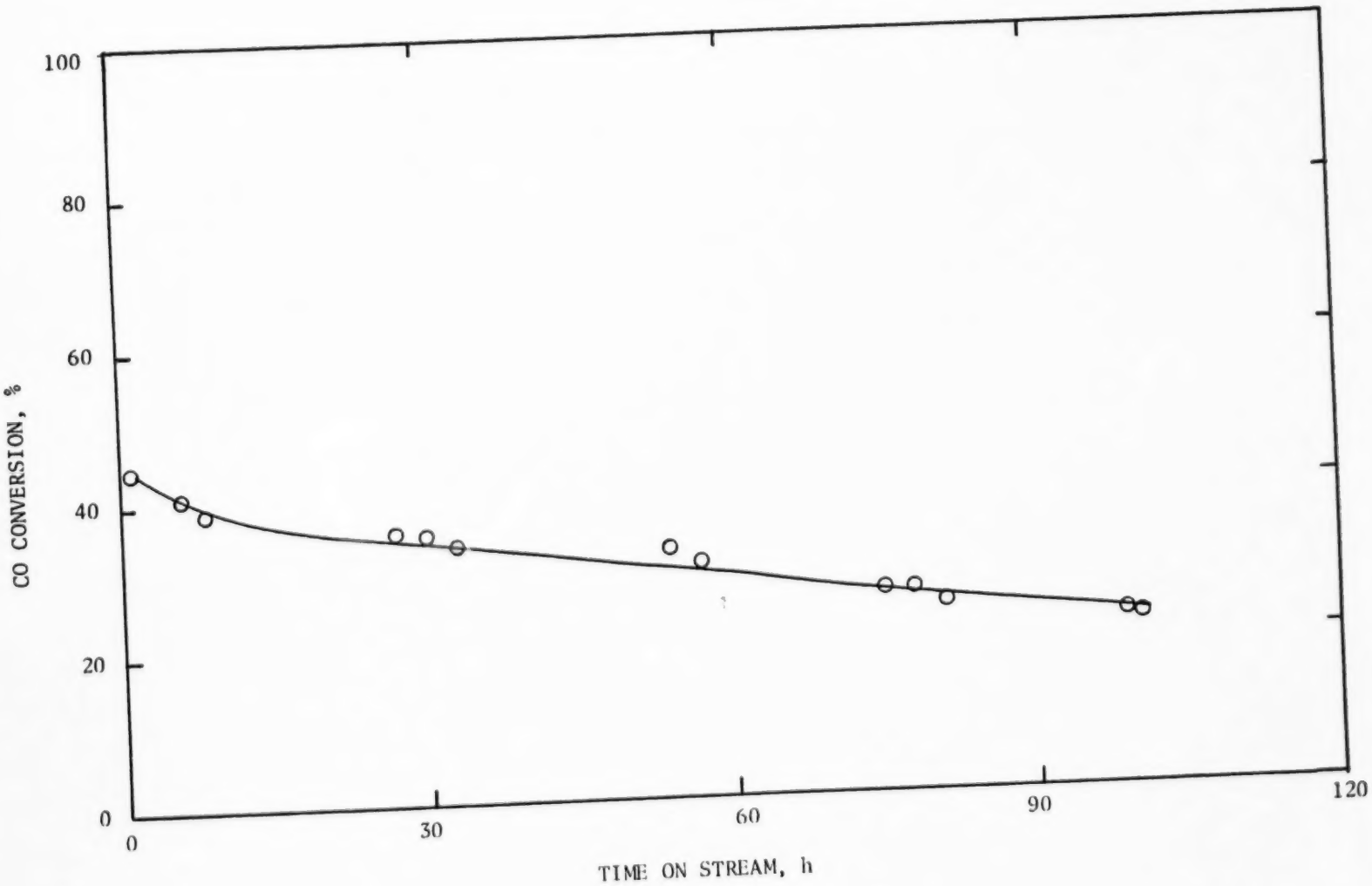

Figure 47. Variation of Carbon Monoxide Conversion with Time-on-Stream.

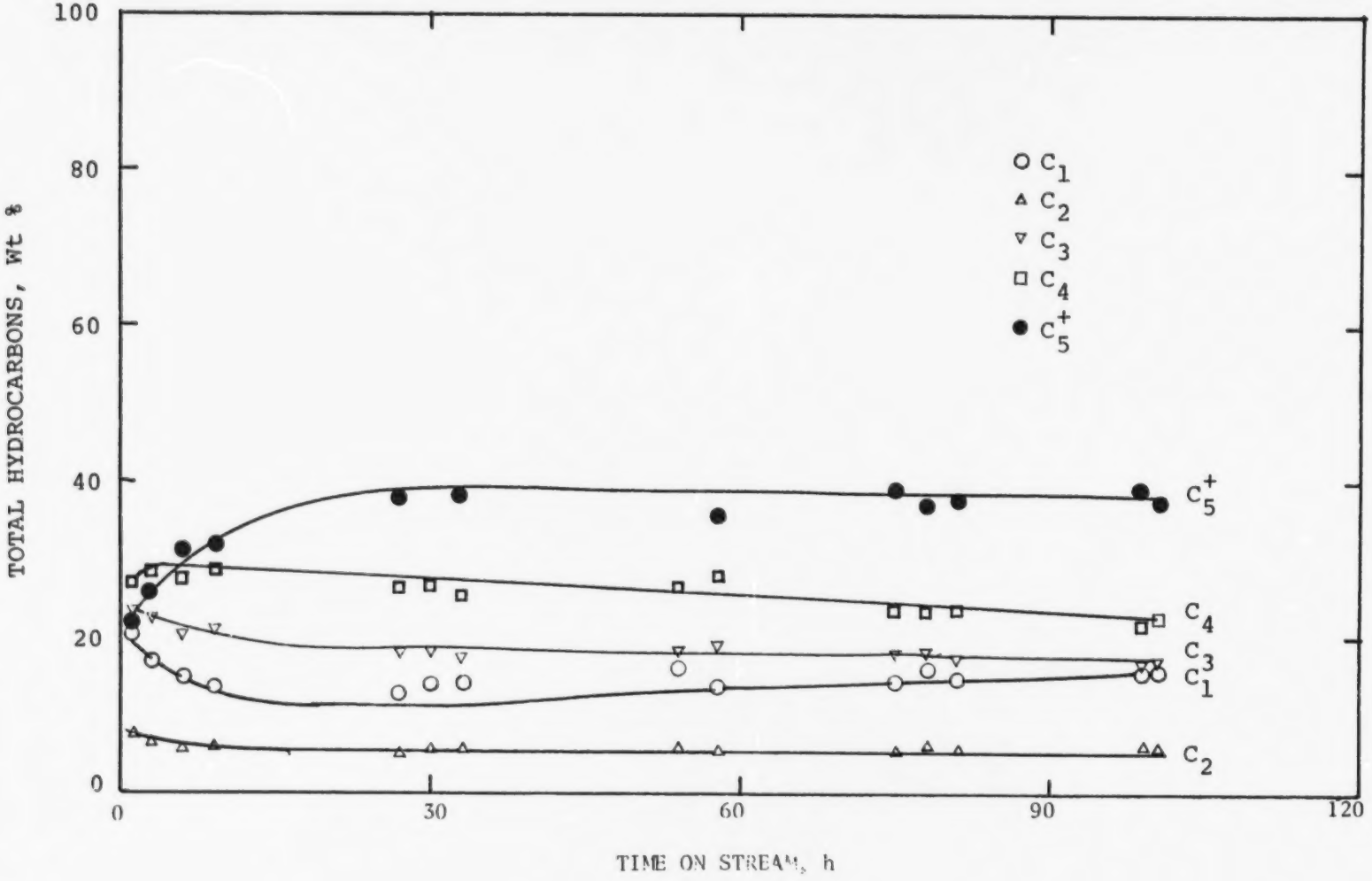

Figure 48. Hydrocarbon Product Distribution with Time-on-Stream

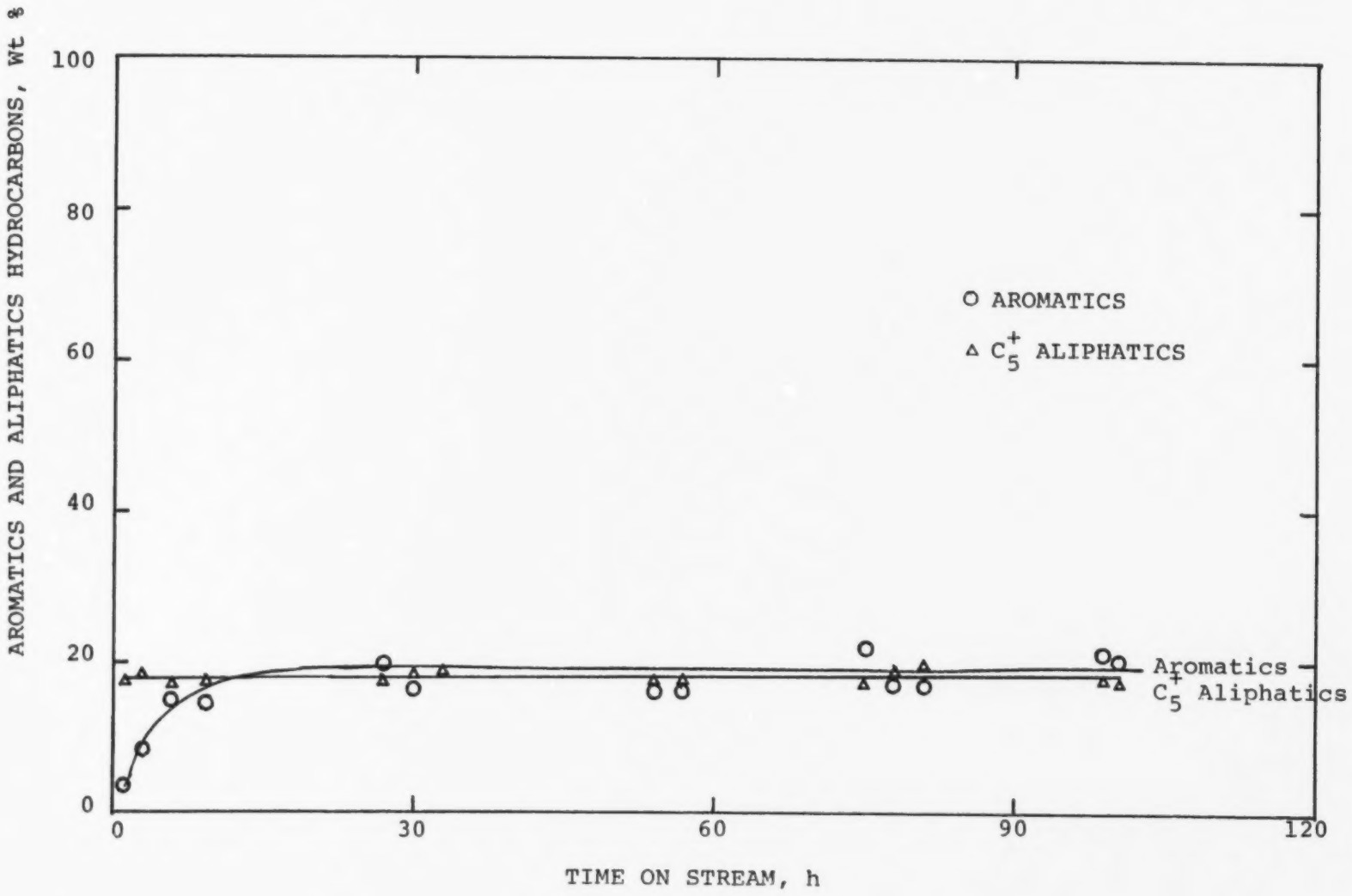

Figure 49. Aromatics and Aliphatics Hydrocarbons in the Hydrocarbon Product with Time-on-Stream

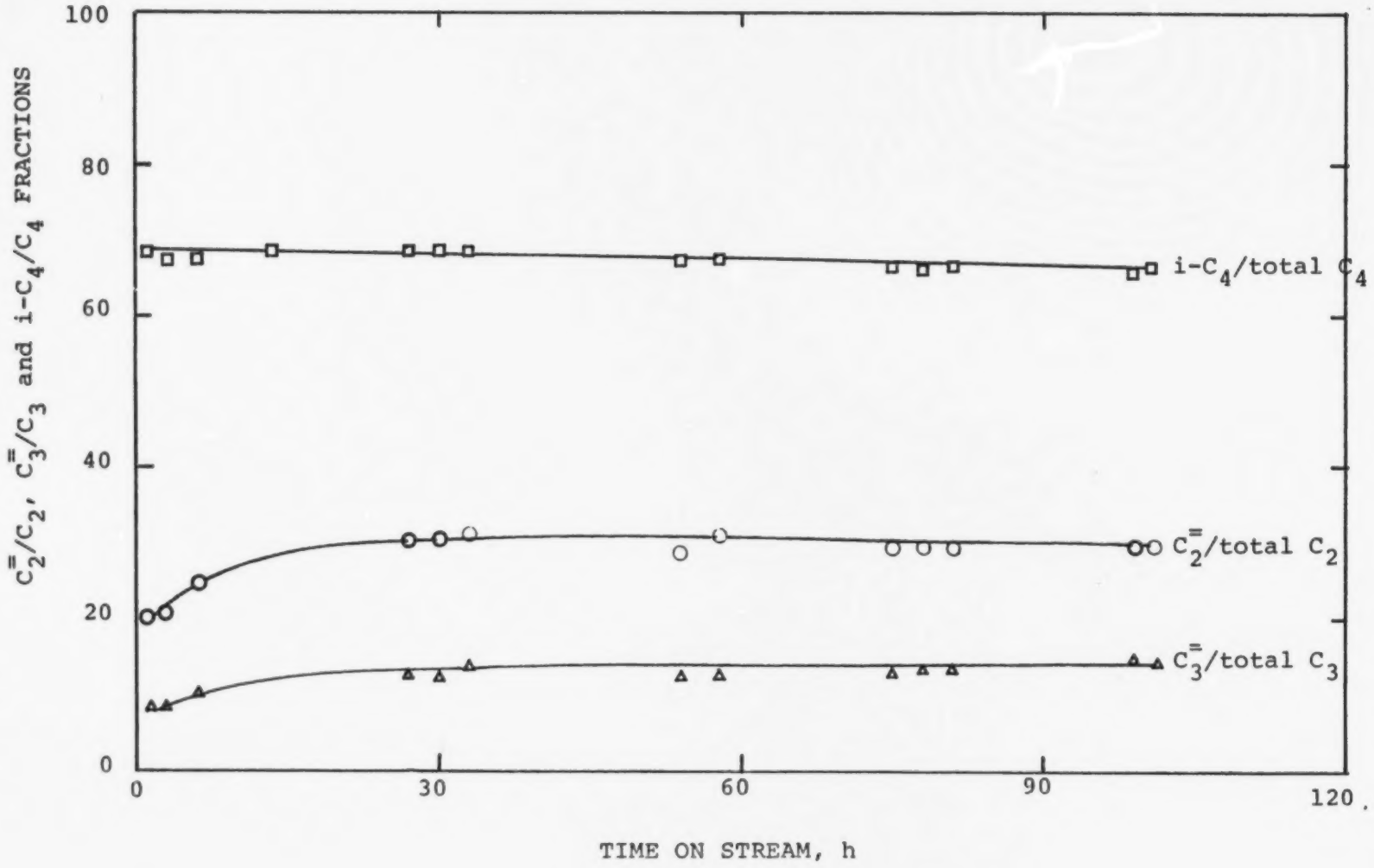

Figure 50. $C_2^=/C_2$, $C_3^=/C_3$ and i-C_4/C_4 Fractions in the Hydrocarbon Product with Time-on-Stream.

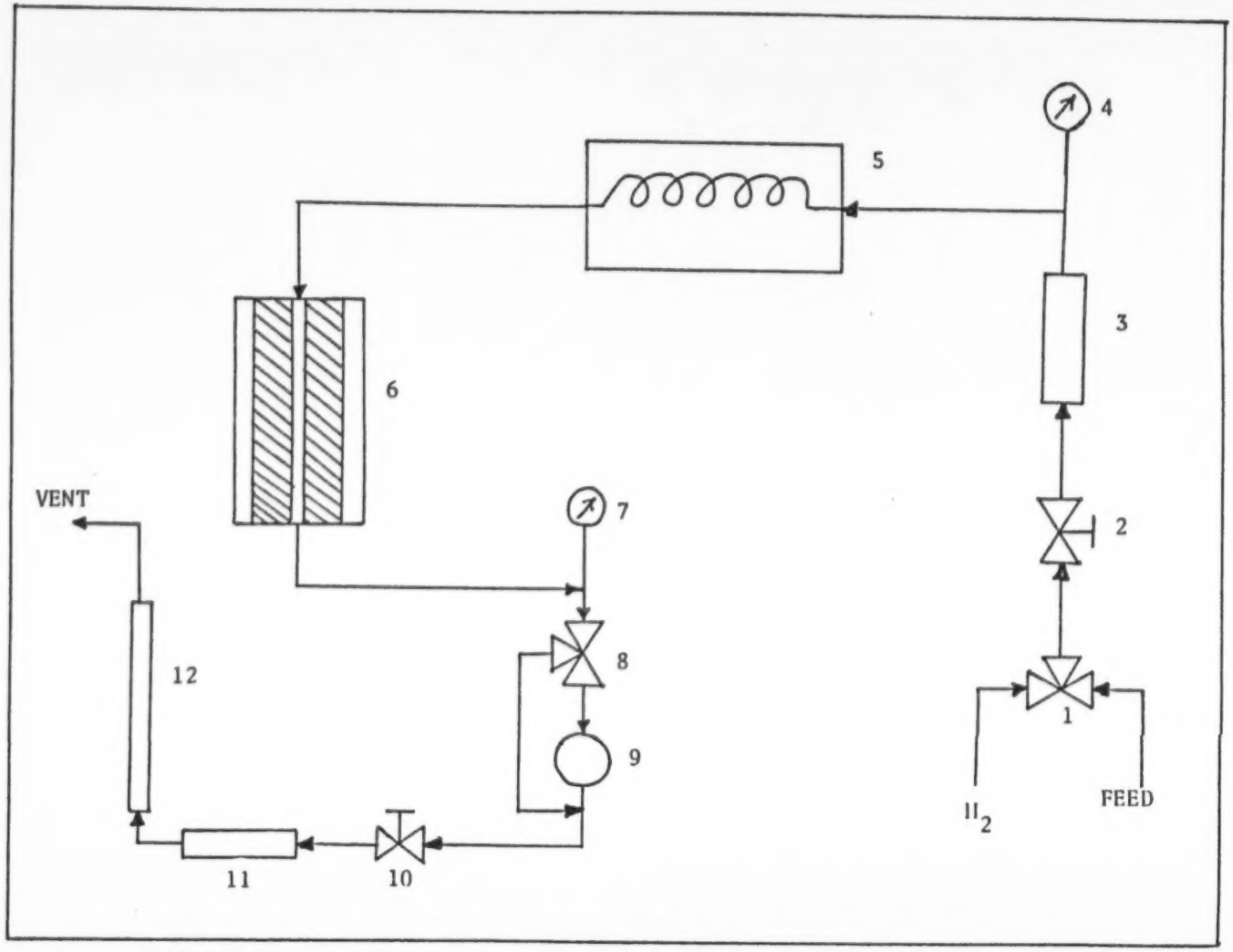

Figure 51. HIGH PRESSURE MICROREACTOR SYSTEM. 1) Three Way Valve 2) Needle Value 3) Mass Flow Transducer 4) Inlet Pressure Gauge 5) Preheater 6) Reactor& Furnace 7) Outlet Pressure Gauge 8) Three Way Valve 9) B.P.REG. 10) Needle Value 11) Sample Trap 12) Bubble - Flow Meter

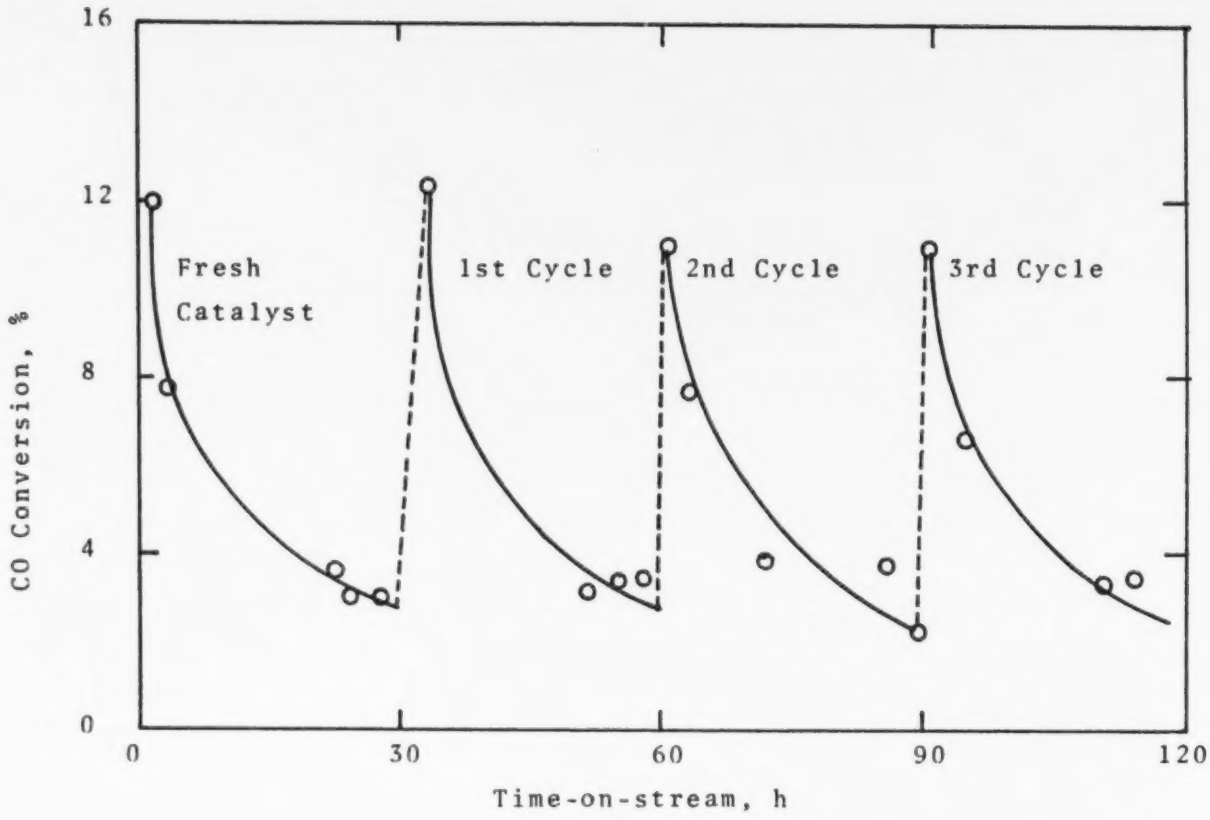

Figure 52. Variation of Carbon Monoxide Conversion with Time-on-Stream.

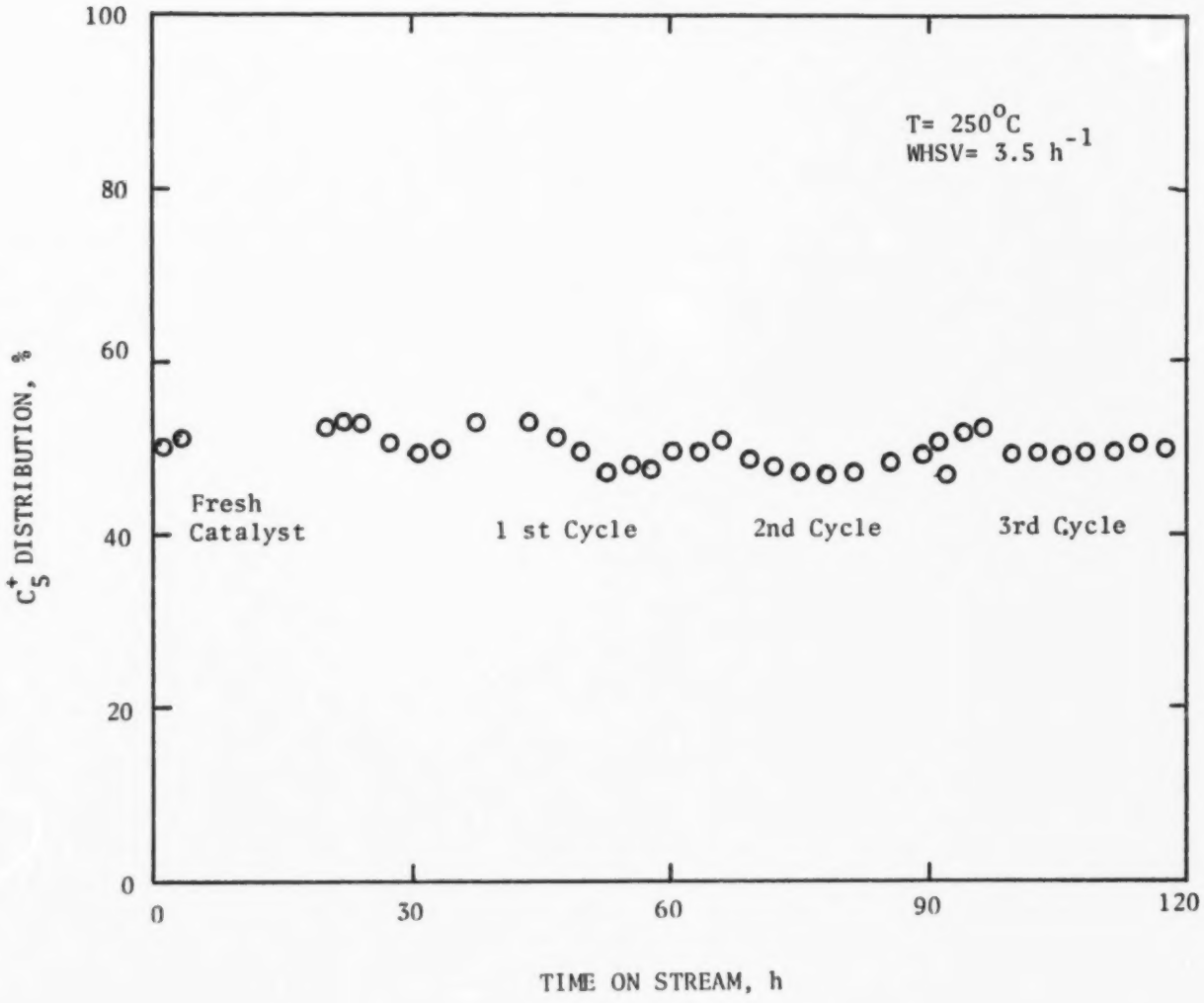

Figure 53. C_5^+ Hydrocarbon Distribution with Time-on-Stream

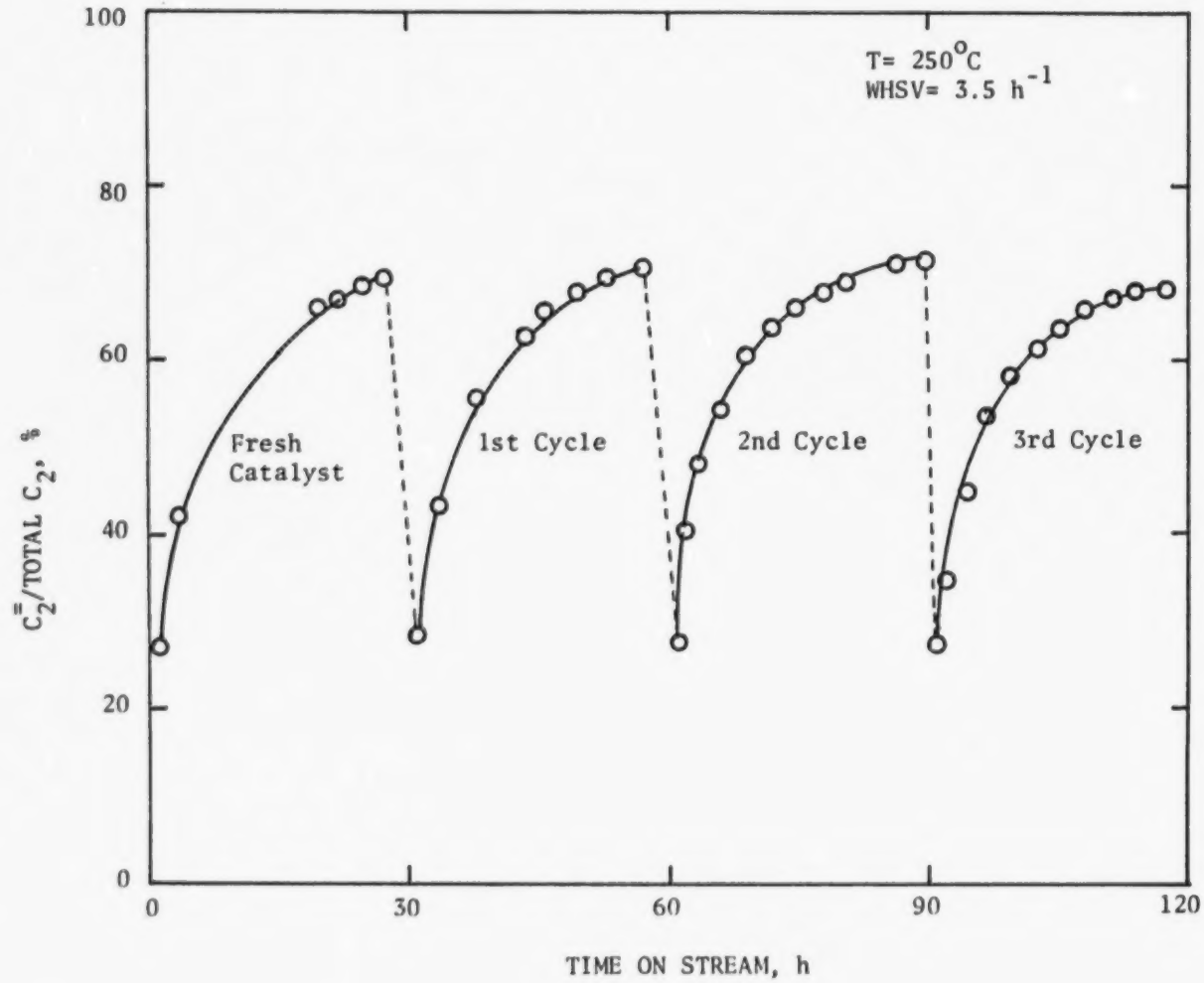

Figure 54 $C_2^=/C_2$ Fraction in the Hydrocarbon Product with Time-on-Stream.

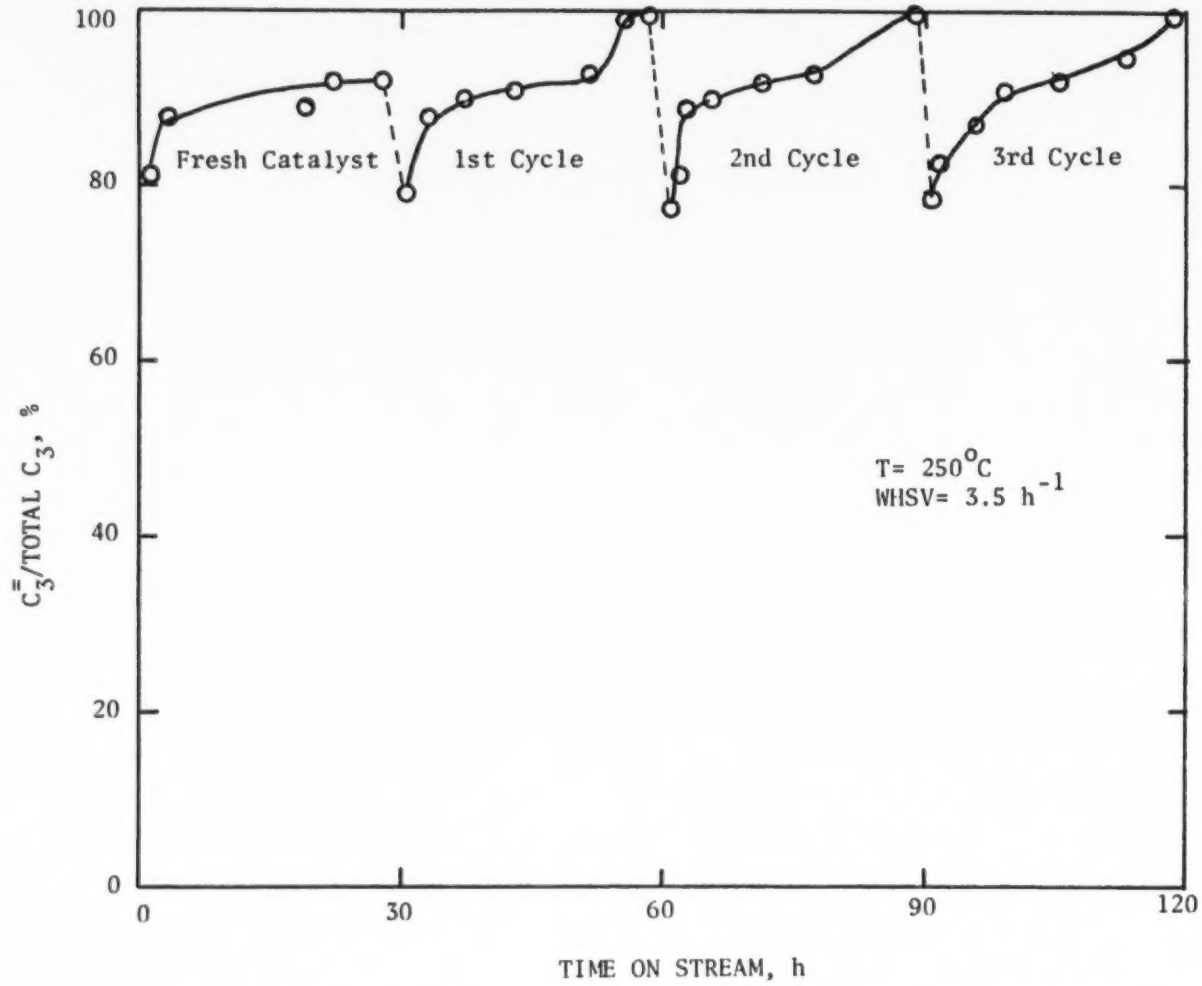

Figure 55. $C_3^=/C_3$ Fraction in the Hydrocarbon Product with Time-on-Stream.